Tesis Doctoral

Sistemas de Control Híbridos Fraccionarios: Modelado, Análisis y Aplicaciones en Robótica Móvil y Mecatrónica

Seyed Hassan HosseinNia

Escuela de Ingenierías Industriales
Departamento de Ingeniería Eléctrica, Electrónica y Automática

Director
Fdo: (Dr. D. Blas Manuel Vinagre Jara)

2013

PhD Thesis

Fractional Hybrid Control Systems: Modeling, Analysis and Applications to Mobile Robotics and Mechatronics

by

Seyed Hassan HosseinNia

in the

School of Industrial Engineering

Department of Electrical, Electronics and Automation Engineering

Director

Dr. Blas Manuel Vinagre Jara

2013

UNIVERSIDAD DE EXTREMADURA

Tesis Doctoral

Sistemas de Control Híbridos Fraccionarios: Modelado, Análisis y Aplicaciones en Robótica Móvil y Mecatrónica

Por

Seyed Hassan HosseinNia

Director

Dr. D. Blas Manuel Vinagre Jara

TRIBUNAL CALIFICADOR

Presidente

Dr. D. Sebastián Dormido Bencomo

Secretario

Dr. Dña. Inés Tejado Balsera

Vocales

Dr. D. Vicente Feliu Batlle

Dr. D. Alfonso Baños Torrico

Dr. D. Igor Podlubny

2013

UNIVERSIDAD DE EXTREMADURA

Abstract

School of Industrial Engineering
Department of Electrical, Electronics and Automation Engineering

by Seyed Hassan HosseinNia

Hybrid systems are heterogeneous dynamic systems whose behavior is determined by interacting continuous-variable and discrete-event dynamics, and they arise from the use of finite-state logic to govern continuous physical processes or from topological and networks constraints interacting with continuous control. The wide applicability of hybrid systems has inspired a great deal of research from both control theory and theoretical computer science. In addition, differential equations with fractional-order have been recently proved to be valuable tools for modeling of many physical phenomena. Regarding the importance of hybrid system and fractional-order calculus there is a lack of research in fractional-order hybrid systems in the specialized literature concerning control applications.

In this thesis, modeling, stability analysis and control of fractional-order hybrid systems are presented as new challenges. Fractional differential inclusions are introduced as a mathematical tool to model fractional-order hybrid systems and some fractional-order systems are modeled using fractional differential inclusions. Fractional-order switching systems and reset control systems are the type of fractional-order hybrid systems which are mostly studied in this dissertation. Currently, reset control focuses on using structures which allow new resetting rules in order to avoid Zeno solutions to

be caused and improve the performance of the system. As a comparative study, the properties of some modified reset strategies are studied which reset controller states to fixed or variable nonzero values and are able to eliminate or reduce the overshoot in first and higher order systems, respectively. Thereafter, a general advanced reset control is proposed with both fixed and variable resetting to nonzero values. In addition, stability analysis is generalized for the fractional-order switching and reset systems. Using the developed stability tools, a fractional-order robust controller is designed for switching systems. Common Lyapunov method and its equivalence in frequency domain are extended to fractional-order switching systems. A frequency domain stability analysis is also generalized for fractional-order reset control systems.

Cruise control and adaptive cruise control of a car Citroën C3 are considered as a practical application. In this experiment, a hybrid controller including two different fractional-order PI controller is designed to act over both the throttle and the brake pedals of the vehicle. The proposed fractional-order reset controller is applied to the servomotor as another application. Furthermore, the developed stability theorem is applied to gain and order scheduling control of an experimental platform called Smart Wheel.

Resumen

Escuela de Ingenierías Industriales
Departamento de Ingeniería Eléctrica, Electrónica y Automática

Seyed Hassan HosseinNia

Los sistemas híbridos son sistemas dinámicos heterogéneos cuyo comportamiento está determinado por la interacción de dinámicas correspondientes a variables continuas y eventos discretos, y surgen de la utilización de la lógica de estados finitos para gobernar procesos físicos continuos, o de restricciones topológicas y de redes que interactúan con un control continuo. La gran aplicabilidad de los sistemas híbridos ha inspirado una gran cantidad de investigación en teoría de control y ciencias de la computación. Por otra parte, las ecuaciones diferenciales de orden fraccionario han demostrado ser valiosas herramientas para el modelado de muchos fenómenos físicos. En cuanto a la importancia de los sistema híbridos y el cálculo fraccionario hay una falta de investigación en sistemas híbridos de orden fraccionario en la literatura específica sobre las aplicaciones de control.

En esta tesis se presentan, como nuevos retos, el modelado, el análisis de estabilidad y el control de sistemas híbridos de orden fraccionario. Se utilizan inclusiones diferenciales de orden fraccionario como herramientas matemáticas para modelar sistemas híbridos de orden fraccionario, y algunos sistemas de orden fraccionario se modelan utilizando inclusiones diferenciales fraccionarias. Los tipos de sistemas híbridos estudiados en esta tesis son los sistemas conmutados y los sistemas de control reset. Actualmente, el control reset se centra en el uso de estructuras que permiten nuevas reglas de puesta a cero con el fin de evitar las soluciones tipo Zeno y mejorar el rendimiento del sistema. Como estudio comparativo, se estudian las propiedades de algunas estrategias de control reset modificado que resetean los estados del controlador a valores fijos o variables distintos de cero y son capaces de eliminar o reducir la sobreoscilación de sistemas de primer orden y orden superior, respectivamente. Cabe destacar que también, se propone una estrategia de control reset avanzado que permite resetear a valores tanto fijos como variables distintos de cero. Además, se generaliza el análisis de la estabilidad para sistemas conmutados y sistemas reset de orden fraccionario. Utilizando las herramientas de análisis de estabilidad desarrolladas, se propone un método para diseñar controladores fraccionarios robustos para sistemas conmutados. El método común de Lyapunov y su equivalencia en el dominio de frecuencia se utilizan para el caso de sistemas de conmutados de orden fraccionario. También se generaliza el análisis de estabilidad en el dominio de la frecuencia para sistemas reset de orden fraccionario.

El control de crucero y el control de crucero adaptativo de un vehículo Citröen C3 se considera como una aplicación práctica. En este experimento, se diseña una ley de control híbrido que incluye dos controladores PI fraccionarios diferentes para las acciones del acelerador y del freno del vehículo. El controlador reset avanzado de orden fraccionario propuesto se aplica a un servomotor como otra aplicación. Por otra parte, el teorema de estabilidad desarrollado se aplica al control de ganancia y orden programados de la plataforma denominada Smart Wheel.

Acknowledgements

This work has been partially supported by the Ph.D. Grant of the ministry of science and research of Iran and the University of Extremadura.

Foremost, I would like to express my sincere gratitude to my advisor Prof. Blas M. Vinagre for the continuous support of my Ph.D study and research, for his patience, motivation, enthusiasm, and immense knowledge. His guidance helped me in all the time of research and writing of this thesis. I could not have imagined having a better advisor and mentor for my Ph.D study.

My sincere thanks also goes to Prof. Richard Magin, for offering me the summer internship opportunities in his group at Department of Bioengineering of University of Illinois at Chicago (USA) and leading me working on diverse exciting projects.

I also take this opportunity to convey my great thanks to my colleague Dr. Inés Tejado for her kind and patient help in my papers and for the hard working together before deadlines. Also to my fellow labmates Dr. Emiliano Pérez, Daniel Torres, Francisco Romero and Isaías González and to my roommates Seyed Sadegh Mohammadi and Soroush Salmani. It has been a great pleasure to be with such a good friends during all these years.

Last but not the least, I would like to thank my family: my parents, for giving birth to me at the first place and supporting me spiritually throughout my life, and my brother Mahmoud for all his support during my stay here in Spain.

Agradecimentos

Este trabajo ha sido parcialmente financiado por la beca predoctoral del Ministerio de Ciencia e Investigación de Irán y por la Universidad de Extremadura

En primer lugar, quisiera expresar mi sincera gratitud a mi director, Profesor Blas M. Vinagre, por el apoyo continuo de mi estudio e investigación de doctorado, por su paciencia, motivación, entusiasmo e inmenso conocimiento. Su guía me ayudó durante todo el tiempo que duró la investigación y la escritura de esta tesis. No hubiera podido imaginar tener un mejor director y mentor para mis estudios de doctorado.

Mi sincero agradecimiento también al Profesor Richard Magin, por ofrecerme la oportunidad de trabajar durante un verano en su grupo en el Departamento de Bioingeniería de la Universidad de Illinois en Chicago (USA), y por guiarme trabajando en diversos proyectos excitantes.

También aprovecho esta oportunidad para dar muchas gracias a mi colega Dra. Inés Tejado por su amable y paciente ayuda en mis artículos y por el duro trabajo juntos antes de que se acabaran los plazos. También a mis compañeros de laboratorio, Dr. Emiliano Pereira, Daniel Torres, Francisco Romero e Isaías Gonzáles, y a mis compaẽros de piso, Seyed Sadegh Mohammadi y Soroush Salmani. Ha sido un gran placer compartir con amigos tan buenos todos estos años.

Finalmente, aunque no menos, me gustaría dar las gracias a mi familia: a mis padres, por haberme dado la vida en primer lugar y por apoyarme espiritualmente a lo largo de ella, y a mi hermano Mahmoud por todo su apoyo durante mi estancia aquí en España.

Contents

List of Figures

List of Tables

Abbreviations

ACC	**A**daptive **C**ruise **C**ontrol
CC	**C**ruise **C**ontrol
CI	**C**legg **I**tegral
DI	**D**ifferntial **I**nclusions
FCI	**F**ractional **C**legg **I**tegral
FDI	**F**ractional **D**ifferntial **I**nclusions
FHS	**F**ractional-order **H**ybrid **S**ystem
FOC	**F**ractional-**O**rder **C**alculus
FORE	**F**irst **O**rder **R**eset **E**lement
FRCS	**F**ractional-order **R**eset **E**lement
FPCI	**F**ractional order **P**roportional **C**legg **I**ntegral
FPI	**F**ractional order **P**roportional **I**ntegral
GOSC	**G**ain and **O**rder **S**cheduling **C**ontrol
GSC	**G**ain **S**cheduling **C**ontrol
HS	**H**brid **S**ystem
IO	**I**nteger-**O**rder
PCI	**P**roportional **C**legg **I**ntegral
PCID	**P**roportional **C**legg **I**ntegral **D**erivative
SwS	**Sw**itching **S**ystem

Chapter 1

About This Thesis

This chapter presents the motivation, objectives and main contributions of this Thesis.

1.1 Problem statement and motivation

Many complicated control systems today such as those for flight control, manufacturing systems, and transportation have big amounts of computer code at their highest level. More generally, programmable logic controllers are widely used in industrial process control. We also see that todays products incorporate logical decision-making into even the simplest control loops (e.g., embedded systems). Indeed, all control systems today apply continuous controls and perform logical checks that determine the mod –and hence the control algorithms– the continuous-variable system is operating under at any given moment. As such, these hybrid control systems offer a challenging set of problems.

Therefore, HS are certainly pervasive today. But they have been with us at least since the days of the relay. Traditionally, though, the hybrid nature of systems and controllers has been suppressed by converting them into either purely discrete or purely continuous entities. The reason is that science and engineerings formal modeling, analysis, and control toolboxes deal largelyand largely successfullywith these pure systems. Engineers have pushed headlong into the application areas above. And the successes in flight control alone attest to the fact that it is possible to build highly complex, highly reliable systems. Yet ever more complex systems continue to arise (e.g., flight

vehicle management and intelligent vehicle/highway systems). And the trend toward embedded systems is sure to continue.

Why Fractional Calculus? Many real dynamic systems are better characterized using a non-integer order dynamic model based on fractional calculus or, differentiation or integration of non-integer order. Traditional calculus is based on integer order differentiation and integration. The concept of fractional calculus has tremendous potential to change the way we see, model, and control the nature around us. Denying fractional derivatives is like saying that zero, fractional, or irrational numbers do not exist. From control engineering point of view, improving and developing the control is the major concern. Existing evidences have confirmed that the best fractional order controller outperforms the best integer order controller. It is also clear that FC has been effectively applied in a wide range of fields, such as feedback control, systems theory, and signals processing, showing some advantages over traditional integer order techniques.

It is time to focus on developing formal modeling, analysis, and control methodologies for fractional order hybrid systems.

1.2 Objectives

The thesis is considered of interest from several points of view. From the scientific point of view, it is intended to develop mathematical models that can represent a more general class of dynamical systems, and tools and techniques to study the behavior of such systems. Furthermore, from the viewpoint of control theory, the possible contributions in techniques and methods to control the above mentioned systems would enlarge the theoretical corpus. Finally, from the viewpoint of the engineering applications, the cases considered (autonomous vehicles and active orthosis for assistance to disabled people) fall into two fields now of undeniable interest. The main objectives of this thesis can be summarized as follows:

1. Modeling of FHS (as FDIs and others). The first step in analysis and/or control of FHS is to model it as a generalized form of differential inclusions (DI) for fractional order control (FOC), which will be referred as FDI.

2. Control of FHS. Fractional order control of HS together with hybrid FOC of an ordinary system will lead us to FHS. Several techniques will be developed in this thesis.

3. Stability analysis of FHS. Many tools are introduced for the stability of the HS which cannot be used in FHS. Some of these methods and tools will be generalized for FHS:

   - Common Lyapunov method.
   - Frequency domain analysis related to quadratic stability.
   - Robust Controller design for SwS.
   - Fractional order reset system and its control

4. Validation of the tools and strategies by simulation.

   - Application case I: autonomous vehicles.
   - Application case II: servomotor
   - Application case III: smart wheel

5. Validation of the tools and strategies by experiments.

   - Application case I: autonomous vehicles.
   - Application case II: servomotor
   - Application case III: smart wheel

1.3 Contributions and related publications

The main contributions of this Ph.D. Thesis are the following:

1. The development of hybrid models in fractional order dynamics

2. The development of stability analysis in frequency domain. An equivalent of common Lyapunov method is proposed to ensure the stability of SwS.

3. Proposal of a different type of the robust controllers using the developed stability theorem.

4. Proposal of a fractional order Clegg integrator and proportional-Clegg integrator controllers

5. Generalization of stability analysis of the fractional order reset control systems

6. The proposal and experimental application, as well as validation, of a fractional hybrid controller for mobile robots in particular CC and ACC of vehicle.

7. The proposal and experimental application, as well as validation, of a fractional-order reset controllers for servomotor application.

8. Application of stability analysis to the smart wheel

These results have been spread in the journals, books, conferences and talks cited next.

Journal

- **S.H. HosseinNia**, I. Tejado, B.M. Vinagre, V. Milanés, J. Villagrá, Experimental Application of Hybrid Fractional Order Adaptive Cruise Control at Low Speed, IEEE Transaction on Control System Technology, Under review

- **S.H. HosseinNia**, I. Tejado, B.M. Vinagre, On the Stability of Fractional Order Switching Systems, Computer and Mathematics With application, Under review

- I. Tejado, **S.H. HosseinNia**, B.M. Vinagre, YangQuan Chen, Efficient Control of a SmartWheel via Internet with Compensation of Variable Delays, Journal of Mechatronics, 2013

- **S.H. HosseinNia**, I. Tejado, B.M. Vinagre, Fractional-Order Reset Control: Application to a Servomotor, Journal of Mechatronics, 2013

- **S.H. HosseinNia**, I. Tejado, B.M. Vinagre, A Method for the Design of Robust Controllers Ensuring the Quadratic Stability for Switching Systems, Journal Vibration and Control, 2012, doi:10.1177/1077546312470480

- **S.H. HosseinNia**, I. Tejado, B.M. Vinagre, D. Sierociuk, Some Ways to Apply Fractional Order SMC to Switching Systems: Application to a DC-DC Buck Converter, Signal, Image and Video Processing, 2012

- I. Tejado, **S.H. HosseinNia** and Blas M. Vinagre, X. Song, Y.Q. Chen, Dealing With Fractional Dynamics of IP Network Delays, International Journal of Bifurcation and Chaos, 2011

Conference

- **S.H. HosseinNia**, Inés Tejado and Blas M. Vinagre, Advanced Reset Control: A Comparative Study, 52nd IEEE Conference on Decision and Control, Italy, 2013, submitted
- **S.H. HosseinNia**, Inés Tejado and Blas M. Vinagre, Basic Properties and Stability of Fractional Order Reset, Control Systems, The 12th European Control Conference (ECC13), Zurich, Switzerland, July, 2013
- **S.H. HosseinNia**, Inés Tejado and Blas M. Vinagre, Fractional Order Hybrid Systems and Their Stability, 14th International Carpathian Control Conference, Krakow-Rytro, Poland, 2013
- F. Romero, J. Alonso, **S.H. HosseinNia**, B. Vinagre, J.M. Font-Llagunes, Muscle Forces Adaptation in Assited Walking Using a Powered SCKAFO, Journal of Biomechanics, 45 (1) (2012) S521
- **S.H. HosseinNia**, Inés Tejado and Blas M. Vinagre, Robust Fractional order PI Controller for Switching Systems, 5th IFAC symposium on Fractional differentiation and its applications, China, 2012
- **S.H. HosseinNia**, Inés Tejado and Blas M. Vinagre, Stability of Fractional Order Switching Systems, 5th IFAC symposium on Fractional differentiation and its applications, China, 2012
- I. Tejado, **S.H. HosseinNia**, B.M. Vinagre, Comparing Fractional Order PI Controllers With Variable Gain and Gain-Order for the Networked Control of a Servomotor, IFAC Conference on Advances in PID Control PID'12 Brescia, 28-30 March 2012
- **S.H. HosseinNia**, F. Romero, I. Tejado, F.J. Alonso, B.M. Vinagre, Controller Design for A Stance-Control Knee-Ankle-Foot Orthosis Based on Optimization

Techniques, International Conference in Biomedical Electronics and Device, Portugal, 2012

- **S.H. HosseinNia**, I. Tejado, B.M. Vinagre, V. Milans, J. Villagr, Low Speed Control of an Autonomous Vehicle Using a Hybrid Fractional Order Controller, 2nd International Conference on Control, Instrumentation, and Automation (ICCIA), Iran, 2011

- J.M. Font-Llagunes, F. Romero, **S.H. HosseinNia**, F.J. Alonso, B.M. Vinagre, U. Lugrs, A Powered Lower Limb Orthosis to Assist the Gait of Incomplete Spinal Cord Injured Patients, XXIX Congreso de la Sociedad Espaola de Ingeniera Biomdica, Spain, 2011

- **S.H. HosseinNia**, I. Tejado, B.M. Vinagre, V. Milans, J. Villagr, ACC of a Commercial Vehicle Using Fractional Order Controllers for Throttle and Brake, Workshop de Robtica: Robtica Experimental, Escuela Superior de Ingenieros de la Universidad de Sevilla, Spain, 2011

- I. Tejado, **S.H. HosseinNia**, B.M. Vinagre, Network-based Experiences With a Servomotor Applying Gain and Order Scheduling Control, Symposium on Fractional Signals and Systems, Coimbra, Portugal, 2011

- **S.H. HosseinNia**, F. Romero, B. M. Vinagre, F. J. Alonso, I. Tejado, Hybrid Modeling and Fractional Control of a SCKAFO Orthosis for Gait assistance, ASME 2011 International Design Engineering Technical Conferences & Computers and Information in Engineering Conference, 2011, Washington D.C., USA

- I. Tejado, V. Milanes, J. Villagra, J. Godoy, **S.H. HosseinNia** and Blas M. Vinagre, Low Speed Control of an Autonomous Vehicle by Using a Fractional PI Controller, 2011 IFAC World Congres, Italy, 2011

- **S.H. HosseinNia**, B. M. Vinagre, F.J. Alonso, Simulacin del control hbrido de un modelo simplificado de rtesis activa para ayuda a la marcha, XVIII Congreso Nacional Ingeniera Mecnica, Spain, 2010

- **S.H. HosseinNia**, B. M. Vinagre, V. Milans and C. Gonzlez, Controller for Urban Intersections Based on Hybrid Automaton, 13th International IEEE Conference on Intelligent Transportation Systems 2010

- **S.H. HosseinNia**, D. Sierociuk, A. J. Calderon, B. M. Vinagre, Augmented System Approach for Fractional Order SMC of a DC-DC Buck Converter, 4th IFAC workshop on Fractional differentiation and its applications 2010
- **S.H. HosseinNia**, B. M. Vinagre, Direct Boolean Integer and Fractional Order SMC of Switching Systems Application to a DC-DC Buck Converter, 4th IFAC workshop on Fractional differentiation and its applications, 2010

In all, the work reported in this Thesis has been disseminated in:

- Seven journal papers
- Eigteen conference papers

1.4 Overview of contents

This Thesis is organized as follows:

- Chapter 1 contains this introduction about the Thesis.
- Chapter 2 presents the current state of the art of HS, and FOC and its application to HS, remarking on some interesting research trends of these topics in Spain.
- Chapter 3 states the modeling the fractional order HS and some application will be introduced.
- Chapter 4 studies design of a robust fractional-order controller for switching systems and states a comparative study of the different reset control system to avoid the Zeno solution and finally, introduces a general fractional-order reset controller which avoid the Zeno solution.
- Chapter 5 is divided into four sections. After preliminaries about the stability of fractional order system and integer-order hybrid system, the stability of switching system will be studied in the second section and the next section will study the stability of fractional order reset system. And, finally some examples are simulated to show the efficiency of the proposed methods.

- Chapter 6 presents the experimental results obtained when applying different fractional-order hybrid controllers and stability analysis of the a Citröen C3 vehicle, servomotor, smart wheel and a biomechanical application.
- Concluding remarks and future works will be presented in chapter 7.

Chapter 2

State of the Art

In this chapter, a current survey of HS and its control, as well as a historical review of FOC and its emerging application to hybrid system, are summarized. The aim is to provide a snapshot assessment of the current state of research in the fields and to present a broad perspective on recent results. The below lists are quite far from aiming at completeness, failing to mention literal hundreds of other published texts related to hybrid systems and FOC. The main reason why they are not mentioned here is that their subjects are of minor importance for the purpose of this Thesis. As one can see from the surveys below, numerous control strategies have been applied to hybrid systems during the last decades. However, there are not so many references and works related to the application of FOC to such systems, especially in Spain. This fact justifies the final purpose of this Thesis.

2.1 Historical review of HS and its control

Many dynamical systems combine behaviors that are typical of continuous-time dynamical systems with behaviors that are typical of discrete-time dynamical systems. For example, in a switched electrical circuit, voltages and currents that change continuously according to classical electrical network laws also change discontinuously due to switches opening or closing. Some biological systems behave similarly, with continuous change during normal operation and discontinuous change due to an impulsive stimulus [3, 4]. In particular, continuous components arise as differential equations specifying

how the concentrations of various molecular species evolve over time. Discrete components of models of biological systems arise from state transitions (e.g., from healthy to abnormal states), abstractions and approximations, nonlinear effects, and the presence of inherently discrete processes, often observed in systems governed by one or a few molecules [5]. Embedded systems and, more generally, systems involving both digital and analog components form another class of examples [3]. Finally, modern control algorithms often lead to both kinds of behavior, due to either digital components used in implementation or logic and decision making encoded in the control algorithm. These examples fit into the class of hybrid dynamical systems, or simply hybrid systems.

Over the last few decades, in research areas such as computer science, feedback control, and dynamical systems, researchers have given considerable attention to modeling and solution definitions for hybrid systems. Perhaps the earliest related reference is the work in [6] where a class of continuous-time systems with both continuous and discrete states (the state is referred to as hybrid state) exhibiting transitions was proposed in the context of optimal control. More recent contributions can be find in [3, 4, 7–24] among several others.

Switching systems have been the subject of interest for the past decades, for their wide application areas. Switching systems are a class of hybrid systems consisting of several subsystems and a switching rule indicating the active subsystem at each instant of time.The continuous dynamics of switching systems are described by a set of time-invariant differential equations which involve (at least partially) the same states. Each of these differential equations represent the dynamics of a time-invariant system, often referred to as constituent systems of the switching system. The discrete dynamics are represented by some logic- or event-driven switching unit that alternates the linear dynamics at distinct time-instances. Referring to [25] a switching system can be happened for a number of reasons such as, switching process, multiple control objectives, performance and constraints and adaptive control. For examples, longitudinal dynamics of an automobile can show a switching process where each gear the dynamics can be described by a different continuous model [26]. In the wind-turbine power generators for reasons of security and performance the generator operates in different modes depending on the current wind-speed can be an example of multi control objectives [27]. Rest control can be fit into performance and constraints where the performance of the controller can be improved by switching off the integral part of the controller

when the error crossing zero [28]. For processes with uncertainties and largely varying disturbances, adaptive controllers can be applied to account for the changing operating conditions. Switching dynamical systems arise naturally as a consequence of the introduction of the multiple-models, switching and tuning paradigm in [29].

Recent efforts in the research of switching systems typically focus on the analysis of dynamic behaviors, such as stability, controllability and observability, and aim to design controllers which guarantee stability and optimize their performance. To be more precise, the study of the stability of switching systems gives rise to a number of interesting and challenging mathematical problems, which have been of increasing interest in the last decades [30–33]. Typically, the approach adopted to analyze these systems is to employ theories that have been developed for differential equations. Actually, most results are based on Lyapunov stability theory. Existence of quadratic Lyapunov functions for each of the constituent LTI systems is not sufficient for the stability of switching systems. However, it is well known that a switching system is stable if there exists some common Lyapunov function that satisfies the conditions of the Lyapunov theory simultaneously for all constituent subsystems (see e.g. [34–39]). In [40], the authors established a number of converse theorems and showed that such a common Lyapunov function always exists when the switching linear system is stable for arbitrary switching. However, general conditions for determining the existence of a common Lyapunov function for switching systems are unknown. A frequency domain method equivalent to the common Lyapunov one may make the control and stability analysis easier. To this respect, a frequency domain equivalent of common Lyapunov function was proposed in [41] based on strictly positive realness (SPR) of the system in order to analyze the quadratic stability of switching systems.

Reset controllers are standard controllers endowed with a reset mechanism, i.e., a strategy that resets to zero the controller state (or part of it) when some condition holds. The reset condition is typically the zero crossing of the controller input, but other choices are possible as well (e.g. see [28, 42–45]). This kind of control was firstly introduced by Clegg in the 50's to overcome the fundamentals limitations of linear controllers; more precisely, to reduce phase lag while retaining the integrator's desirable magnitude slope in the frequency response [42]. Thus, Clegg integrator (CI) was introduced as a solution for improving feedback performance, due to its ability to provide the magnitude slope of a linear integrator (-20 dB/dec) but with a phase

(about $-38°$) much more favourable in terms of phase margins and robustness. The potential advantages of using CI to meet stringent design specifications have been reported in many papers (e.g. [46, 47]). Additional reset structures, such as first order reset elements (FORE) [43, 44] and improved reset controllers [48], were proposed later to improve the performance of CI.

Recently, there has been a renewed interest in this class of systems due to their advantages with respect to conventional control solutions. Essentially, it has been shown that resetting to zero at the zero crossings of the error is completely inadequate since it may cause Zeno solutions in the system response (see e.g. [28] and references therein). As a result, current trends focus on using new reset structures which allow reset to occur on more complicated and sophisticated sets so as to improve the performance of the system. To this end, several and different solutions have been reported in the literature. For example, the controller states were reset to certain non-zero values in [48, 49] to make the system response be even faster in comparison with the linear solution. In [28, 50, 51], a PI+CI controller was used to reduce considerably both the percentage of overshoot and the settling time by resetting only a percentage of the integral term of the PI controller. The authors of [52] proposed a new class of FORE, together with set-point regulation, which allow new resetting rules. A modified version of this reset strategy was applied in [53] to a diesel engine. In our previous works, we investigated the possibilities of using fractional order CI (FCI) together with classic PI controllers as base controller [54, 55]. It was demonstrated that FCI is also able to handle the mentioned problems in reset control by adjusting its order adequately.

While the application of switching systems, reset control system and more generally hybrid system can undoubtedly be beneficial, studying fractional-order generalization of such systems is by no means trivial. In this thesis, we focus on modeling, control and stability analysis of fractional-order hybrid system and in particular fractional-order switching systems, and reset control systems. Next section will review fractional-order calculus and its application in FHS.

2.2 Historical review of FOC and FHS

Fractional-order calculus (FOC) is a more than 300 years old topic, being the first reference probably associated with Leibniz and L´Hôpital in 1695 where half-order derivative was mentioned. However, the first indication of the potential of FOC may be shown by Bode in the 1940s, without using the term "fractional", with his study to keep invariant the performance of a feedback amplifier in closed-loop to changes in the amplifier gain. In the 90.s decade, Prof. Oustaloup, of University of Bordeaux (France), and Prof. Podlubny, of Technical University of Kosice (Slovak Republic), presented important studies on fractional-order control strategies, which established the starting point of FOC on automatic control applications. In particular, Oustaloup [56] proposed the CRONE (French abbreviation for Commande Robuste dOdre Non Entier, meaning Non-integer-Order Robust Control) method for the control of dynamics systems, demonstrating its superior performance versus the traditional PID controller and introducing the robustness property. Nowadays, there exist three generations of CRONE controllers (see [57]). With respect to Podlubnys work [58], he introduced the generalization of the traditional PID controller to non-integer-orders, namely the $PI^{\lambda}D^{\mu}$ controller, where λ and μ are the orders of the integrator and differentiator, respectively. Podlubny also demonstrated the better response of this kind of controllers in comparison with the classical ones, especially to control fractional-order systems.

Thereafter and during the last decades, further research activities to define new effective tuning methods for fractional-order controllers have been proposed in the literature as an extension of classical control theory, mainly for traditional PID controllers due to its widespread industrial use. A classification of these tuning techniques is presented in [59]. In this respect, some analytical methods, concerning phase and gain margins, flat phase or dominant poles, can be found in [59–63], as well as some numerical methods in [64, 65] and tuning rules in [66–68]. These tuning methods are basically based on techniques in the frequency domain but also by optimizing certain performance indices or providing the controlled system with extra specifications given by the additional tuning parameters of fractional-order controllers with respect to classical ones. Besides, it is worth mentioning that there exist interactive software tools for the design of fractional-order PID controllers [69, 70].

At the same time, the better understanding of the potential of fractional calculus, i.e., the generalization of the classical calculus to orders of integration and differentiation not necessarily integer, and the increasing number of applications in many areas of science and engineering have led to the importance of both the analysis and study of fractional-order models, to better characterize the behavior of a system, and the design of fractional-order controllers, which allow the controlled system to attain better performance in comparison with classical integer-order controllers (see e.g. [65, 71] for fundamentals of fractional-order systems and controllers). Although the problem of stability is a very essential and crucial issue for control systems, including fractional-order systems, due to the complexity of the relations, it has been discussed and investigated only in some recent literature. For more details of stability for different classes of fractional-order systems, e.g. see [58, 72–74] for linear time invariant systems, [75, 76] for delayed systems, [77, 78] for nonlinear systems, [79, 80] for fractional-order interval systems. Likewise, some extensions of Lyapunov theory have been developed to fractional-order systems [81, 82].

Recently, some works are reported on fractional-order hybrid systems (FHS), and fractional-order differential inclusions (FDI). In [83–87], the authors mainly focused on the mathematical part of FDIs and their solution. Particularly, existence of the solution of a certain class of FDI like FDI with Dirichlet boundary conditions, impulsive FDI and FDI with infinite delay are investigated in [83, 84, 86]. Furtheremore, existence of solutions for nonlinear FDIs of order $\alpha \in (1, 2]$ with families of mixed and closed boundary conditions are studied in [87]. Kaczorek investigated the realization problem for positive fractional hybrid 2D linear systems proposing a method for computation of positive fractional realizations of a given proper 2D transfer matrix [88, 89]. Hedrih [90] obtained eigen main chains, eigen modes and main coordinates using an analytical approach, for a fractional-order hybrid multi-pendulum system dynamics. Balochian et. al. have lately reported some new works on variable structure control of FDIs [91, 92]. In [91] the stabilization of a particular class of multi-input linear systems of fractional-order differential inclusions with state delay using variable structure control is considered whereas the sufficient condition for stabilization problem of a linear time invariant fractional-order switched system with order, $1 < \alpha < 2$ by a single Lyapunov function whose derivative is negative and bounded by a quadratic function within the activation regions of each subsystem are presented in [92].

To this respect, common Lyapunov theory will be generalized for fractional-order switching systems, and stability conditions will be provided based on such a common Lyapunov method and its equivalence in frequency domain. It is important to remark that stability in frequency domain may be useful for the design, in the frequency domain, of integer or fractional-order controllers to stabilize fractional or integer-order switching systems, respectively.

Although mentioned works have contributed greatly to the research in the field, but, despite the recent general interest on fractional-order systems, fractional-order Hybrid systems have not received much attention. Therefore, new studies of modeling, control and stability analysis are required to face analysis and control of FHS. The research activity related to FOC is more than 15 years old at University of Extremadura. This interest started with Dr. Vinagre's Ph.D. Thesis in 2001 [93]. Since then, four Ph.D. Theses has been developed under his supervision [94–97]. As a result, and in collaboration with other international scientists, an important number of papers and books have been published (e.g. see [60, 65, 71, 93, 98–117]).

In this thesis we focus on modeling, control and stability of FHS Given this motivation, the objective of this thesis in one hand is to develop a theoretical framework to design fractional-order hybrid controller and study stability for fractional-order hybrid systems in general, extending classical theory to such systems. On the other hand applying the developed methods on the following practical applications:

1. Mobile robotics: CC and ACC of Citroën vehicle;
2. Reset control of a servomotor;
3. Stability analysis of the smart wheel controlled using gain and order scheduling PI control in [97, 106]

In this research, as an application, fractional-order hybrid controller is designed to control throttle and brake in low speed control of Citroën C3 vehicle. Regarding to the different dynamics of the car during the acceleration and deceleration, different controllers (multi-controller) are designed which represent an application of FHS. fractional-order gain scheduling which is another example of multi-controllers can be

another application of FHS, which is reported in [106, 111] and its stability is analyzed in this dissertation. In addition, the developed fractional-order reset controller is applied to a servomotor to investigate another experiments in the family of HS.

Chapter 3

Fractional-Order Hybrid Systems

In this chapter we review the differential inclusions and generalize DI for fractional-order systems. Hybrid automaton will be briefly reviewed and some examples will show the modeling of HS/FHS as DI/FDI.

3.1 Differential inclusions

In a hybrid dynamical system, the state sometimes flows (continuously) while at other times it makes jumps. Whether flow occurs or a jump occurs depends on the state's location in the state space. Thus, a hybrid dynamical system is usually described by two functions, f and g, and two sets C and D. The function f generates a differential equation that governs flow while the function g generates a reset equation that governs jumps. The function f is often only specified for variables that can flow while the function g is often only specified for variables that can jump. The set C indicates where in the state space flow may occur while the set D indicates where in the state space jumps may occur. Where these sets overlap, both flowing and jumping may be possible.

A widely used model of a continuous-time dynamical system is the first-order differential equation $\dot{x} = f(x, u)$, with x and u belonging to an n-dimensional Euclidean space $\mathbb{R}^n$. This model can be expanded in two directions that are relevant for hybrid systems. First, we can consider differential equations with state constraints, that is, $\dot{x} = f(x, u)$ and $x \in C,\ u \in C_u$, where C and C_u are subset of $\mathbb{R}^n$. Second, we can consider the

situation where the right-hand side of the differential equation is replaced by a set that may depend on x. Both situations lead to the differential inclusion $\dot{x} \in F(x)$, where F is a set-valued mapping. Combining the two generalizations leads to constrained differential inclusions $\dot{x} \in F(x,u),\ x \in C,\ u \in C_u$.

A typical model of a discrete-time dynamical system is the first-order equation $x^+ = g(x,u)$, with $x, u \in \mathbb{R}^n$. The notation x^+ indicates that the next value of the state is given as a function of the current state x through the value $g(x)$. As for differential equations, it is a natural extension to consider constrained difference equations and difference inclusions, which leads to the model $x^+ \in G(x,u),\ x \in D,\ u \in D_u$, where G is a set-valued mapping and D and D_u are subset of $\mathbb{R}^n$. Since a model of a hybrid dynamical system requires a description of the time driven dynamics, the event driven dynamics, and the regions on which these dynamics apply, we include both a constrained differential inclusion and a constrained difference inclusion in a general model of a hybrid system in the form

$$\begin{aligned} \dot{x} \in F(x,u), x \in C, u \in C_u, \\ x^+ \in G(x,u), x \in D, u \in D_u. \end{aligned} \tag{3.1}$$

This model captures a wide variety of dynamic phenomena including systems with logic-based state components, which take values in a discrete set, as well as timers, counters, and other components. We refer to a hybrid system in the form described by the former equations as $\mathcal{H}$. We call C the flow set, F the flow map, D the jump set, and G the jump map.

3.2 Hybrid Automaton

There is a growing literature, mainly in computer science, that deals with hybrid systems as an outgrowth of automata theory. The main idea is to successively add time

constraints on events and simple dynamics (such as clocks and timers) to finite automata in order to build on automata results. A simple example is a room-thermostat-heater system where the temperature of the room evolves according to laws of thermodynamics and the state of the heater (on/off); the thermostat senses the temperature, performs certain computations and turns the heater on and off. In general, hybrid automata have been used to model and analyze a variety of embedded systems including vehicle control systems, air traffic control systems, mobile robots, and processes from systems biology.

Informally, a hybrid automaton is a (possibly infinite) state machine augmented with differential equations. It is a standard model for describing a hybrid system. Several different but equivalent formal definitions exist.

Hybrid automata come in several flavors: The Alur-Henzinger hybrid automaton is a popular model; it was developed primarily for algorithmic analysis of hybrid systems model checking. The HyTech model checking tool is based on this model. The Hybrid Input/Output Automaton model has been developed more recently. This model enables compositional modeling and analysis of hybrid systems. Another formalism which is useful to model implementations of hybrid automaton is the lazy linear hybrid automaton.

Hybrid automaton is a collection,

$$\mathcal{H} = (Q,\ X,\ f,\ D,\ E, G,\ R) \tag{3.2}$$

where,

- $q \in Q$ is discrete state,
- $X \in \mathbb{R}^n$ is continuous state,
- $Init \subseteq Q \times \mathbb{R}^n$ is initial state,
- $f : Q \times X \to TX$ is a vector field,
- $D : Q \to P(X)$ is domain,

- $E \subseteq Q \times Q$ is a set of edges,
- $G : E \to P(X)$ is a guard condition,
- $R : E \times X \to P(X)$ is a reset map.

3.3 Modeling of fractional-order Hybrid System

Differential equations with fractional-order have recently proved to be strong tools in the modeling of many physical phenomena. Many fractional-order controllers such as fractional-order PID [65, 98, 101, 118], fractional-order state feedback control [119], fractional-order sliding mode control [107, 108], are proposed to control dynamical system. In addition, many fractional-order system are studied and controlled [109, 120, 121]. Regarding to this application and the importance of the hybrid system, there is lack of research in fractional-order hybrid system. Although there exist some works reported in fractional-order differential inclusions, there still is lack of research in modeling, control and analysis of fractional-order differential inclusions. As mentioned in previous sections, many system around us are hybrid and many system needs hybrid controllers regarding to the applications. Therefore, applying fractional-order controller or analyzing the control of fractional-order hybrid system is necessary. Modeling, control, simulation and stability analysis of fractional-order hybrid system needs it own tools which have to be developed. The first step in the analysis of the hybrid fractional-order system is to model the system. In the next section a generalization of fractional-order differential inclusions will be studied.

3.3.1 fractional-order Differential Inclusions

The integer-order differential inclusions is described in (3.2) at section 3.1. As a generalization of differential inclusions in the fractional-order system we can have,

$$\begin{aligned} D^{\alpha}x \in F(x,u), x \in C, u \in C_u, \\ x^{+} \in G(x,u), x \in D, u \in D_u. \end{aligned} \tag{3.3}$$

where, D^{α} is the fractional-order differentiator. As it mentioned before, there are many system which can be represent as fractional-order hybrid differential inclusions.

Following some example will show the application of the integer and fractional-order hybrid differential inclusions.

3.4 Some Examples

In this section first we study the well-known bouncing ball system to introduce the modeling of HS using DI. Then, some class of Hybrid system such as switching systems, multi-controller system and reset control system will modeled using DI/FDI.

3.4.1 Bouncing ball

A canonical example of a hybrid system is the bouncing ball, a physical system with impact. Here, the ball (thought of as a point-mass) is dropped from an initial height and bounces off the ground, dissipating its energy with each bounce. The ball exhibits continuous dynamics between each bounce; however, as the ball impacts the ground, its velocity undergoes a discrete change modeled after an inelastic collision. A mathematical description of the bouncing ball follows. Let x_1 be the height of the ball and x_2 be the velocity of the ball. A hybrid system describing the ball is as follows [122]: The flow map for this system follows from the forces acting on the ball. For $x_1 > 0$, gravity acts on the ball generating the flow map,

$$f(x) := \begin{bmatrix} x_2 \\ -\gamma \end{bmatrix} \text{if}, x_1 > 0, \tag{3.4}$$

where γ denotes the gravitational constant, according to Newtons laws of motion. Since flowing below the level of the floor will not be possible, the flow map does not need to be defined for $x_1 < 0$. Alternatively, one can view the flow map as a set-valued mapping with empty values for $x_1 < 0$. One may also consider defining the flow map for $x_1 = 0$. The jump map can be taken to be

$$g(x) := \begin{bmatrix} x_1 \\ -cx_2, \end{bmatrix} \tag{3.5}$$

where $0 < c < 1$ is a coefficient of restitution. This is saying that when the height of the ball is zero (it has impacted the ground), its velocity is reversed and decreased by a factor of c. Effectively, this describes the nature of the inelastic collision.

Following the discussion above, the balls velocity is allowed to jump when $x_1 = 0$ and $x_2 < 0$. Thus, the jump set may be taken to be

$$C := \left\{ x \in \mathbb{R}^2 | x_1 = 0, x_2 < 0 \right\}. \tag{3.6}$$

One may also consider choosing the jump set to be the closure of the set D given above. This would add the point $(x_1, x_2) = (0, 0)$ to the jump set, resulting in a closed set. The effect on solutions of closed jump sets will be discussed in the next chapter.

The state of the bouncing ball system changes continuously when the ball is above the floor. Thus, one may consider taking the flow set as

$$D := \left\{ x \in \mathbb{R}^2 | x_1 > 0 \right\}. \tag{3.7}$$

The bouncing ball is an especially interesting hybrid system, as it exhibits Zeno behavior. Zeno behavior has a strict mathematical definition, but can be described informally as the system making an infinite number of jumps in a finite amount of time. In this example, each time the ball bounces it loses energy, making the subsequent jumps (impacts with the ground) closer and closer together in time. To show the flow and jump, this hybrid system is solved using the hybrid toolbox released by Sanfelice in [20] and it is shown in Fig. 3.1. The restitution time is set as $c = 0.8$ and the simulation is run for 20 jumps.

In addition, the bouncing ball can be formulate as following hybrid automaton format,

- $Q = \{q_0\}$
- $X = (x_1, x_2) \in \mathbb{R}^2$
- $Init = \{q_0\} \times \{x \in \mathbb{R}^2 : x_1 \geq 0\}$
- $\dot{x} = f(q_0, x) = [x_2, -g]^T$
- $R(q_0, \{x : x_1 = 0, x_2 \leq 0\}) = (q_0, (x_1, -cx_2))$, where q_0 is the discrete state.

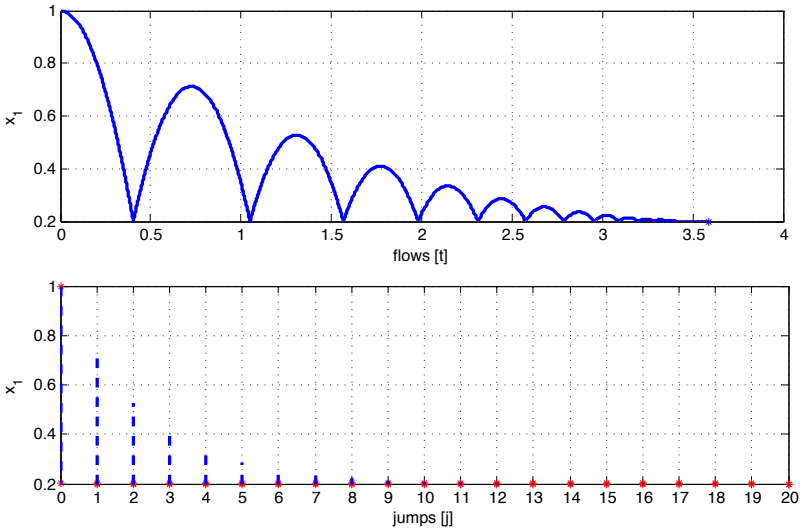

FIGURE 3.1: Solution of the bouncing ball hybrid system.

3.4.2 Systems with Switches and Relays

Physical systems with switches and relays can be naturally modeled as hybrid systems. Sometimes, the dynamics may be considered merely discontinuous, such as in a blown fuse. In many cases of interest, however, the switching mechanism has some hysteresis, yielding a discrete state on which the dynamics depends. This situation is depicted by the multi-valued function H shown in Fig. 3.2. Suppose the function H models

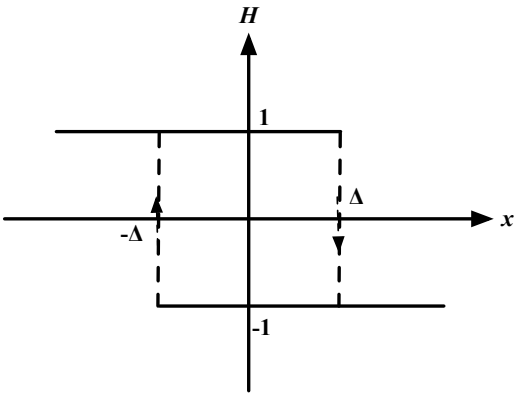

FIGURE 3.2: Hysteresis Function.

the hysteretic behavior of a thermostat. We may model a thermostatically controlled room as follows

$$\dot{x} = f(x, H(x - x_0)), \tag{3.8}$$

where x and x_0 denote room and desired temperature, respectively. The function f denotes dynamics of temperature, which depends on the current temperature and whether the furnace is switched On or Off. Note that this system is not just a differential equation whose right-hand side is piecewise continuous. There is memory in the system, which affects the value of the vector field. Indeed, such a system naturally has a finite automaton associated with the hysteresis function H, as pictured in Fig. 3.3. Notice that, for example, the discrete state changes from +1 to -1 when the continuous state enters the set $\{x \geq \Delta\}$. That is, the event of x attaining a value greater than or equal to Δ triggers the discrete or phase transition of the underlying automaton.

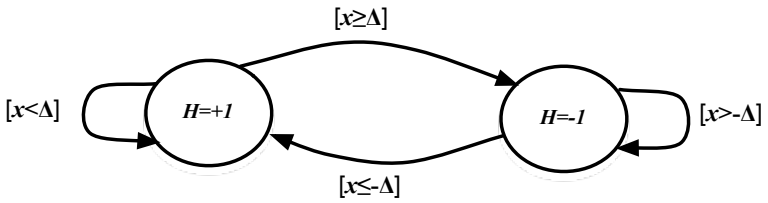

FIGURE 3.3: Finite Automaton Associated with Hysteresis Function.

3.4.2.1 Temperature Control of a Solid

In [99, 123], a fractional-order model for temperature is identified and controlled. For the mathematical description of the controlled object was chosen two-term differential equation of the fractional-order. This mathematical description can be approximated by differential equation of first order. The mathematical model of the controlled object described by two-term differential equation as follows:

$$D^{\alpha}T(t) = -\frac{a_0}{a_1}T(t) + u(t), \tag{3.9}$$

where T is temperature, $u(t)$ is control input and $a_0 = 0.598, a_1 = 39.69, \alpha = 1.26$. Fig. 3.4 can show the bang-bang control of the temperature model. Regarding to this controller system can be represent as a hybrid model. The flow map can be described as follows:

$$\begin{bmatrix} D^{\alpha}T(t) \\ D^{\alpha}u(t) \end{bmatrix} = \begin{bmatrix} -\frac{a_0}{a_1} & 1 \\ 0 & 0 \end{bmatrix} \begin{bmatrix} T(t) \\ u(t) \end{bmatrix} \tag{3.10}$$

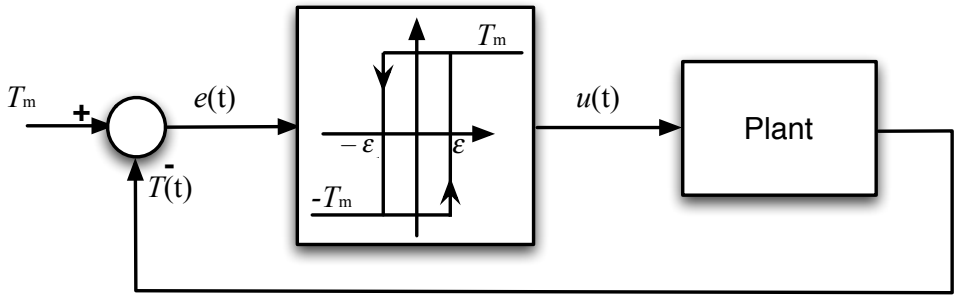

FIGURE 3.4: Temperature control.

The control input i.e. $u(t)$ belongs to $\{-T_m, T_m\}$ where T_m is the desired temperature. Concerning to the hysteresis switch, the control input will be T_m when $\{T \in \mathbb{R} | T < T_m + \varepsilon\}$ and the control input will be $-T_m$ when $\{T \in \mathbb{R} | T > T_m - \varepsilon\}$. Then the flow map is taken to be:

$$C := \{(T, u) \in \mathbb{R} \times \{-T_m, T_m\} \, | u = T_m \& T < T_m + \varepsilon \text{ or } u = -T_m \& T > T_m - \varepsilon\} \, . \tag{3.11}$$

The jump set is taken to be:

$$D := \{(T, u) \in \mathbb{R} \times \{-T_m, T_m\} \, | u = T_m \& T = T_m + \varepsilon \text{ or } u = -T_m \& T = T_m - \varepsilon\} \, . \tag{3.12}$$

Regarding the jump map, since the role of jump changes is to toggle the logic mode and since the state component T does not change during jumps, the jump map will be

$$\begin{bmatrix} T \\ u \end{bmatrix}^+ = \begin{bmatrix} T \\ -u \end{bmatrix} . \tag{3.13}$$

3.4.3 Switching system

The past decades have witnessed an enormous interest in switching systems whose behaviour can be described mathematically using a mixture of logic based switching and difference/differential equations. By a switching system we mean a hybrid dynamical system consisting of a family of continuous-time subsystems and a rule that orchestrates the switching among them [34, 124, 125]. A primary motivation for studying such systems came partly from the fact that switching systems and switching multi-controller

systems have numerous applications in control of mechanical systems, process control, automotive industry, power systems, traffic control, and so on. In addition, there exists a large class of nonlinear systems which can be stabilized by switching control schemes, but cannot be stabilized by any continuous static state feedback control law [30]. Another motivation arises from the application of switching systems theory to the field of network-based control systems. These new types of control systems can be handled as switching systems (e.g. refer to [126–130] and references therein).

3.4.3.1 DC-DC buck converter

DC-DC buck converter can be an example of switching system. The formulation in the form of a bilinear system defined on $\mathbb{R}^n$ is,

$$\begin{bmatrix} \dot{v}_c \\ \ddot{v}_c \end{bmatrix} = \begin{bmatrix} 0 & 1 \\ -\frac{1}{LC} & -\frac{1}{RC} \end{bmatrix} \begin{bmatrix} v_c \\ \dot{v}_c \end{bmatrix} + \begin{bmatrix} 0 \\ \frac{1}{LC} \end{bmatrix} uV_g. \tag{3.14}$$

where $u \in \{0, 1\}$. Suppose,

$$u = \frac{1}{2}(1 - \text{sgn}(S)), \tag{3.15}$$

where S is desired surface and $S\dot{S} < 0$ is satisfied regarding to the sliding mode condition(see [107]). Then, defining

$$\xi = \begin{bmatrix} v_c \\ \dot{v}_c \end{bmatrix} \tag{3.16}$$

the hybrid state of the closed-loop system is given by

$$x := \begin{bmatrix} v_c \\ \dot{v}_c \\ q \end{bmatrix} \in \mathbb{R}^3. \tag{3.17}$$

The flow map for the closed-loop system is given by

$$f(x) := \begin{bmatrix} 0 & 1 & 0 \\ -\frac{1}{LC} & -\frac{1}{RC} & \frac{V_g}{LC} \\ 0 & 0 & 0 \end{bmatrix} x \tag{3.18}$$

Considering the controller as $u = q, q = 0, 1$, the jump will happen $q = 0$ and e when $q = 0$, the jump will happen if $S < 0$ and the jump will happen when $q = 1$, if $S > 0$. Defining,

$$C_0 := \{S|S > 0\}$$
$$C_1 := \{S|S < 0\}$$
$$D_q := \{S|S = 0\},$$

the flow set is taken to be

$$C := \left\{(\xi, q) \in \mathbb{R}^2 \times \{0, 1\} \,|q \in \{0, 1\}, \xi \in C_q\right\}. \tag{3.19}$$

The jump set is taken to be

$$D := \left\{(\xi, q) \in \mathbb{R}^2 \times \{0, 1\} \,|q \in \{0, 1\}, \xi \in D_q\right\}. \tag{3.20}$$

The jump map for the closed-loop system will be

$$g(x) := \begin{bmatrix} v_c \\ \dot{v}_c \\ 1 - q \end{bmatrix}. \tag{3.21}$$

3.4.4 Sample-and-Hold Control Systems

In a typical sample-and-hold control scenario, a continuous-time plant is controlled by a digital controller. The controller samples the plants state, computes a control signal, and sets the plants control input to the computed value. The controllers output remains constant between updates. Sample-and-hold devices perform analog-to-digital and digital-to-analog conversions.

The closed-loop system resulting from this control scheme can be modeled as a hybrid system. Sampling, computation, and control updates in sample-and-hold control are associated with jumps that occur when one or more timers reach thresholds defining the update rates. When these operations are performed synchronously, a single timer

state and threshold can be used to trigger their execution. In this case, a sample-and-hold implementation of a control law samples the state of the plant and up- dates its input when a timer reaches the threshold $T > 0$, which defines the sampling period. During this up- date, the timer is reset to zero. For the static, state-feedback law $u = \kappa(\xi)$ for the plant $\dot{\xi} = f(\xi, u)$, a hybrid model uses a memory state z to store the samples of u, as well as a timer state t to determine when each sample is stored. The state of the resulting closed-loop system, which is depicted in Fig. 3.5, is taken to be $x(\xi, z, \tau)$. During flow, which occurs until τ reaches the threshold T, the state of the plant evolves according to, $\dot{\xi} = f(\xi, z)$, the value of z is kept constant, and τ grows at the constatnt rate of one. In other words, $\dot{z} = 0$ and $\dot{\tau} = 1$. This behavior corresponds to the flow set $C = \mathbb{R}^n \times \mathbb{R}^m \times [0, T]$, while the flow map is given by $F(x) = (f(\xi, z), 0, 1)$ for all $x \in C$.

When the timer reaches the threshold T, the timer state τ is reset to zero, the memory state z is updated to $\kappa(\xi)$, but the plant ξ does not change. This behavior corresponds to the jump set $D := \mathbb{R}^n \times \mathbb{R}^m \times \{T\}$ and the jump map $G(x) := (\xi, \kappa(\xi), 0)$ for all $x \in D$ [3].

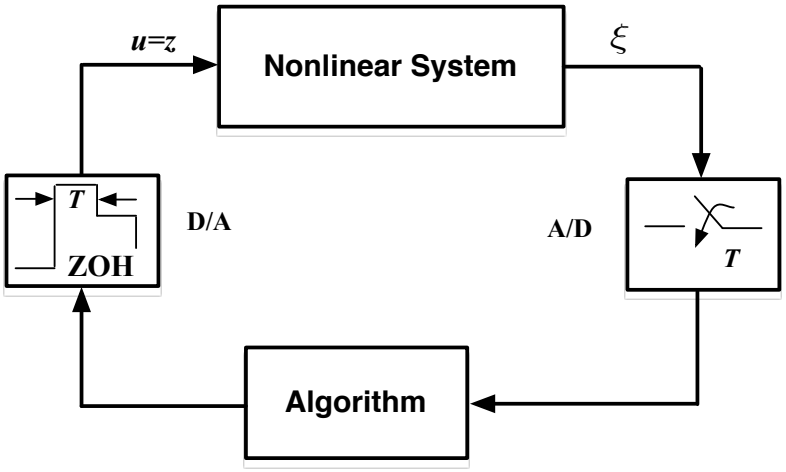

FIGURE 3.5: Digital control of a continuous-time nonlinear system with sample-and-hold devices performing the analog-to-digital (A/D) and digital-to-analog (D/A) conversions. Samples of the state ξ of the plant and updates of the control law $\kappa(\xi)$ computed by the algorithm are taken after each amount of time T . The controller state z stores the values of $\kappa(\xi)$.

3.4.5 Multi Controllers system

In several control applications, the design of a continuous-time feedback controller that performs a particular control task is not possible. For example, in the problem of globally stabilizing a multi-link pendulum to the upright position with actuation on the first link only, topological constraints rule out the existence of a continuous-time feedback controller that accomplishes this task globally and robustly. However, it is often possible to overcome such topological obstructions using hybrid feedback control to combine continuous-time feedback laws that achieve certain subtasks [20].

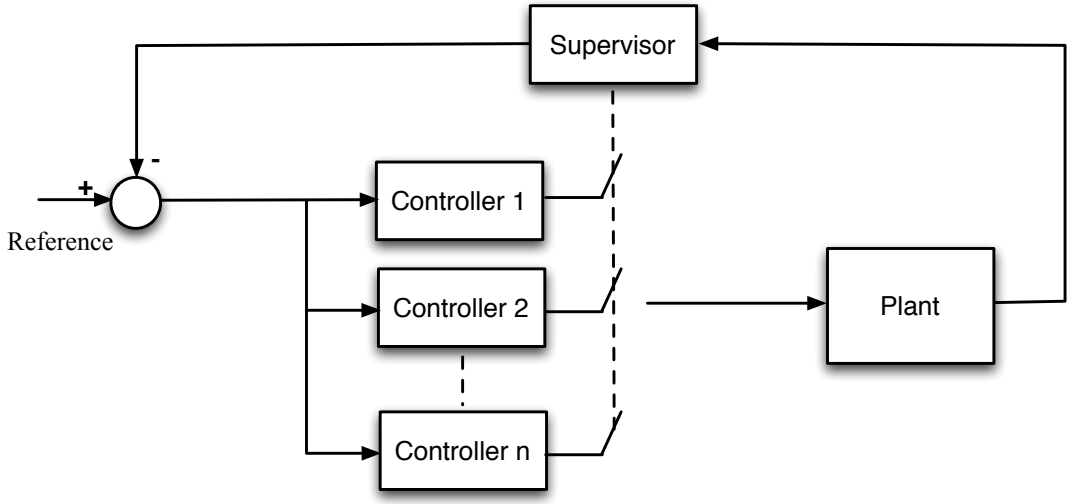

FIGURE 3.6: Multi controller schematic

For instance, suppose that two state feedback control laws $\kappa_1 : \mathbb{R}^p \to \mathbb{R}^m, \kappa_2 : \mathbb{R}^p \to \mathbb{R}^m$ have been designed to stabilize the origin of a nonlinear control system $\dot{\xi} = \tilde{f}(\xi, u)$. The feedback law κ_1 produces efficient transient responses, but only works near the origin. The feedback law κ_2 produces less efficient transients but works globally. The goal is to build a hybrid feedback law that globally asymptotically stabilizes the origin while using κ_1 near the origin and uses κ_1 far from the origin.

The controller will use a logic variable q, which here we assume to take values in the set $\{1, 2\}$, to keep track of which controller is currently being applied. Then, the state of the closed-loop system is given by

$$x := \begin{bmatrix} \xi \\ q \end{bmatrix} \in \mathbb{R}^{p+1}. \tag{3.22}$$

Since the logic variable does not change during flows, the flow map for the closed-loop system is given by

$$f(x) := \begin{bmatrix} \tilde{f}(\xi, \kappa_q(\xi)) \\ 0 \end{bmatrix}. \tag{3.23}$$

Hysteresis is used as follows to determine when it is appropriate to switch between controllers. A jump should occur when $q = 2$ and the state ξ is close to the origin, say in a set D_2, and a subsequent jump should not occur unless $q = 1$ and the state ξ attempts to leave a larger set C_1. This behavior is generated by allowing flows when $q = 1$ and $\xi \in C_1$ or when $q = 2$ and $\xi \in \mathbb{R}^p$ $D_2 =: C_2$, while allowing jumps when $q = 2$ and $\xi \in D_2$ or when $q = 1$ and $\xi \in \mathbb{R}^p$ $C_1 =: D_1$. Thus,the flow set is taken to be

$$C := \{(\xi, q) \in \mathbb{R}^p \times \{1, 2\} \,|q \in \{1, 2\}\,, \xi \in C_q\}\,. \tag{3.24}$$

The jump set is taken to be

$$D := \{(\xi, q) \in \mathbb{R}^p \times \{1, 2\} \,|q \in \{1, 2\}\,, \xi \in D_q\}\,. \tag{3.25}$$

Regarding the jump map, since the role of jump changes is to toggle the logic mode and since the state component ξ does not change during jumps, the jump map for the closed-loop system will be

$$g(x) := \begin{bmatrix} \xi \\ 3 - q \end{bmatrix} \tag{3.26}$$

Finally, in order for the hybrid feedback law to work as intended, there should be a relationship between D_2 and C_1. In particular, if trajectories of

$$\tilde{f}(\xi, \kappa_1(\xi)) \tag{3.27}$$

start in D_2 they should remain in a closed set that is a strict subset of C_1; moreover any trajectory of this system that starts in C_1 and remains in C_1 should converge to the origin. Since the local controller is locally asymptotically stabilizing, both of these properties can be induced by first picking C_1 to be a sufficiently small neighborhood of the origin and then picking D_2 to be another sufficiently small neighborhood of the origin [20].

3.4.5.1 A fractional-order multi controllers

As mentioned before many system has recently been controlled with fractional-order PI. For instance, let us consider a first order system with two different dynamics as follows (see Fig. 3.7):

$$G_i(s) = \frac{K_i}{s + \tau_i}, i = 1, 2, \tag{3.28}$$

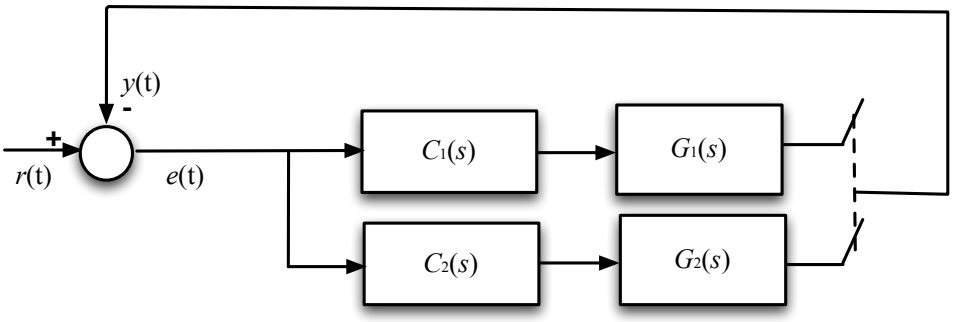

FIGURE 3.7: Closed loop system with two controllers.

Now consider following fractional-order PI to control this system,

$$C_i(s) = k_{p_i} + \frac{k_{i_i}}{s^{\alpha_i}}, i = 1, 2. \tag{3.29}$$

Closed loop transfer function of the system can be represent as,

$$\frac{Y(s)}{R(s)} = \frac{a_i s^{\alpha_i} + b_i}{s^{\alpha_i+1} + (\tau_i + a_i)s^{\alpha_i} + b_i}, i = 1, 2. \tag{3.30}$$

where $a_i = K_i k_{p_i}$ and $b_i = K_i k_{i_i}$. Assuming $\alpha_i = \frac{q_i}{p_i}$ and replacing 3.30 to the state space form yields,

$$\begin{bmatrix} D^{\frac{1}{q_i}} x_1 \\ D^{\frac{1}{q_i}} x_2 \\ \vdots \\ D^{\frac{1}{q_i}} x_{p_i+1} \\ \vdots \\ D^{\frac{1}{q_i}} x_{p_i+q_i-1} \\ D^{\frac{1}{q_i}} x_{p_i+q_i} \end{bmatrix} = \begin{bmatrix} 0 & 1 & 0 & \cdots & 0 & \cdots & 0 \\ 0 & 0 & 1 & \cdots & 0 & \cdots & 0 \\ \vdots & \vdots & \vdots & \ddots & \vdots & \ddots & \vdots \\ 0 & 0 & 0 & \cdots & 1 & \cdots & 0 \\ \vdots & \vdots & \vdots & \ddots & \vdots & \ddots & \vdots \\ 0 & 0 & 0 & \cdots & 0 & \cdots & 1 \\ -b_i & 0 & 0 & \cdots & -(\tau_i + a_i) & \cdots & 0 \end{bmatrix} \begin{bmatrix} x_1 \\ x_2 \\ \vdots \\ x_{p_i+1} \\ \vdots \\ x_{p_i+q_i-1} \\ x_{p_i+q_i-1} \end{bmatrix} + \begin{bmatrix} 0 \\ 0 \\ 0 \\ \vdots \\ 0 \\ \vdots \\ 1 \end{bmatrix} U(r(t)), i = 1, 2 \tag{3.31}$$

where $U(r(t)) = a_i D^{\alpha_i} r(t) + b_i r(t)$. Thus, it is obvious that the closed loop system has fractional-order in following general form:

$$D^{\alpha_i} x = A_i x + B_i U_i. \tag{3.32}$$

Now assume that the controller one i.e. $c_1(e)$ will be activated if $e = r(t) - y(t) > -\varepsilon$ and the other controller i.e. $c_2(e)$ will be activated if $e = r(t) - y(t) < \varepsilon$. Thus, the flow set and the flow map are taken to be,

$$\begin{bmatrix} D^{\alpha_i} x \\ D^{\alpha_i} i \end{bmatrix} = \begin{bmatrix} A_i x + B_i U_i \\ 0 \end{bmatrix}, \tag{3.33}$$

$$C := \left\{ (x, i) \in \mathbb{R}^{\alpha_i + 1} \times \{1, 2\} \,|\, i = 1 \& y(t) < r(t) + \varepsilon \text{ or } i = 2 \& y(t) > r(t) - \varepsilon \right\}. \tag{3.34}$$

The jump set is taken to be:

$$D := \left\{ (x, i) \in \mathbb{R}^{\alpha_i + 1} \times \{1, 2\} \,|\, i = 1 \& y(t) = r(t) + \varepsilon \text{ or } i = 2 \& y(t) = r(t) - \varepsilon \right\}. \tag{3.35}$$

Regarding the jump map, since the role of jump changes is to toggle the logic mode and since the state component x does not change during jumps, the jump map will be

$$\begin{bmatrix} x \\ i \end{bmatrix}^{+} = \begin{bmatrix} x \\ 3-i \end{bmatrix}. \tag{3.36}$$

Gain scheduling and gain and order scheduling control can be another example of the multi controller system [97, 106].

3.4.6 Reset Control Systems

Reset controllers were introduced to overcome the limitations of linear controllers. For instance, in the time domain it is not possible to fulfil all characteristic and specification like rise time, overshoot, settling time, or in the frequency domain water-bed effect will not let the system satisfies all the specifications [28, 42–45]. So, the main reason for using reset controllers is that, just by including the mechanism of resetting, they are able to overcome fundamental limitations in linear systems.

The reset controller was first introduced by studying Clegg integrator (CI) to reduce phase lag while retaining the integrator's desirable magnitude slope in the frequency response [42]. The CI was introduced as a solution for improving feedback performance, due to its ability to provide the magnitude slope of a linear integrator (-20 dB/dec) but with a phase (about $-38°$) much more favourable in terms of phase margins and robustness. The other reset controllers, such as first order reset element (FORE) controller [43, 44] and improved reset controller [48], PI+CI [50, 51, 131] were proposed later to improve the CI.

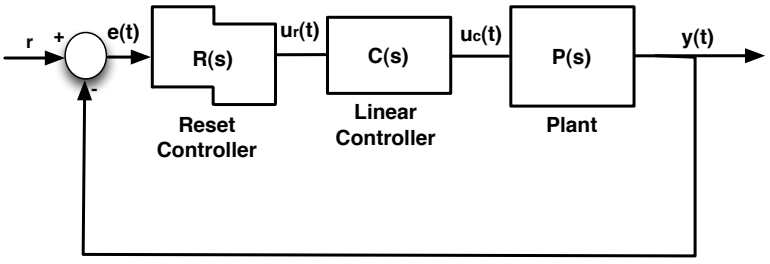

FIGURE 3.8: Block diagram of the reset control system

The block diagram of a general reset control system is shown in Fig. 3.8. It can be observed that the dynamics of the reset controller can be described by the fractional-order differential inclusion (FDI) equation as:

$$\begin{aligned} D^{\alpha}x_r(t) &= A_r x_r(t) + B_r e(t),\ e(t) \neq 0, \\ x_r(t^+) &= A_{R_r} x_r(t),\ e(t) = 0, \\ u_r(t) &= C_r x_r(t) + D_r e(t), \end{aligned} \tag{3.37}$$

where $0 < \alpha \leq 1$ is the order of differentiation, $x_r(t) \in \mathbb{R}^{nr}$ is the reset controller state and $u_r(t) \in \mathbb{R}$ is its output. The matrix $A_{R_r} \in \mathbb{R}^{n_r \times n_r}$ identifies that subset of states x_r that are reset (the last $\mathcal{R}$ states) and use the structure $A_{R_r} = \begin{bmatrix} I_{n_{\bar{\mathcal{R}}}} & 0 \\ 0 & 0_{n_{\mathcal{R}}} \end{bmatrix}$ and $n_{\bar{\mathcal{R}}} = n_r - n_{\mathcal{R}}$.

The linear controller $C(s)$ and plant $P(s)$ have, respectively, state-space representations as follows:

$$\begin{aligned} D^{\alpha}x_c(t) &= A_c x_c(t) + B_c u_r(t), \\ u_c(t) &= C_c x_c(t), \end{aligned} \tag{3.38}$$

and

$$\begin{aligned} D^{\alpha}x_p(t) &= A_p x_p(t) + B_p u_c(t), \\ y(t) &= C_p x_p(t), \end{aligned} \tag{3.39}$$

where $A_p \in \mathbb{R}^{n_p \times n_p}$, $B_p \in \mathbb{R}^{n_p \times 1}$, $C_p \in \mathbb{R}^{1 \times n_p}$, $A_c \in \mathbb{R}^{n_c \times n_c}$, $B_c \in \mathbb{R}^{n_c \times 1}$ and $C_c \in \mathbb{R}^{1 \times n_c}$.

The closed-loop reset control system can then be described by the following FDI:

$$\begin{aligned} D^{\alpha}x(t) &= A_{cl} x(t) + B_{cl} r,\ x(t) \notin \mathcal{M} \\ x(t^+) &= A_R x(t),\ x(t) \in \mathcal{M} \\ y(t) &= C_{cl} x(t) \end{aligned} \tag{3.40}$$

where $x = \begin{bmatrix} x_p \\ x_c \\ x_r \end{bmatrix}$, $A_{cl} = \begin{bmatrix} A_p & B_pC_c & 0 \\ -B_cD_rC_p & A_c & B_cC_r \\ -B_rC_p & 0 & A_r \end{bmatrix}$, $A_R = \begin{bmatrix} I_{n_p} & 0 & 0 \\ 0 & I_{n_c} & 0 \\ 0 & 0 & A_{R_r} \end{bmatrix}$, $B_{cl} = \begin{bmatrix} 0 & B_cD_r & B_r \end{bmatrix}^T$ and $C_{cl} = \begin{bmatrix} C_p & 0 & 0 \end{bmatrix}$. The reset surface $\mathcal{M}$ is defined by:

$$\mathcal{M} = \{x \in \mathbb{R}^n : C_{cl}x = r,\ (I - A_R)x \neq 0\}\,. \tag{3.41}$$

where $n = n_r + n_c + n_p$. In absence of the linear controller $C(s)$ the state space realization of the closed loop system can also be stated as (3.40) where, $x = \begin{bmatrix} x_p \\ x_r \end{bmatrix}$, $A_{cl} = \begin{bmatrix} A_p - B_pD_rC_p & B_pC_r \\ -B_rC_p & A_r \end{bmatrix}$, $A_R = \begin{bmatrix} I_{n_p} & 0 \\ 0 & A_{R_r} \end{bmatrix}$, $B_{cl} = \begin{bmatrix} B_pD_r & B_r \end{bmatrix}^T$, $C_{cl} = \begin{bmatrix} C_p & 0 \end{bmatrix}$.

Chapter 4

Fractional-order Hybrid Control Design

This part is divided into two section. First section is studying the design of the robust integer- and fractional-order controller for the switching system. In the next section, a comparative study between some reset strategies is given in order to show their benefits in terms of prevention of Zeno solutions and reduction of overshoot.

4.1 Robust Fractional-Order Control Design for Switching Systems

In this section, we investigate control of switching systems. A frequency-domain design method is developed for switching systems for both integer or fractional-order controllers, taking into account specifications regarding performance and robustness and ensuring the stability of the controlled system. Some examples are given to show the applicability and effectiveness of the proposed tuning method.

4.1.1 Quadratic stability in frequency domain

In [41], authors propose an equivalent to common Lyapunov stability conditions in frequency domain. The relation between SPRness and the quadratic stability can be

stated in the following theorem. For further information about the specification of state space system, refer to Section 5.2.

Theorem 4.1 ([41]). *Consider $c_1(s)$ and $c_2(s)$, two stable polynomials of order n, corresponding to the systems $\dot{x} = A_1 x$ and $\dot{x} = A_2 x$, respectively, then the following statements are equivalent:*

1. $\frac{c_1(s)}{c_2(s)}$ *and* $\frac{c_2(s)}{c_1(s)}$ *are SPR.*
2. $|\arg(c_1(j\omega)) - \arg(c_2(j\omega))| < \frac{\pi}{2}\ \forall\ \omega$.
3. A_1 *and* A_2 *are quadratically stable, which means that* $\exists P = P^T > 0 \in \mathbb{R}^{n\times n}$ *such that* $A_1^T P + P A_1 < 0$, $A_2^T P + P A_2 < 0$.

4.1.2 Problem statement

It is well known that a switching system can be potentially destabilized by an appropriate choice of switching signal, even if the switching is between a number of Hurwitz-stable closed-loops systems. Even in the case where the switching is between systems with identical closed loop characteristic polynomials, it is sometimes possible to destabilize the switching system by means of switching ([27]). Likewise, the concept of robustness with respect to parameter variations is well defined for LTI systems. However, this issue is somewhat more difficult to quantify for switched linear systems. In particular, robustness may be defined with respect to a number of design parameters, including, not only the parameters of the closed-loop system matrices, but also with respect to switching signal.

Let us illustrate the importance of designing a robust controller for switching systems by means of a particular example. Consider a switching system given by the following second order transfer function:

$$G_i(s) = \frac{2}{(\tau_i s + 1)^2},\ i = 1, 2, \tag{4.1}$$

with $\tau_1 = 1$ and $\tau_2 = 0.1$. One can state than only the time constant τ of the system changes. As can be observed in Fig. 4.1(a), both subsystems has the same phase

margin of 90 deg. Applying quadratic stability conditions in frequency domain to the closed-loop system, we have:

$$\left|\arg((3-\omega^2)+2j\omega)-\arg((3-0.01\omega^2)+0.2j\omega)\right| \not< \frac{\pi}{2}, \forall\omega. \tag{4.2}$$

Figure 4.1(b) depicts condition (4.2) graphically. It can be seen that the quadratic stability is not guarantied. As a result, a method to design the robust and stable controllers for such a class of switching systems is required.

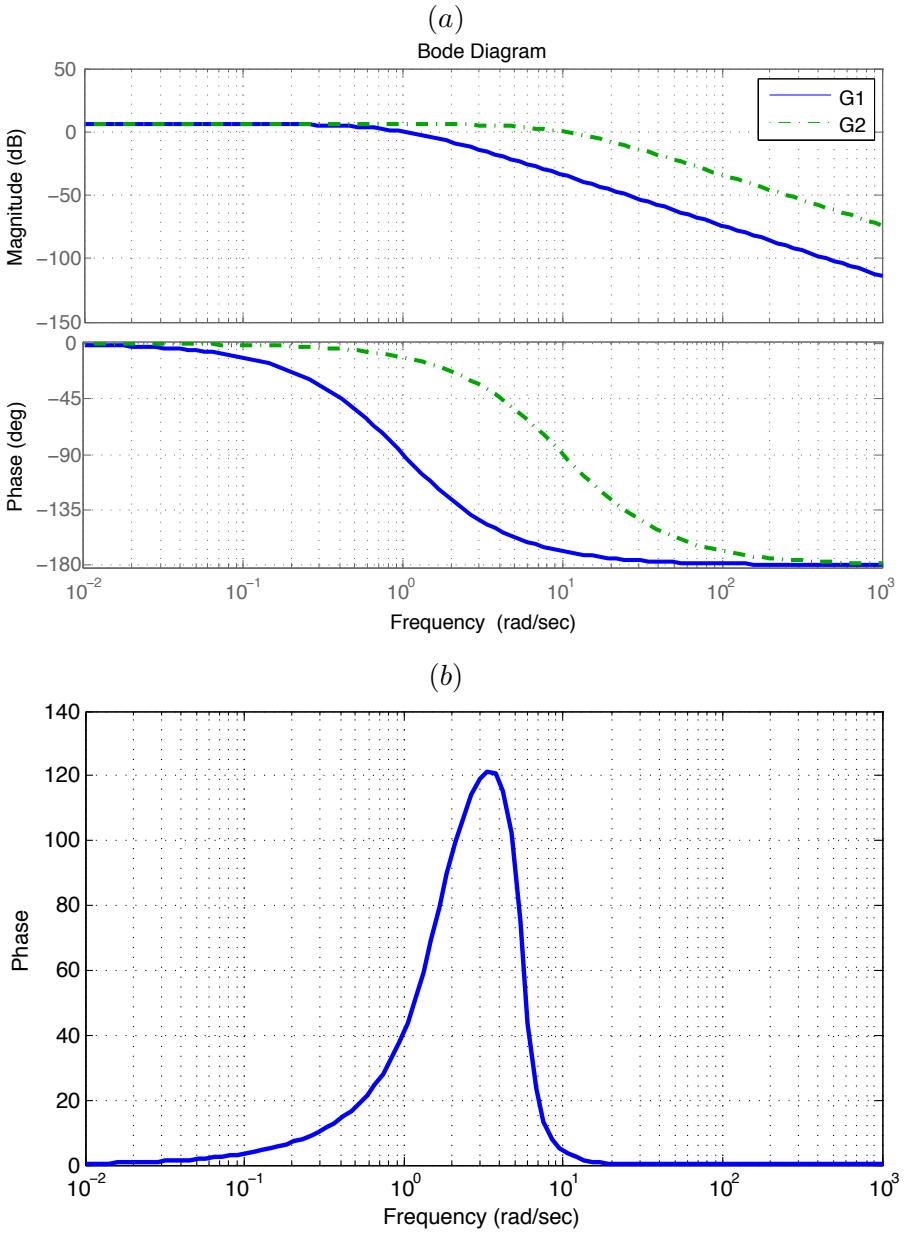

FIGURE 4.1: Frequency domain analysis: (a) Bode plot of the controlled subsystems H_1 and H_2 (b) PID

4.1.3 Design method

As commented in the introduction, the objective is to design controllers for switching systems so that the system fulfills different specifications regarding performance and robustness, and ensuring its stability. A scheme of the control approach is shown in Fig. 4.2 for a general system $G_i(s)$, $i = 1, 2, ..., L$.

Specifications related to phase margin, gain crossover frequency and output disturbance rejection are going to be considered in this design method. Indeed, other kinds of specifications can be met, depending on the particular requirements of the application. It should be noticed that, apart from these design specifications, which can change with the application, the stability conditions have to be also fulfilled. Actually, if the number of subsystems which constitutes the system to be controlled is L, there are $L-1$ stability conditions to be fulfilled. Therefore, denoting the number of specifications as N, a controller with $L + N - 1$ parameters is required in order to fulfil all given specifications and the stability conditions.

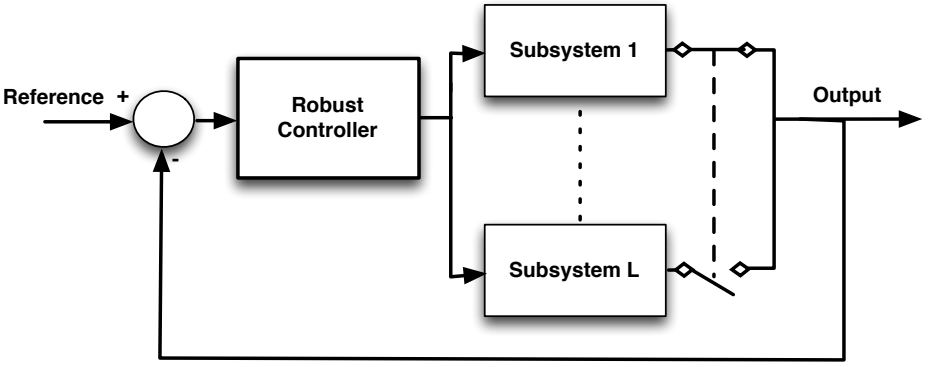

FIGURE 4.2: Scheme of the controlled system

Define G_n is the subsystem with the worse conditions regarding to each specification. Let assume that the phase margin and gain crossover frequency of a subsystem G_n are denoted as ϕ_{m_n} and ω_{cp_n}, respectively, c_i, $i = 1, 2, ..., L$, are the characteristic polynomials of each closed-loop subsystem and $K(j\omega)$ is the controller to be tuned. Thus, the design problem is formulated as follows:

1. Frequency domain specifications:

- Phase margin:

$$\arg(K(j\omega_{cp_n})G_n(j\omega_{cp_n})) + \pi > \phi_{m_n}. \tag{4.3}$$

- Gain crossover frequency:

$$|K(j\omega_{cp_n})G_n(j\omega_{cp_n})|_{dB} = 0dB. \tag{4.4}$$

- Output disturbance rejection:

$$\left| S(j\omega) = \frac{1}{1 + G_n(j\omega)K(j\omega)} \right|_{dB} \leq M, \forall\omega \leq \omega_s, \tag{4.5}$$

  where M is the desired value of the sensitivity function S for frequencies less than ω_s.

2. Stability conditions:

$$|\arg(c_1(j\omega)) - \arg(c_2(j\omega))| < \frac{\pi}{2}, \forall\omega \geq 0,$$

$$\vdots$$

$$|\arg(c_{L-1}(j\omega)) - \arg(c_L(j\omega))| < \frac{\pi}{2}, \forall\omega \geq 0. \tag{4.6}$$

   It is important to remark that (4.3)-(4.5) refer to the worse conditions concerning phase margin, crossover frequency and sensitivity for a subsystem G_n among all subsystems. The same can be done for any other specification, such as, high frequency noise rejection, steady-state error cancellation, etc. (see e.g. [65] for more tuning specifications). The set of conditions (4.6) ensure the stability of the switching system. In the case of the fractional-order systems or time delayed systems, an approximation of fractional-order derivative or delay can be used to apply these specifications.

As an example, in the case of $N = 2$, a list for types of switching systems and their possible controllers is given in Table 4.1 –any other type of controller can be tuned using the same idea. As can be stated, the use of fractional-order controllers may have the advantage of allowing more specifications or subsystems to be fulfilled or controlled, respectively, and, consequently, more robust performances to be attained.

TABLE 4.1: Type of switching system and possible controllers when $N = 2$

L	Type of controller	Transfer function
2	PID	$K_p + \frac{K_i}{s} + K_d s$
2	Fractional PI (FPI)	$K_p + \frac{K_i}{s^\lambda}$
2	Fractional PD (FPD)	$K_p + K_d s^\mu$
3	PID with noise filter (NPID)	$K_p + \frac{K_i}{s} + \frac{K_d s}{1+s/N}$
4	Fractional PID (FPID)	$K_p + \frac{K_i}{s^\lambda} + K_d s^\mu$

To determine the controller parameters, the set of nonlinear equations (4.3)-(4.6) has to be solved. To do so, the optimization toolbox of Matlab can be used to reach out the better solution with the minimum error. More precisely, the function *FMINCON* is able to find the constrained minimum of a function of several variables. It solves problems of the form $\min_x f(x)$ subject to: $C(x) \leq 0$, $C_{eq}(x) = 0$, $x_m \leq x \leq x_M$, where $f(s)$ is the function to minimize; $C(x)$ and $C_{eq}(x)$ represent the nonlinear inequalities and equalities, respectively (non-linear constraints); x is the minimum we are looking for; and x_m and x_M define a set of lower and upper bounds on the design variables, x.

In this particular case, the specification (4.3) will be taken as the main function to minimize, and the rest of specifications, i.e., (4.4)-(4.6), will be taken as constrains for the minimization, all of them subjected to the optimization parameters defined within the function *FMINCON*. The success of this optimization process depends mainly on the initial conditions considered for the parameters of the controller.

Now we give some examples of application of the proposed method for designing robust and stable controllers for switching systems. Specifically, three cases will be considered next for different numbers of design specifications and systems with different numbers of subsystems: the velocity control of a car and the control of a switching system with $L = 4$ given two design specifications, and the velocity control of a servomotor given three design specifications.

Example 4.1. *Velocity control of a vehicle with first order dynamics given two design specifications.*

In [110, 113], we proposed a hybrid model of a vehicle taking into account its different dynamics when accelerating and braking as follows

$$G_1(s) \simeq \frac{4.39}{s + 0.1746}, \tag{4.7}$$

$$G_2(s) \simeq \frac{4.45}{s + 0.445}, \tag{4.8}$$

where G_1 and G_2 refer to the throttle and brake dynamics, respectively.

For the viewpoint of the comfort of car's occupants, phase margin and crossover frequency has to be chosen around 80 deg and 0.8 rad/sec, respectively, in order to obtain a smooth closed-loop response with an overshoot close to 0. Therefore, given two specifications, $N = 2$, and two subsystems, $L = 2$, controllers with three parameters are required to this application. In particular, two different three-parameter controllers are designed: a fractional PI (FPI) and a traditional PID controllers of the forms given in Table 4.1. Solving the set of equations (4.3)-(4.6) for the previous specifications, the parameters of both controllers are:

- FPI: $K_{p_1} = 0.15$, $K_{i_1} = 0.07$, $\alpha = 0.71$;
- PID: $K_{p_2} = 0.1$, $K_{i_2} = 0.11$ and $K_d = 0.223$.

Figure 4.3 shows the frequency response of the controlled car when applying the FPI and PID controllers. As can be seen, the design specifications are fulfilled for both subsystems for both designed controllers –the phase margin obtained with the FPI is even higher than 80 deg. An important issue that should be noticed is that the system controlled with PID has constant magnitude for high frequency, which may cause the system sensitive to high frequency noises and, consequently, instability. The phase difference between the two characteristic polynomials of the closed-loop controlled subsystems for both cases is shown in Fig. 4.4. It is observed that the maximum phase differences are 27.35 and 10.57 deg when using the FPI and PID, respectively, so the controlled system is stable in both cases.

To show the system performance in time domain, a manoeuvre which simulates the car acceleration to 20 km/h and, after that, the braking to 0 km/h –stop completely– for different switching, including a comparison of its velocity for the FPI and PID cases is depicted in Fig. 4.5. As observed in this figure, the car has an adequate performance for

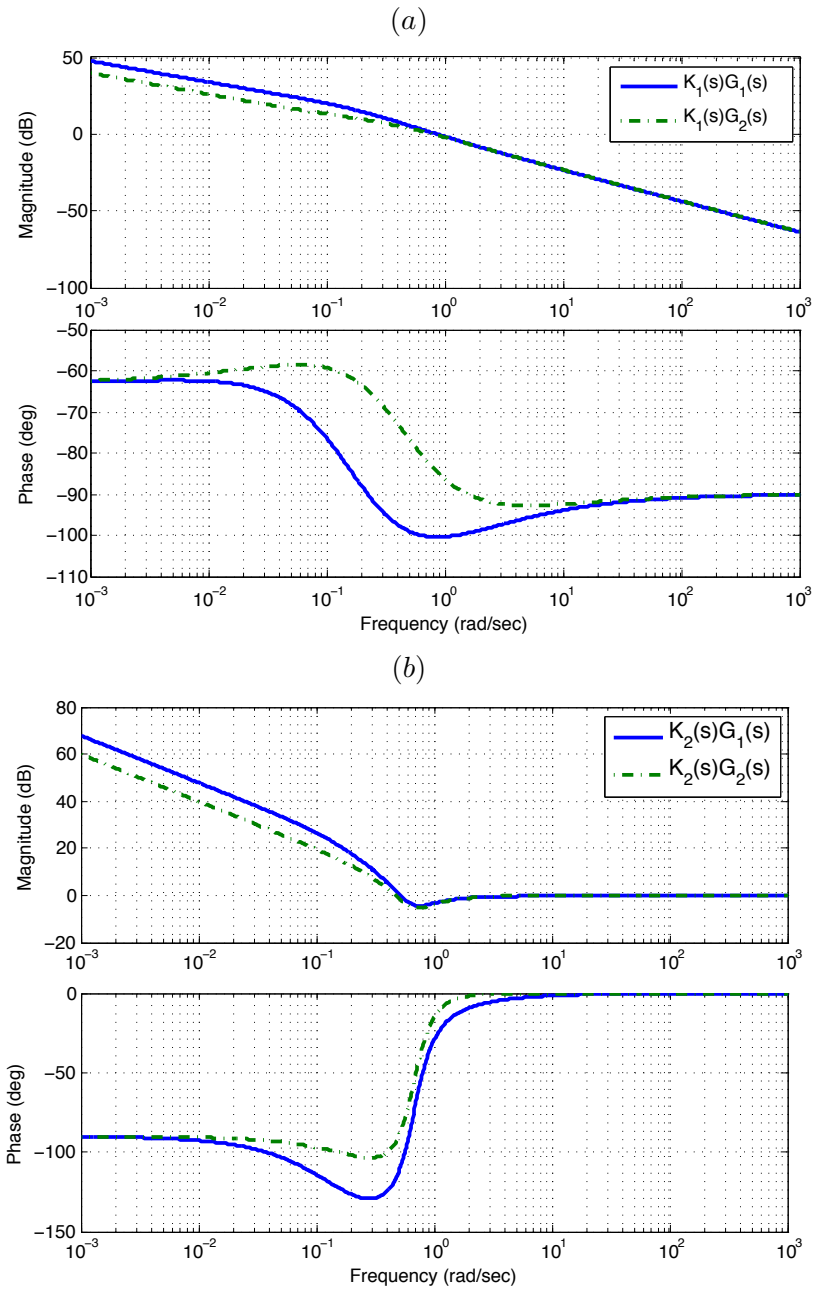

FIGURE 4.3: Bode plots of the controlled system in Example 4.1 when applying: (*a*) FPI (*b*) PID

both the throttle and the brake actions when applying the FPI controller (dash-dotted black line), achieving the reference velocity in a suitable time and without overshoot in both cases. Although both controllers fulfilled the specifications, the response when using the PID (dashed red line) has a considerable high value of overshoot. As a result, it can be said that the occupants' comfort is guaranteed when applying the proposed FPI controller.

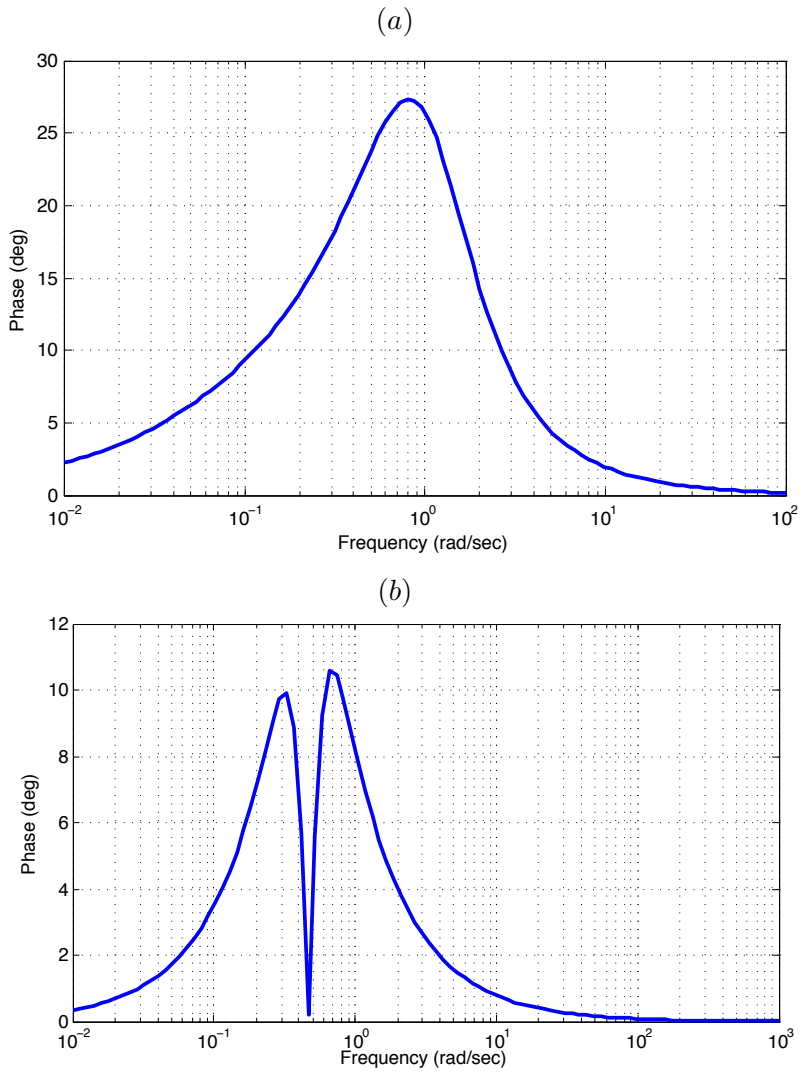

FIGURE 4.4: Phase difference between the two characteristic polynomials of the closed-loop system in Example 4.1 when applying: (*a*) FPI (*b*) PID

Example 4.2. *Control of a switching system with $L = 4$ given two design specifications.*

Now consider a switching system given by:

$$G_1(s) = \frac{1.5}{5s+1}, \tag{4.9}$$

$$G_2(s) = \frac{1.2}{3s+1}, \tag{4.10}$$

$$G_3(s) = \frac{1.1}{2s+1}, \tag{4.11}$$

$$G_4(s) = \frac{1}{s+1}. \tag{4.12}$$

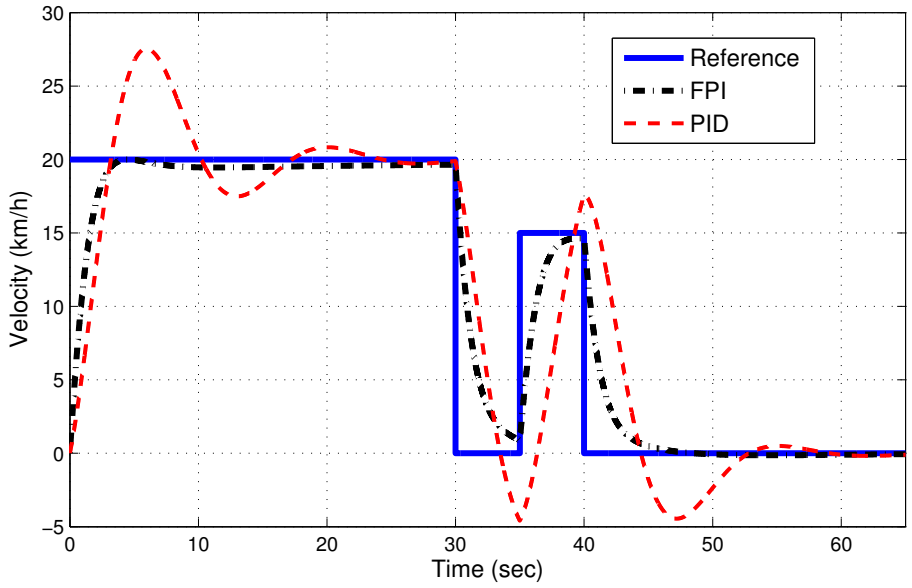

FIGURE 4.5: Time response of the controlled system with both FPI and PID during random switching

The aim is to design a robust controller so that the controlled system is stable during a defined switching – from subsystem 1 to subsystem 2, subsystem 2 to subsystem 3, subsystem 3 to subsystem 4 and vice versa– and has zero steady state error and fast response with settling time less than 2 sec. Equivalently, the design specifications are chosen as a phase margin of 80 deg at 5 rad/sec. Therefore, a five-parameter controller is required, i.e., a fractional-order PID (FPID) of the form given in Table 4.1 will be tuned next. In addition, the three stability conditions to be fulfilled are:

$$|\arg(c_1(j\omega)) - \arg(c_2(j\omega))| < \frac{\pi}{2}, \forall\omega \geq 0, \tag{4.13}$$

$$|\arg(c_2(j\omega)) - \arg(c_3(j\omega))| < \frac{\pi}{2}, \forall\omega \geq 0, \tag{4.14}$$

$$|\arg(c_3(j\omega)) - \arg(c_4(j\omega))| < \frac{\pi}{2}, \forall\omega \geq 0. \tag{4.15}$$

Then, solving the set of equations (4.3), (4.4) and (4.13)-(4.15), the FPID parameters are: $K_p = 10.20$, $K_i = 30.18$, $K_d = 2.80$, $\lambda = 0.83$ and $\mu = 0.47$.

Figure 4.6(a) and 4.6(b) show the Bode plot and the phase difference between each pair of subsystems, respectively. It is obvious that the controlled system fulfilled the design specifications –$\omega_{cp} > 5$ rad/sec and $\phi_m > 80$ deg– and is stable. As can be seen, the worst case corresponds to the first subsystem, but is still within the margin of the

specifications.

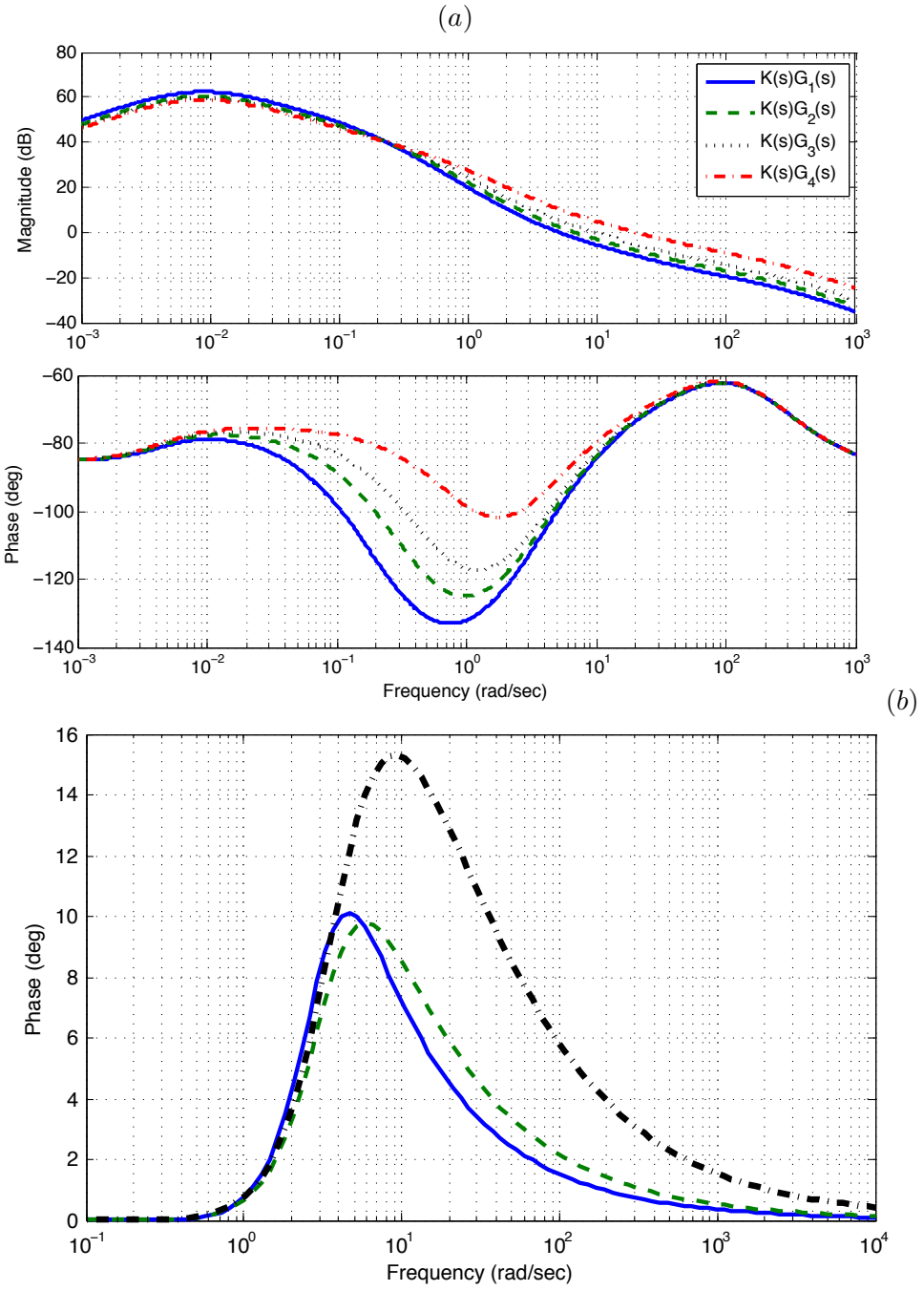

FIGURE 4.6: Simulation result applying FPID in Example 4.2: (*a*) Bode plot of the controlled system (*b*) Phase difference between the each pair of characteristic polynomials of the closed-loop system in Example 4.2: (4.13) –solid line–, (4.14) –dashed line– and (4.15) –dash-dotted line–

In order to show the performance of the system by applying the designed controller, the closed-loop response is simulated for constant and variable references, as shown in Fig. 4.7. It can be observed that all the subsystems fulfill the settling time less than 2 sec.

Example 4.3. *Velocity control of a servomotor given three design specifications.*

Let us now consider the velocity of a servomotor described by:

$$G_1(s) = \frac{0.55}{62s+1}, \tag{4.16}$$

$$G_2(s) = \frac{0.55}{100s+1}, \tag{4.17}$$

where dynamics (4.16) corresponds to the normal servomotor dynamics and dynamics (4.17) may be caused when the brake is activated ([95]). In this example, we will design a controller using specifications of phase margin, gain crossover frequency and output disturbance rejection as follows: $\phi_m = 80$ deg at $\omega_{cp} = 0.6$ rad/sec and a desired value of the sensitivity function of $M = -20$dB for frequencies less than 0.1rad/sec. Among all four-parameter controllers, a PID with noise filter (NPID) of the form in Table 4.1 is chosen. Then, solving the set of four equations, the parameters of the controller are: $K_p = 81.35$, $K_i = 35.195$, $K_d = 95.71$, $N = 19.86$.

The fulfillment of the design specifications and stability is proved by Fig. 4.8(a), 4.8(b) and 4.9, which represent the Bode plot, phase difference of closed-loop polynomials and sensitivity function, respectively. Finally, Fig. 4.10 shows the time response of the controlled system for variable reference. It can be observed that its performance is adequate, even during switching.

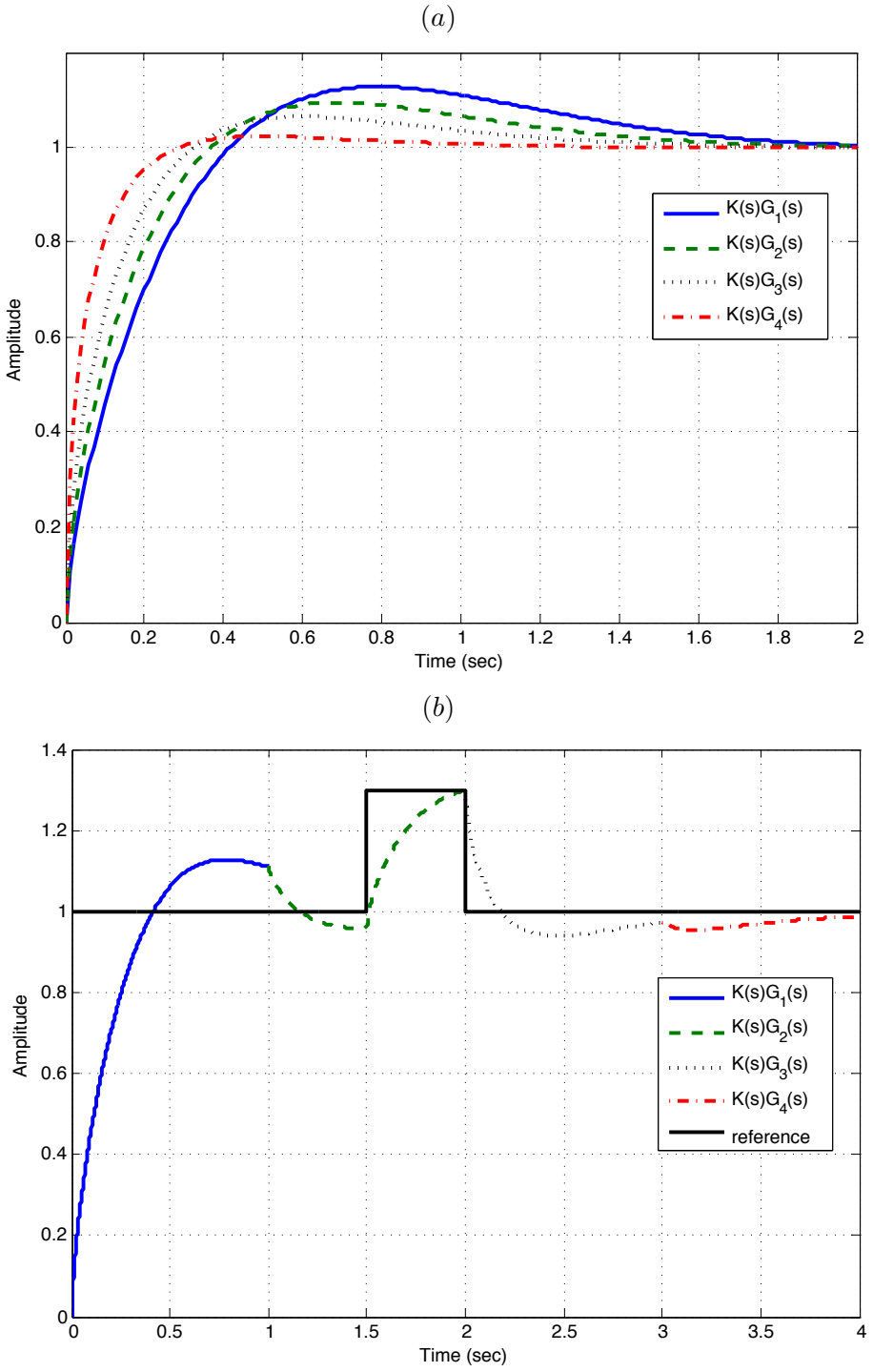

FIGURE 4.7: Step response of system in Example 4.2 (a) constant reference (b) variable reference. Each colour is related to the subsystem which is activated which shows the controller maintain its stability during the switching

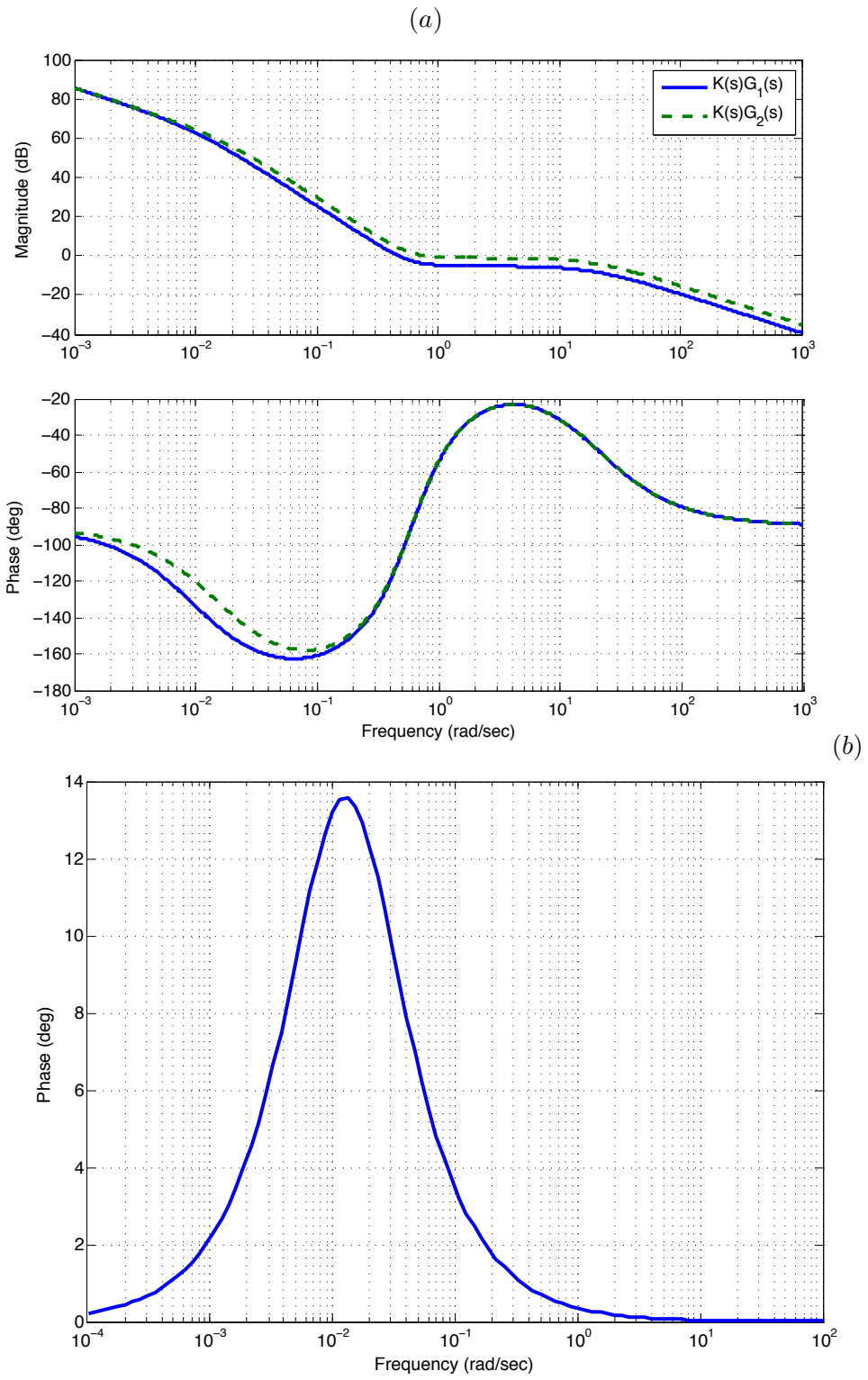

FIGURE 4.8: Simulation result applying NPID in Example 4.3: (a) Bode plot of the controlled system (b) Phase difference of characteristic polynomials of the closed-loop system

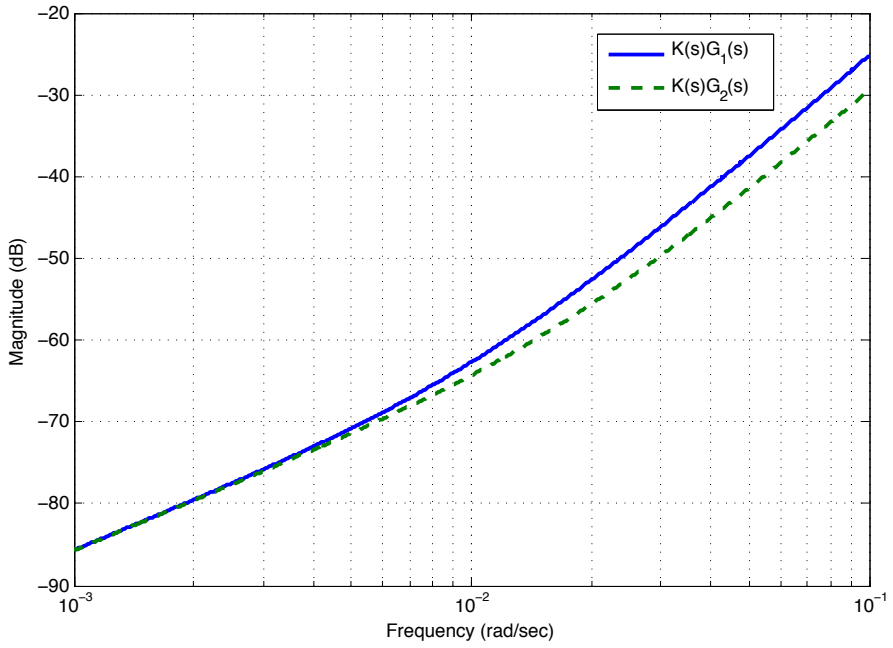

FIGURE 4.9: Sensitivity function S in Example 4.3

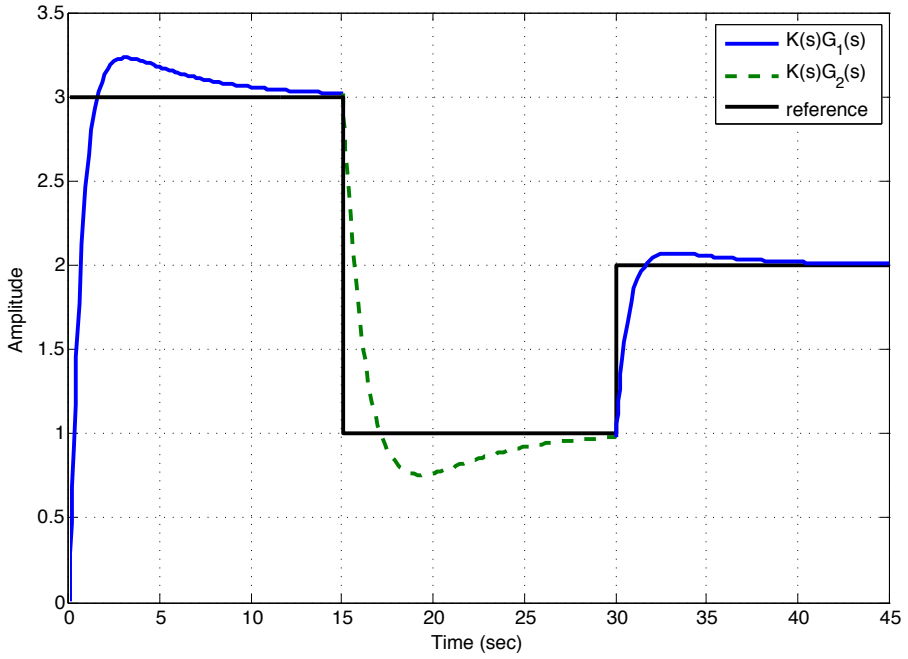

FIGURE 4.10: Step response of system in Example 4.3 for variable reference

4.2 Advanced Reset Control: A Comparative Study

Currently, reset control focuses on using structures which allow new resetting rules in order to avoid Zeno solutions to be caused and improve the performance of the system. This section investigates the properties of some modified reset strategies which reset controller states to fixed or variable nonzero values and are able to eliminate or reduce the overshoot in first and higher order systems, respectively. Based on them, a general advanced reset control is proposed with both fixed and variable resetting to nonzero values. A comparative study between advanced and modified reset strategies is given in order to show their benefits in terms of prevention of Zeno solutions and reduction of overshoot. As a result, some guidelines is considered for the design of such controllers depending on the application are offered.

Given this context, in this section we study the particular features of different reset control strategies, of integer and fractional order, to improve the performance of a system, especially in terms of prevention of Zeno solutions and traditional time domain specifications. The main objective is to continue the investigation on different resetting rules and provide the reader a comparative study which may help to make a decision of using a reset structure. The contribution of this section is twofold: (1) propose a more general reset structure which combines the features of the modified reset controllers, which will be referred to as advanced reset control, and (2) provide some guidelines for designing such controllers depending on the application.

4.2.1 Properties of the Reset Controllers

In this section, fundamentals of the reset CI and FORE controllers are given and, then, compared with FCI.

4.2.1.1 FORE and Clegg Integrator

FORE is a simple reset compensator with a first order base compensator given by

$$FORE(s) = \frac{K}{s+b}. \tag{4.18}$$

For a given system its describing function (DF) is calculated as the ratio between the fundamental component of its sinusoidal response and the sinusoidal input. Suppose $y(t)$ is the response of the reset compensator to the sinusoidal input $e(t) = A\sin(\omega t)$ the DF of the system can be defined as:

$$N(A,\omega) = \frac{2j\omega}{\pi A}\int_0^{\pi} y(t)e^{-j\omega t}dt. \tag{4.19}$$

Applying (4.19) the DF of the FORE system is obtained as follows [28, 44]:

$$N(A,\omega)_{FORE} = \frac{K}{b+j\omega}\left(1 + j\frac{2\omega^2\left(1+e^{-b\frac{\pi}{\omega}}\right)}{\pi\left(b^2+\omega^2\right)}\right), \tag{4.20}$$

and substituting $b = 0$ and $K = 1$ in (4.20) yields the DF for the CI:

$$N(A,\omega)_{CI} = \frac{4}{\pi\omega}\left(1 - j\frac{\pi}{4}\right), \tag{4.21}$$

Therefore, it is clear that CI gives a phase lead of almost 52° with respect to an integrator (it also increases the gain with a factor of about 1.62). Figure 4.11 shows this fundamental property of the CI and FORE through the Nichols diagram, that is, the achievement of a phase lead up to 52° with respect their base linear compensator.

4.2.1.2 Fractional-Order Clegg integrator (FCI)

FCI was firstly proposed in [132]. It has been shown that it can have a tunable phase lag and its DF can be represented as:

$$N(A,\omega)_{FCI} = \frac{4}{\pi\omega^{\alpha}}\left(\sin\left(\alpha\frac{\pi}{2}\right) + \frac{\pi}{4}e^{-j\alpha\frac{\pi}{2}}\right), \tag{4.22}$$

Figure 4.12 compares the phase difference between both the FCI (solid line) and the FI (dotted line) with respect to the integer-order linear integrator (II) for different values of the order α. As observe, the phase lag depends on the value of α for both cases, but is always higher when using the FCI for $\alpha < 1$. In particular, when $\alpha = 1$, the phase difference between the FCI and the II is about 52° (actually, the FCI is the CI) and 0 for the other case. Note that this phase difference can be viewed as the phase margin to be added to the system. Taking into account the better performance of the FCI against the FI, we will focus on the FCI in this section.

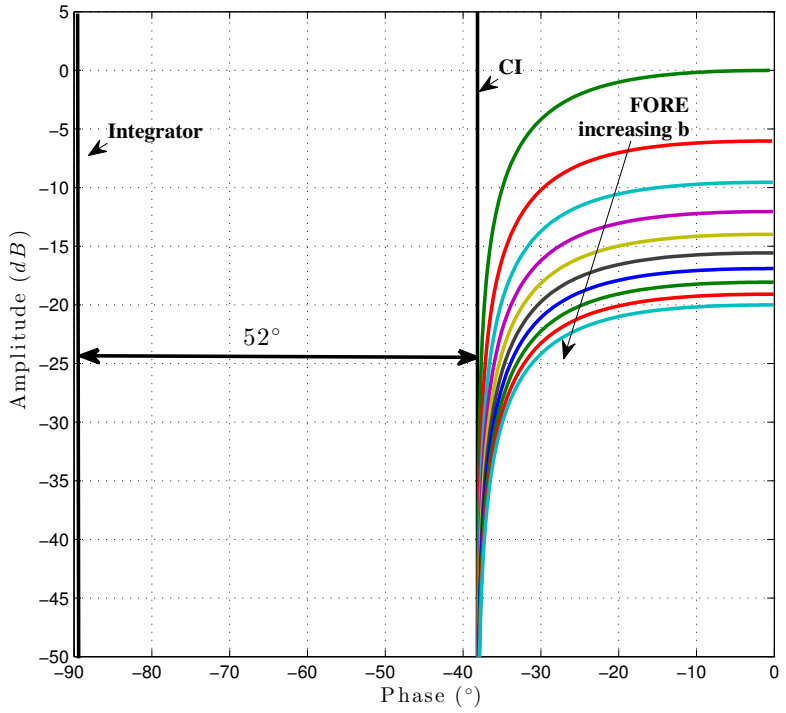

FIGURE 4.11: Nichols chart of FORE and CI with respect to the classical integrator

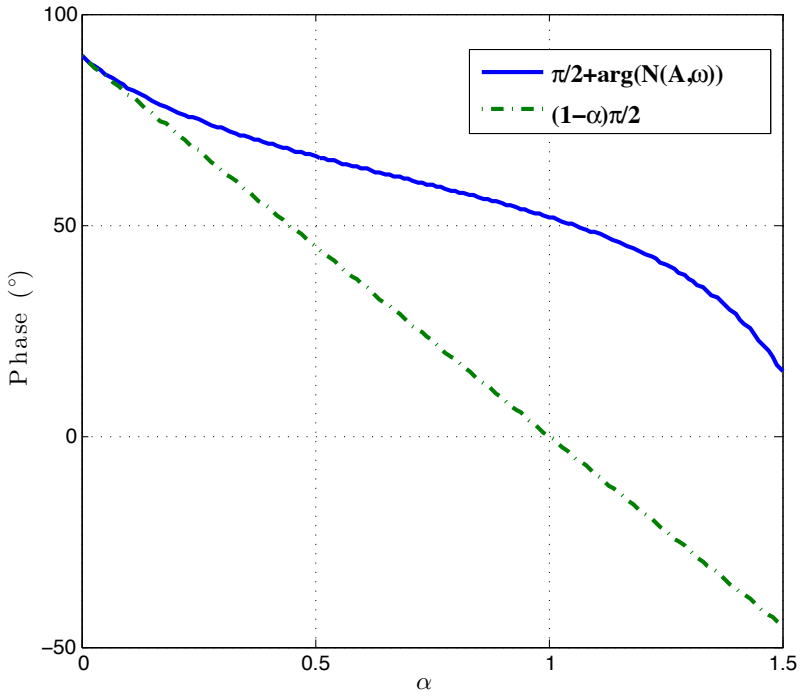

FIGURE 4.12: Phase difference between both the FCI and the FI in comparison with integer-order linear integrator (II). (FCI *vs* II: $\frac{\pi}{2} + \arg(N(A,\omega)_{FCI})$), FI *vs* II: $(1-\alpha)\frac{\pi}{2}$)

Example 4.4. *Comparing different rest controllers to reduce the overshoot*

One of the motivation of using reset control is to reduce the overshoot in a step response. For example, consider the same feedback system as in [45] where the loop transfer function and controller are

$$P(s) = \frac{1}{s^2 + 0.2s}, \tag{4.23}$$

and

$$C(s) = s + 1, \tag{4.24}$$

respectively. The system shows the 70% of overshoot and the aim is to design the different reset controller to reduce the overshoot. In [45] used a FORE with $b = 1$ and reduced the overshoot to about 40%. In this example, this method is compared with CI, FI and FCI. Fractional-order parameter in FCI and FI is set as $\alpha = 0.5$.

The simulation results is shown in Fig. 4.13. As it can be seen, the CI has the 41% of overshoot a bit more than FORE but faster response. The FI as it is was expected has the worse response– almost no improvement in reducing the overshoot but the FCI has the best response which reduce the overshoot to around 19%. It should be commented that there are other ways to reduce the overshoot but as it is mentioned before, it may cause the limitation in the response and the aim in this particular example was obtaining faster response lower overshoot at the same time.

4.2.2 Modified Reset Controllers

This section recalls the formulations and main properties of different modified reset controllers reported in the literature to avoid the occurrence of Zeno solutions. In particular, the following reset strategies will be summarized:

1. Improved reset control: an optimized reset controller which resets to a nonzero value periodically.

2. PI+CI reset control: a combination of linear and reset PI which leads the system to reset to a nonzero value.

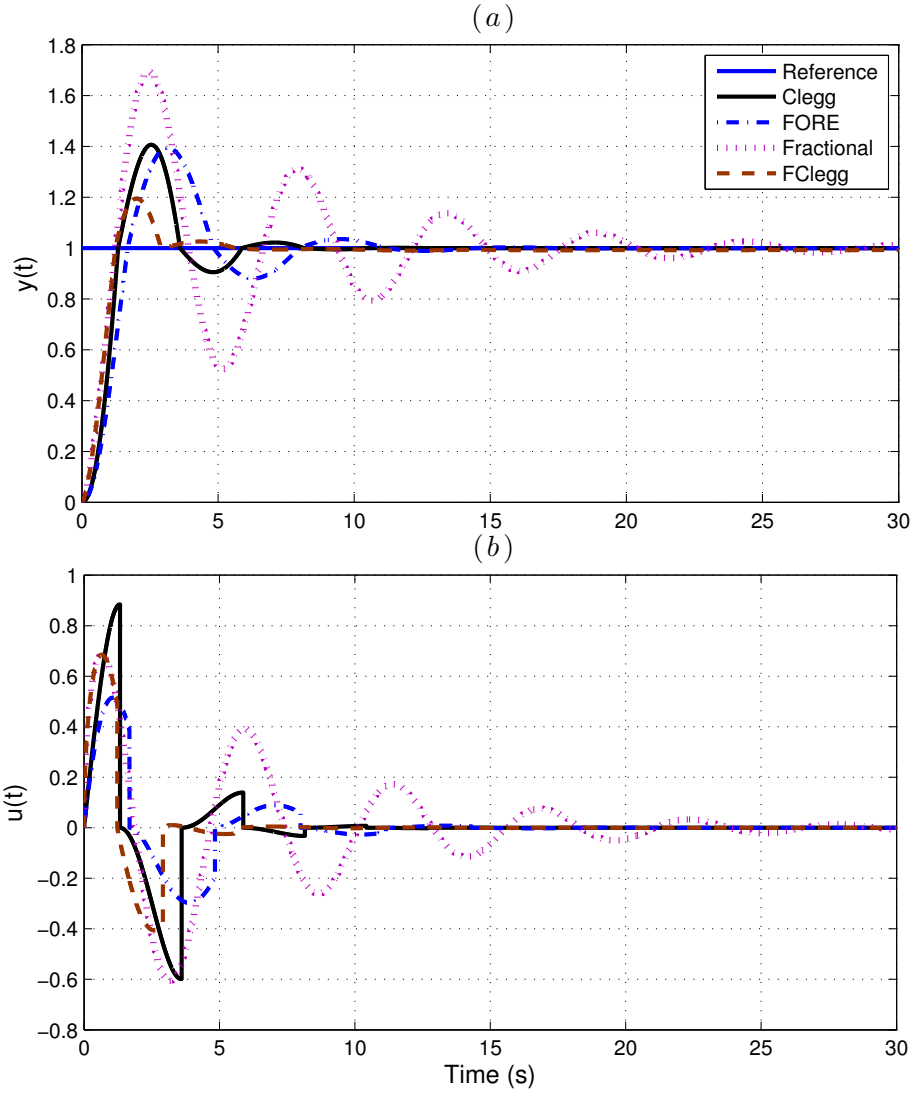

FIGURE 4.13: Comparing the response of the system with different reset controller (*a*) time response, (*b*) control input

3. Reset control with feedforward: combines classic reset with feedforward control and is capable of resetting to DC gain of the system.

It is important to mention that all these controllers can be useful to avoid such problems but, depending on the application, one of them may show better performance in comparison with the other. That discussion will be addressed in Section 4.2.6 through several examples. Firstly, let us to formulate the dynamics of reset control systems.

4.2.2.1 Improved reset controller

In [48, 49], the authors studied a reset controller, called improved reset controller, where its states are reset to certain nonzero values, which makes the system response be even faster in comparison with the linear solution. It can be represented as follows:

$$\begin{aligned} \dot{x}_r &= A_r x_r + B_r e, \ t \neq t_k \\ x_r(t_k^+) &= E_k x_p + F_k x_r + G_k r, \ t = t_k \\ u_r &= C_r x_r + D_r e \end{aligned} \tag{4.25}$$

The main idea of this controller is to let free its after-reset state $x_r(t^+)$ (not necessarily equal to zero) and compute it and its parameters E_k, F_k, G_k, C_r and D_r in order to minimize a quadratic performance function of the form:

$$J_k = e^T(t_{k+1})P_0 e(t_{k+1}) + \dot{e}^T(t_{k+1})Q_0\dot{e}(t_{k+1}) + \int_{t_k}^{t_{k+1}} e^T(s)P_1 e(s)ds$$

where P_0, Q_0 and P_1 are weighting vectors.

4.2.2.2 PI+CI controller

In [50, 51, 131], a PI+CI controller was used to reduce considerably both the percentage of overshoot and the settling time by resetting only a percentage of the integral term of a PI controller, namely P_{reset}. Its transfer function is given by

$$R(s) = k_p\left(1 + \frac{1 - P_{reset}}{\tau_i s} + \frac{P_{reset}\text{CI}}{\tau_i}\right), \tag{4.26}$$

where k_p is the proportional gain and τ_i is the integral time constant. It can be written in state space of the form of (3.37) with $\alpha = 1$, $A_r = 0$, $B_r = \begin{bmatrix} 1 \\ 1 \end{bmatrix}$, $A_{R_r} = \begin{bmatrix} 1 & 0 \\ 0 & 0 \end{bmatrix}$, $C_r = \begin{bmatrix} 0 & \frac{k_p}{\tau_i} \end{bmatrix}$, $D_r = k_p$.

4.2.2.3 Reset controller with feedforward

A feedforward controller is combined together with a traditional reset controller in [52, 53], as shown in Fig. 4.14. In order to avoid Zeno solutions, K should be chosen

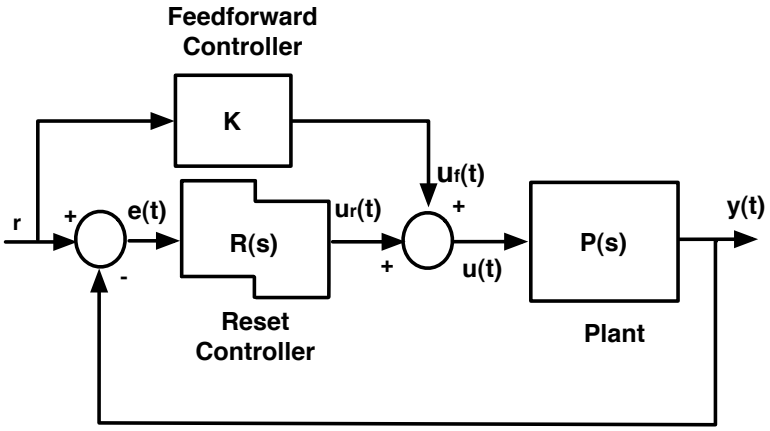

FIGURE 4.14: Block diagram of modified reset control

as DC gain of the system, i.e.,

$$K = \begin{cases} -\frac{1}{C_p A_p^{-1} B_p}, & \text{if } A_p \text{ is invertible} \\ 0, & \text{otherwise} \end{cases} \tag{4.27}$$

In classic reset control, controller resets to zero when error is zero. Therefore, the feedforward controller adds $u = Kr = \frac{1}{P(0)} r$ to classic reset controller. As mentioned above, resetting to zero may cause Zeno solutions, but it can be eliminated by resetting to Kr –a nonzero value. Actually, this feature is also common to improved reset and PC+CI controllers; all these three controllers will force the system to reset to Kr. More precisely, in improved reset control, the controller parameters should be tuned to minimize x_r, which is not possible unless

$$\lim_{t \to \infty} u_r = Kr. \tag{4.28}$$

This condition was not proven in [48, 49] but can be stated from the experiment. This condition is satisfied in PC+CI by a linear integrator and, in the reset controller with feedforward, by the feedforward gain K.

4.2.3 Fractional-Order Proportional-Clegg Integrator

As another solution to eliminate Zeno solution, we consider a FPCI , where an FCI was used instead of classic CI. A fractional order reset controller in general can be

represented in state space by (3.37), where α is the (non-integer) order of the system. The state space representation of FPCI can be obtained by substituting $A_r = 0$, $B_r = 1$, $A_{R_r=0}$, $C_r = \frac{k_p}{\tau_i}$ and $D_r = k_p$ in (3.37).

Assume the transfer function and DF of FPCI given, respectively, by:

$$R(s) = K_p + \frac{K_i}{FCI^{\alpha}}, \tag{4.29}$$

$$N(A,\omega)_{FPCI} = K_p + \frac{4K_i}{\pi\omega^{\alpha}}\left(\sin\left(\alpha\frac{\pi}{2}\right) + \frac{\pi}{4}e^{-j\alpha\frac{\pi}{2}}\right). \tag{4.30}$$

As commented, the key feature of this FPCI is to tune α to achieve an optimized system performance, as will be shown.

Let us consider the transient response output waveform of a FCI for a sinusoidal input for different values of its order α (see Fig. 4.15). For the integer-order case (CI, $\alpha = 1$), a symmetrical waveform can be observed. On the contrary, the fractional-order cases results in asymmetrical responses. On the other hand, the integer-order response shows that reset occurs when the output is in almost its maximum value, whereas reset for the fractional-order ones takes places at another point different to the maximum value. Accordingly, when applying the integer-order CI, Zeno solution happens but, the asymmetrical response of FCI control signal may help to be avoid Zeno solution.

For a better illustration of this fact, let us consider a system $P(s)$ controlled by $R(s)$ with the following transfer functions:

$$P(s) = \tfrac{1}{2s+1},$$
$$R(s) = 1 + \tfrac{20}{\mathrm{FCI}^{\alpha}}.$$

Figure 4.16 shows the output, control signal and phase portrait of the controlled system for different values of α, $0.5 \leq \alpha \leq 1$. It can be observed that the oscillation only occurs when $\alpha = \{0.9, 1\}$. In the rest of the cases, the system response reaches the reference value. As shown in Fig. 4.16(a), the controller resets at about the maximum of the control signal and continues resetting with the same shape and amplitude for the case of $\alpha = \{0.9, 1\}$. However, when $\alpha = \{0.5, 0.7\}$, the controller resets at a point of the control signal lower than the maximum value and no oscillation occurs. Therefore, it is

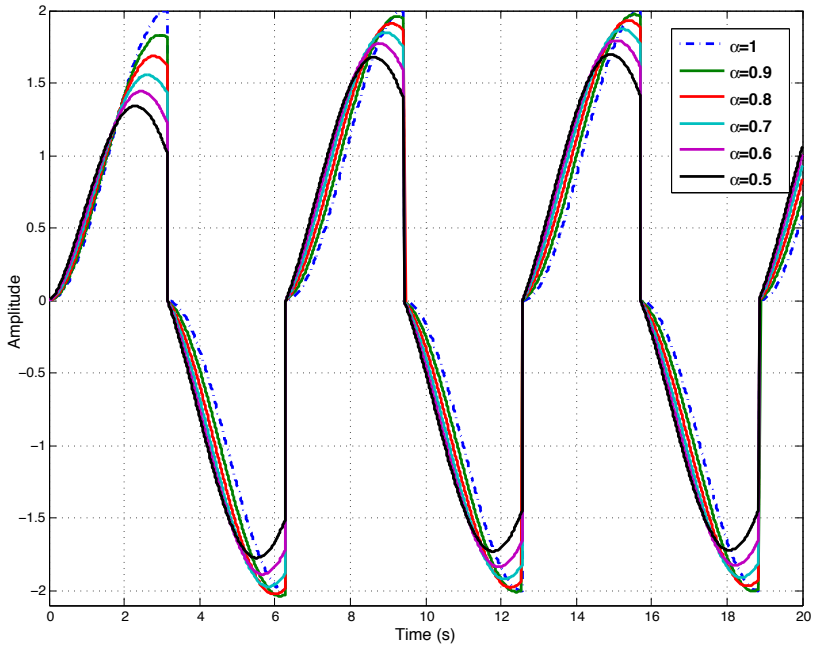

FIGURE 4.15: Output waveform corresponding to a FCI for different values of α

possible to avoid limit cycles, and consequently, to remove the permanent oscillation, tuning α accordingly.

It is worth mentioning that different specifications can be met to design the controller, depending on the particular requirements of the application. As an example, specifications related to phase margin and gain crossover frequency are going to be considered to obtain the values of K_p and K_i in Section 6.2.1. To this respect, DF (4.30) will be used. Likewise, the fractional-order α will be searched to have no oscillation.

4.2.4 Fractional-Order PI+CI

So far we have seen, FCI integrator can increase the phase lag of the system and on the other hand PI+CI can be used to avoid the Zeno solution. Therefore, we study a fractional-order PI+CI (PI$^\alpha$+CI$^\alpha$) which can be represented as:

$$R(s) = k_p \left(1 + \frac{1 - P_{reset}}{\tau_i s^\alpha} + \frac{P_{reset}\text{FCI}}{\tau_i}\right), \tag{4.31}$$

where k_p is the proportional gain and τ_i is the integral time constant. It can be written in state space of the form of (3.37) with $A_r = 0$, $B_r = \begin{bmatrix} 1 \\ 1 \end{bmatrix}$, $A_{R_r} = \begin{bmatrix} 1 & 0 \\ 0 & 0 \end{bmatrix}$,

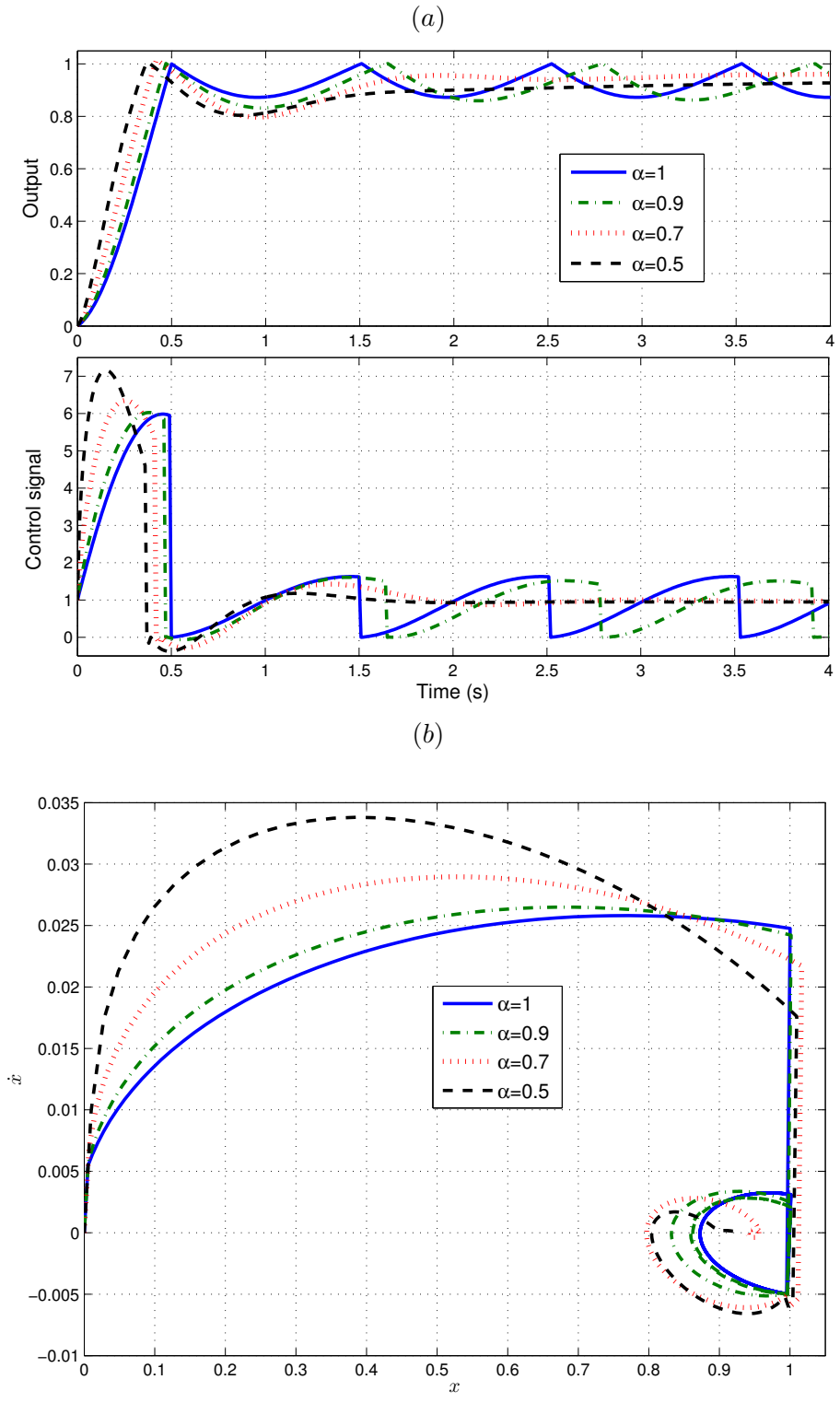

FIGURE 4.16: Simulation results of the controlled system (4.31) for different values of the order α of FCI: (a) Output and control signal (b) Phase portrait (x is the output of the system)

$C_r = \begin{bmatrix} 0 & \frac{k_p}{\tau_i} \end{bmatrix}$, $D_r = k_p$. Describing function of F(PI+CI) is simply given by,

$$F(PI + CI)(j\omega) = kp \left(1 + \frac{1 - P_{reset}}{\tau_i (j\omega)^{\alpha}} + \frac{P_{reset}}{\frac{4\tau_i}{\pi\omega^{\alpha}} \left(\sin\left(\alpha\frac{\pi}{2}\right) + \frac{\pi}{4} e^{-j\alpha\frac{\pi}{2}} \right)} \right), \tag{4.32}$$

In Fig. 4.17(a) and 4.17(b) are showing the describing functions of a PI+CI for several values of the reset ratio preset and PI$^{\alpha}$+CI$^{\alpha}$ compensator for several fractional-order when $P_{reset} = 0.5$, respectively. Figure 4.17(a) shows that PI+CI in comparison with its base PI compensator, allows achieving both a bigger phase margin and a crossover gain frequency. On the other hand, comparing F(PI+CI) when $Preset = 0.5$ with PI compensator also shows the bigger phase margin and a crossover gain frequency (see Fig. Fig. 4.17(b)). Therefore, at the same time using the lower value of α and the lower value of P_{reset}, will result on the system with the bigger phase margin and and a crossover gain frequency. This means that a better performance both in terms of speed of response and relative stability can be obtained by means of PI$^{\alpha}$+CI$^{\alpha}$ compensation, overcoming Zeno problem and obtaining better performance than PI+CI.

4.2.5 Advanced Reset Control

This section presents the main results: the introduction of a general advanced SISO reset control with both fixed and variable resetting to nonzero values.

Taking into account the features of the modified reset control, we can conclude to the following general fractional order reset controller –henceforth referred to as advanced reset controller– where its state is reset to Kr when error crosses zero, which can be represented as

$$\begin{aligned} D^{\alpha} x_r(t) &= A_r x_r(t) + B_r e(t), \ e(t) \neq 0, \\ x_r(t^+) &= A_{R_r} x_r(t) + \tfrac{K}{n_{\mathcal{R}} c_r} B_{R_r} r, \ e(t) = 0, \\ u_r(t) &= C_r x_r(t) + D_r e(t), \end{aligned} \tag{4.33}$$

where matrix $A_{R_r} \in \mathbb{R}^{n_r \times n_r}$ identifies that subset of states $x_r(t)$ that are reset (the last $\mathcal{R}$ states) and has the form $A_{R_r} = \begin{bmatrix} I_{n_{\bar{\mathcal{R}}}} & 0 \\ 0 & 0_{n_{\mathcal{R}}} \end{bmatrix}$, $B_{R_r} = \begin{bmatrix} 0 \\ 1 \end{bmatrix}$, $C_r = c_r \begin{bmatrix} 0 & 1 \end{bmatrix}$ with $n_{\bar{\mathcal{R}}} = n_r - n_{\mathcal{R}}$, $c_r \in \mathbb{R}$. And I and 0 denote identity and zero matrices with proper dimension, respectively.

Meticulously, controller (4.33) is a reset control with feedforward where its feedforward part becomes active when the first time error crosses zero. Actually, it activates the feedforward gain when it is necessary which is the first reset time in order to avoid Zeno solution. Therefore, the advanced reset controller unlike the reset controller with feedforward maintaines the same rise time as the classic controller.

Let us denote the transfer function of the base controller of the reset as $R_{base}(s)$. According to Fig. 4.14, in presence of the error the closed-loop transfer function of the system controlled by the reset controller with feedforward and advanced reset controller are,

$$\frac{(K + R_{base}(s))P(s)}{1 + R_{base}(s)P(s)}. \tag{4.34}$$

and

$$\frac{R_{base}(s)P(s)}{1 + R_{base}(s)P(s)}. \tag{4.35}$$

respectively. Comparing (4.35) and (4.35) with the transfer function of a classic controller (controller with no reset), it is obvious that the advanced reset controller (but not the reset controller with feedforward) preserves some specification of the classic controller like rise time.

Likewise, this controller can be reshaped to reset periodically when $t = t_k$, similarly to the improved reset controller, which will lead us to a more general advanced reset controller as follows:

$$\begin{aligned} D^{\alpha}x_r(t) &= A_r x_r(t) + B_r e(t),\ t \neq t_k, \\ x_r(t_k^+) &= A_{R_r} x_r(t) + B_{R_r}\left(\tfrac{Kr - D_r e(t_k)}{n_{\mathcal{R}} c_r}\right),\ t = t_k, \\ u_r(t) &= C_r x_r(t) + D_r e(t). \end{aligned} \tag{4.36}$$

Due to the fact that reset happens periodically, and not necessarily when error is zero, it should take place to a variable nonzero value, which is function of both DC gain of the system and error.

4.2.6 Examples and Discussion

This section gives some examples of application of the aforementioned advanced and modified reset controllers for first and second order systems. It also provides a comparative simulated study and some guidelines to be considered for designing reset controllers depending on the application.

4.2.6.1 First order systems

In this first example, PI+CI, advanced reset and FPCI strategies are going to be compared for a first order system. Let us consider the system [28]

$$\begin{aligned} \dot{x}_p &= -0.5x_p + 1.5u \\ y &= x_p \end{aligned}, \tag{4.37}$$

whose transfer function is $P(s) = \frac{1.5}{s+0.5}$, controlled by a PI+CI of the form of (4.26) with $k_p = 2$, $\tau_i = 0.15$, and $P_{reset} = 0.21$. Now, consider controller (4.33) in which the reset controller is a proportional-CI (PCI) with resetting to $K = \frac{1}{P(0)}$. Thus, it can be rewritten as

$$\begin{aligned} \dot{x}_r(t) &= e(t), \ e(t) \neq 0, \\ x_r(t^+) &= \tfrac{\tau_i}{k_p P(0)} r, \ e(t) = 0, \\ u_r(t) &= \tfrac{k_p}{\tau_i} x_r(t) + k_p e(t). \end{aligned} \tag{4.38}$$

With respect to FPCI, parameters of PI are chosen equal to the PI+CI case. On one hand the lower fractional-order the higher ability to avoid the Zeno solution and on the other hand the lower fractional-order causes larger settling time so that, setting the fractional-order parameter α to 0.9 would be a trade off to overcome Zeno solution and settling time problem at the same time.

Simulation results are shown in Fig. 4.18 when applying the PI and PCI controller in (a) and using PI+CI, advanced reset controller and FPCI in (b). As observe in Fig. 4.18(a), PI and PCI cause a undesirable overshoot and Zeno solutions, respectively. In Fig. 4.18(b), it can be seen that the three controllers avoid the occurrence of Zeno solution.

Moreover, PI+CI and FPCI controllers reduce the overshoot considerably, whereas advanced reset control eliminate completely it. Taking into account the control signals, on the one hand, the system output tends to $K = 0.33$ when $t \to \infty$ when applying PI controller. On the other, the PCI always resets to zero (when error is zero) which causes the Zeno solution. This problem is solved in PI+CI by adding a linear integrator to the PCI and in the FPCI and the advanced reset controller, by using a FCI which will allow to reset to nonzero values. It can be observed that the control signal with the advanced reset controller reaches 0.33 after the first reset and, consequently, the overshoot is removed. For the PI+CI, the overshoot is reduced a bit. The FPCI cause an undershoot in the system response, which is significantly lower than the overshoot of PI+CI and PI controllers.

Fig. 4.19 compares the output response and control signal of PI^α+CI^α for several value of α. As it can be observed the lower fractional-order lead us to the better performance, i.e. less overshoot and faster response.

4.2.6.2 Second order systems

This example firstly compares advanced reset controller with two of the modified reset controllers –controller with feedforward and improved reset controller– and, then, advanced and reset controllers with variable resetting for second order systems. Thereafter, different fractional-order advanced reset controller is compared to show the performance of the fractional-order controller to reduce the overshoot.

Let us now consider the dynamics of a micro-actuator plant described by [48, 49]:

$$\begin{aligned} \dot{x}_{p_1} &= x_{p_2}, \\ \dot{x}_{p_2} &= -a_1 x_{p_1} - a_2 x_{p_2} + bu, \\ y &= x_{p_1} \end{aligned} \tag{4.39}$$

where x_{p_1}, x_{p_2} are position and velocity of the moving stage with $a_1 = 10^6$, $a_2 = 1810$, and $b = 3{\times}10^6$. This system can be also given by its transfer function $P(s) = \frac{b}{s^2+a_2 s+a_1}$. Consider a reset controller with a PI as base linear controller and a periodic reset action,

so:

$$\begin{aligned} \dot{x}_r &= e, \ t \neq t_k \\ x_r(t_k^+) &= E_1 x_{p_1} + E_2 x_{p_2} + Gr, \ t = t_k, \\ u &= \frac{k_p}{\tau_i} x_r + k_p e \end{aligned} \tag{4.40}$$

with $k_p = 0.08$ and $\tau_i = \frac{8}{3} \times 10^{-4}$. The optimization function J_k was minimized with the following parameters: $P_0 = 2.1, Q_0 = 10^{-6}$, and $P_1 = 0$. The reset time interval $\bigtriangledown t_k = t_k - t_{k-1}$ was fixed to 1 ms. Then, the optimal solution is given by the constant matrices $E_1 = -2.8 \times 10^{-4}$, $E_2 = -6.8 \times 10^{-7}$, and $G = 0.0014$. For the advanced controller (4.38), similar values were used with $\alpha = 1$.

Comparing advanced reset controller, reset controller with feedforward with improved reset controller (4.40), all these three controllers reset to nonzero values. In particular, improved reset controller will reset to $\frac{k_p}{\tau_i}(E_1 x_{p_1} + E_2 x_{p_2} + Gr) + k_p e$. As time tends to infinity, the states x_{p_1} and x_{p_2} and error tend to r, 0 and 0, respectively. Therefore, the control signal u_r tends to $\frac{k_p}{\tau_i}(E_1 + G)\, r = 0.336$, which is very close to the feedforward gain for the unit step input, i.e., $K = \frac{1}{P(0)} = 0.333$. Likewise, improved reset controller resets when $t = t_k$ at each 1 ms, whereas advanced reset controller and reset controller with feedforward reset when $e = 0$.

The step responses and control signals when applying reset controller with feedforward, improved and advanced reset controller are shown in Fig. 4.20. The performance of the system using a PI and a PCI were also obtained. As expected, improved reset, reset controller with feedforward and advanced reset controller are able to eliminate the Zeno solution caused by PCI, and this is because of the control signals reach the steady state value K. Fig. 4.21 compares advanced factional order control for different values of α. It can be seen that the higher the value of α, the lower the overshoot but the slower the response, so that a trade of between an integer and a fractional order advanced reset controller (in this case $\alpha = 1.1$) may be a good way to overcome both Zeno solutions and overshoot at the same time.

The feedforward gain in reset controller with feedforward, the fractional order CI in FPCI cause different rise time in comparison with the classic PI controller. Unlike the improved reset controller and feedforward reset controller, the other introduced controller i.e. PCI, PI+CI and advanced reset controller have similar base controller as classic PI controller which make the system similar rise time. In addition, the

overshoot is reduced when applying advanced reset, and it is completely eliminated with improved reset since it resets periodically before error reaches zero.

Now, let us combine the advanced reset controller and improved reset controller (4.33) in the simplest way to have an advanced reset control with periodic resetting with the following parameters: $\alpha = 1$, $n_{\mathcal{R}} = 1$, $A_r = 0$, $B_r = 1$, $c_r = C_r = \frac{k_p}{\tau_i}$ and $D_r = k_p$. Simulation results using this advanced and improved controllers are illustrated in Fig. 4.22 for $t_k = 1$ ms. It can be seen that advanced reset controller with periodic resetting can even reduce the overshoot obtained with the same controller but resetting when error is zero.

4.2.6.3 Discussion

Taking into account the examples, the following remarks can be stated:

1. Improved reset controller, PC+CI, FPCI, reset controller with feedforward and advanced reset controller are useful strategies to avoid the occurrence of Zeno solutions.

2. A reset controller can avoid the occurrence of Zeno solutions when its control signal reaches a value equal to the inverse of the DC gain of the system multiplied by input.

3. Advanced reset controller and reset controller with feedforward show the best performance for first order systems and are capable of eliminating the overshoot completely.

4. It is recommended the use of advanced reset controller with periodic reset and improved reset control to reduce the overshoot for higher order systems, due to the ability to switch when error is not necessarily zero. Advanced reset control of fractional order can be another choice to reduce the overshoot in such systems.

5. Despite the high ability of the improved reset controller in reducing the overshoot, its design is complicated due to the required optimization process. However, applying the idea of periodic resets of improved reset control to advanced reset control will lead us to a simpler and more useful controller –controller (4.36).

6. In advanced reset control, the feedforward controller is active when the first reset happens. This feature makes this controller different from the one with feedforward, in which the feedforward controller is always on the loop. This fact causes the base controller to be different from classic controllers: the rising time of the reset controller is different from the obtained by the classic one. Improved reset control due to its periodic reset also does not preserve the rise time of the classic controller.

7. In order to design a controller to have a response of a first order system with no overshoot and in a certain rising time, two steps are required: (i) tune the base controller to obtain a certain rise time, and (ii) apply advanced reset control.

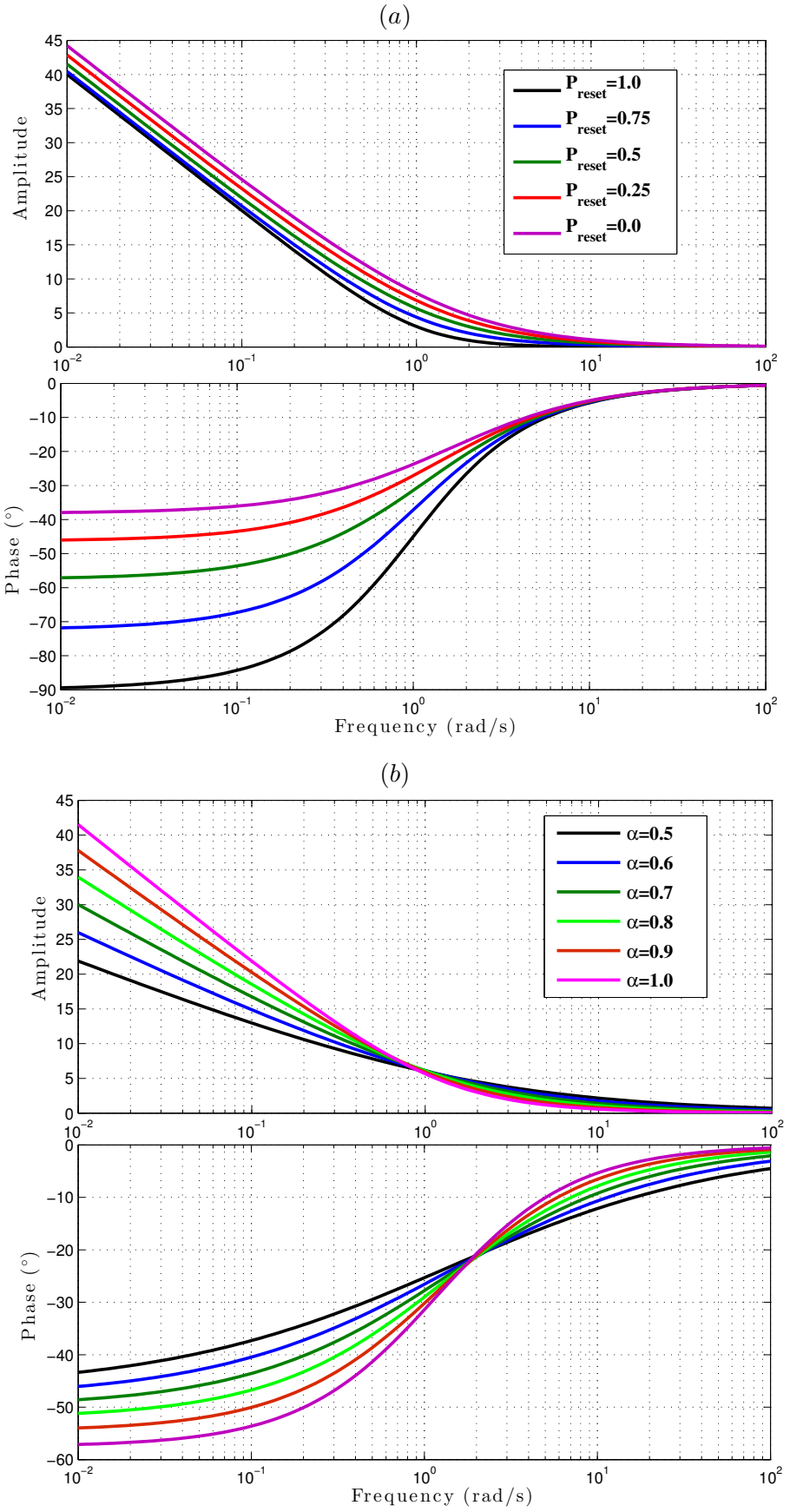

FIGURE 4.17: Describing function when ($k_p = \tau_i = 1$) (a) for different value of P_{reset} and $\alpha = 1$ (b) for different value of α and $P_{reset} = 0.5$

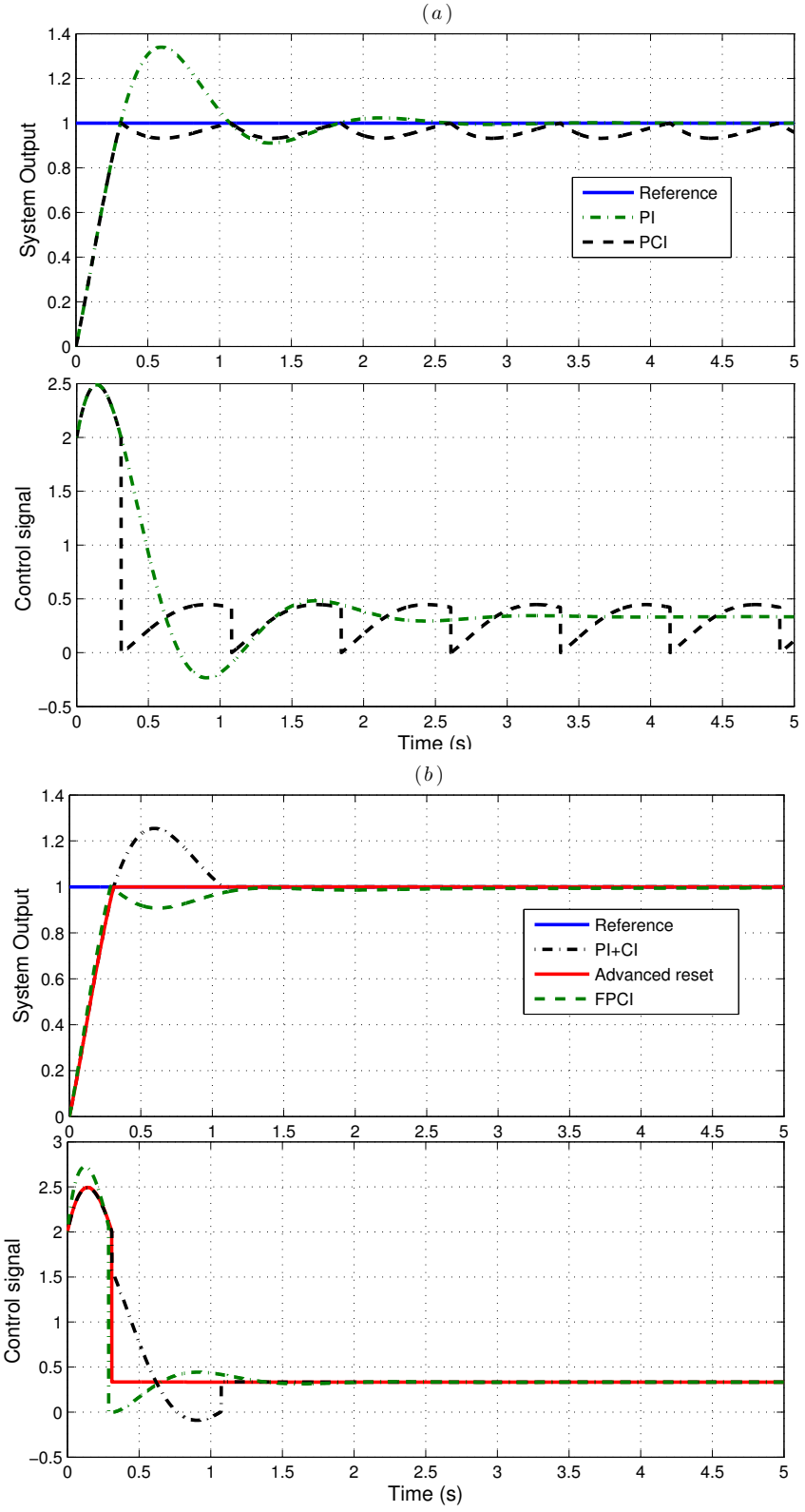

FIGURE 4.18: Comparison of different reset controllers for first order systems: (a) Using PI and PCI (b) Using PI+CI, advanced reset control and FPCI

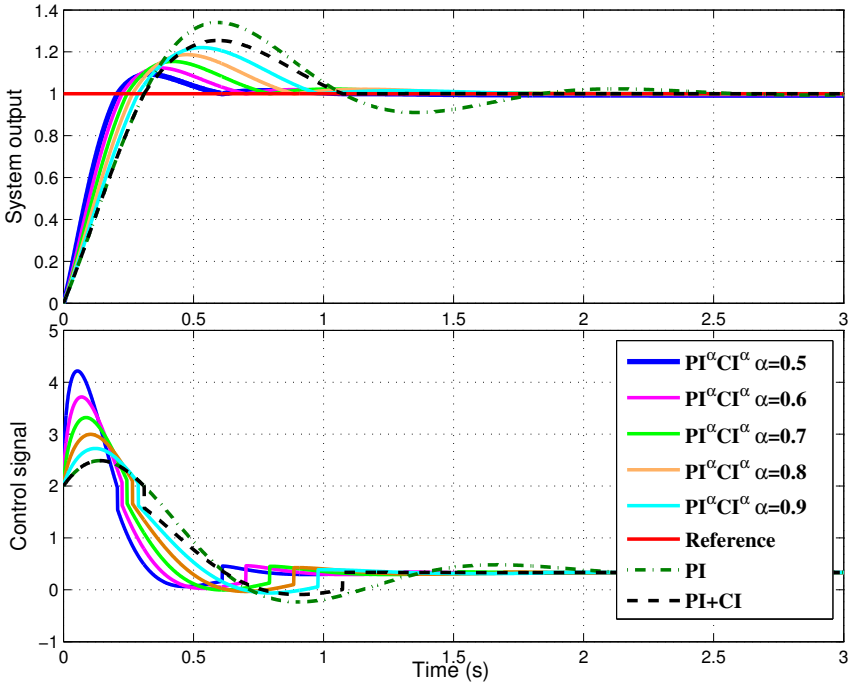

FIGURE 4.19: Simulation result of PI$^\alpha$+CI$^\alpha$

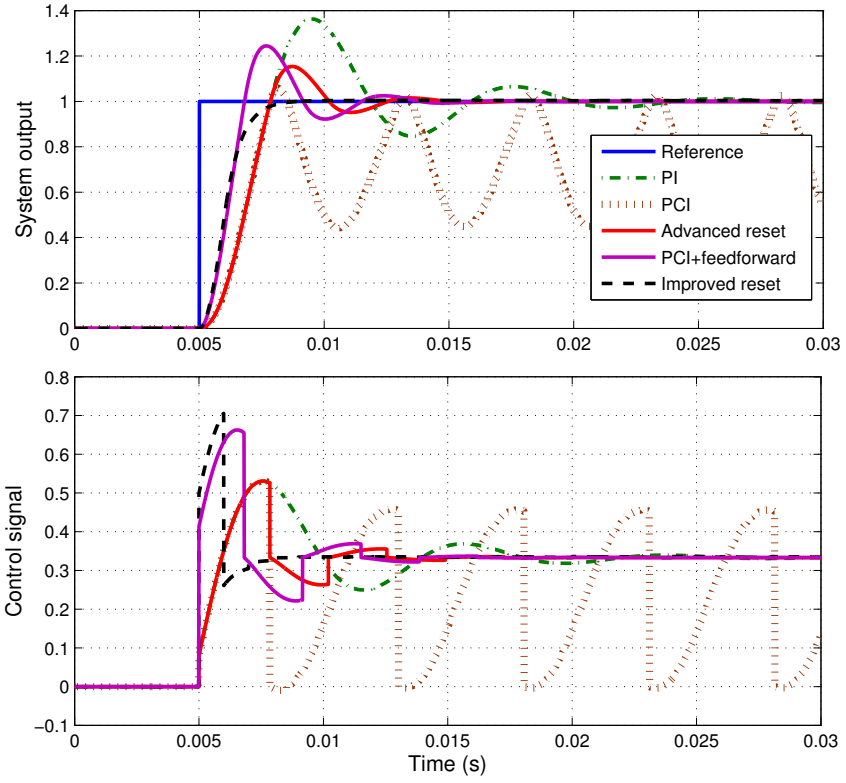

FIGURE 4.20: Comparison of advanced and improved reset and reset with feedforward controllers for second order systems

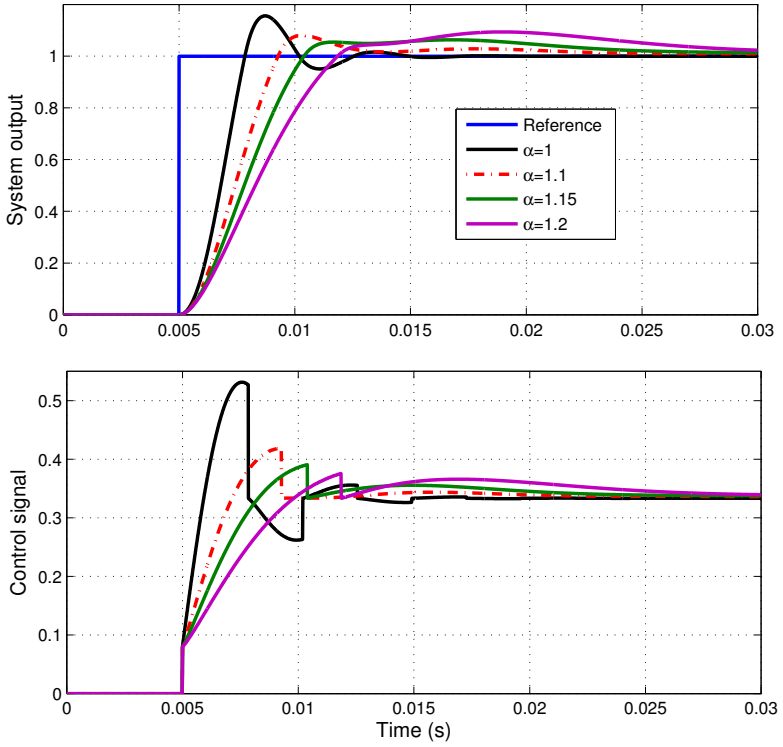

FIGURE 4.21: Comparison of advanced factional order controllers for different values of α for second order systems

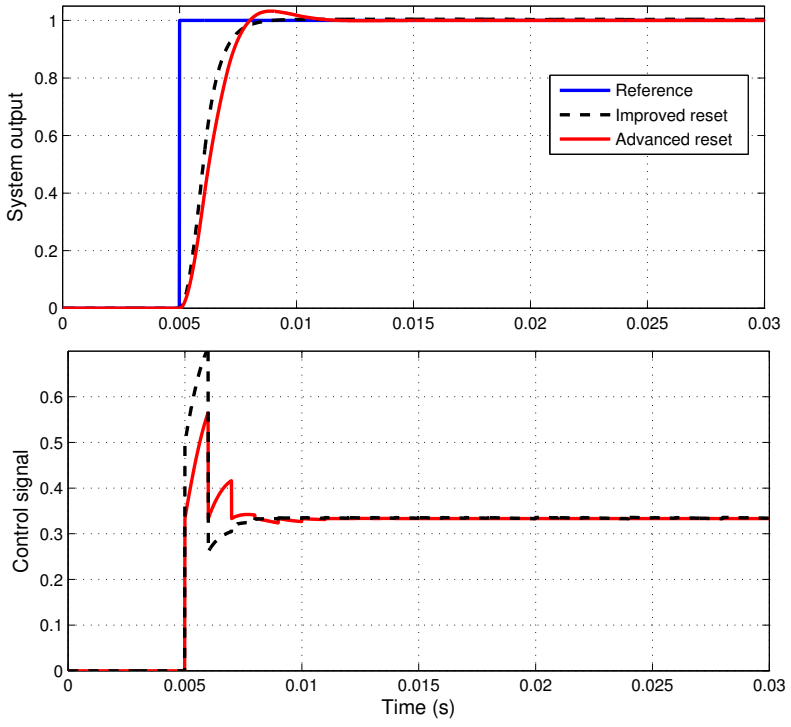

FIGURE 4.22: Comparison of improved reset controller and advanced reset controller with variable reset for second order systems

Chapter 5

Stability of Fractional-Order Hybrid Systems

This part is studying the stability of FHS in particular fractional-order switching system and fractional-order reset control system. Section 5.1 provides a collection of definitions and auxiliary theorems, concerning both switching and fractional-order systems, needed for the proof of the main results. In Section 5.2, the main results are presented, referred to the stability of fractional-order SwS based on common Lyapunov functions, its equivalence in the frequency domain and the stability analysis of the fractional-order reset control system. Finally, section 5.4 gives some examples to illustrate the effectiveness of the proposed theory.

5.1 Preliminaries

When a system becomes unstable, the output of the system goes to infinity (or negative infinity), which often poses a security problem in the immediate vicinity. Also, systems which become unstable often incur a certain amount of physical damage, which can become costly. For the sake of clarity, a collection of important issues concerning stability of switched systems is given in this section, mainly using Lyapunov theory.

5.1.1 Stability theorems and basic definitions

The idea behind Lyapunov's stability theory is as follows: assume there exists a positive definite function with a unique minimum at the equilibrium. One can think of such a function as a generalized description of the energy of the system. If we perturb the state from its equilibrium, the energy will initially rise. If the energy of the system constantly decreases along the solution of the autonomous system, it will eventually bring the state back to the equilibrium. Such functions are called Lyapunov functions. While Lyapunov theorems generalize to nonlinear systems and locally stable equilibria we shall only state them in the form applicable to our system class. Consider an autonomous nonlinear dynamical system

$$\dot{x}\left(t\right) = f(x\left(t\right)),\ x\left(0\right) = x_0, \tag{5.1}$$

where $x(t) \in \mathcal{D} \subseteq \mathbb{R}^n$ denotes the system state vector, $\mathcal{D}$ an open set containing the origin, and $f : \mathcal{D} \to \mathbb{R}^n$ continuous on $\mathcal{D}$. Suppose f has an equilibrium; without loss of generality, we may assume that it is at origin. Then, Lyapunov stability for continuos systems can be summarized in the following theorems.

Theorem 5.1. *Let $x = 0$ be an equilibrium point of (5.1). Assume that there exists an open set $\mathcal{D}$ with $0 \in \mathcal{D}$ and a continuously differentiable function $V : \mathcal{D} \to \mathbb{R}$ such that:*

1. $V(0) = 0$,
2. $V(x) > 0$ *for all* $x \in \mathcal{D}\backslash\{0\}$, *and*
3. $\frac{\partial V}{\partial x}(x)f(x) \leq 0$ *for all* $x \in \mathcal{D}$.

then $x = 0$ is a stable equilibrium point of (5.1).

Theorem 5.2. *If, in addition, $\frac{\partial V}{\partial x}(x)f(x) \leq 0$ for all $x \in \mathcal{D}\backslash\{0\}$, then $x = 0$ is an asymptotically stable equilibrium point.*

Definition 5.3 (Campact set)**.** A set S of real numbers is compact if and only if it is closed and bounded.

Definition 5.4 (pre-attractive)**.** A compact set $\mathcal{A}$ is pre-attractive if there exists a neighborhood of $\mathcal{A}$ from which each solution is bounded and the complete solutions converge to $\mathcal{A}$, that is, $|x(t,j)|_{\mathcal{A}} \to 0$ as $t+j \to \infty$ where $(t,j) \in \text{dom } x$.

Definition 5.5 (pre-asymptotically stable)**.** A compact set $\mathcal{A}$ is pre-asymptotically stable if it is stable and pre-attractive.

Consider a hybrid automaton $\mathcal{H}(C,F,D,G)$, where C and D are domain of continuos and discrete equations and F and G are continuos and discrete equations, respectively.

Definition 5.6. $x = 0 \in \mathbb{R}^n$ is an equilibrium point of $\mathcal{H}$ if:

1. $f(q,0) = 0$ for all $q \in Q$, and
2. $((q,q^{'}) \in E)\hat{}(0 \in G(q,,q^{'})) \Rightarrow R(q,q^{'},0) = \{0\}$.

Definition 5.7. Let $x = 0 \in \mathbb{R}^n$ be an equilibrium point of $\mathcal{H}$. $x = 0$ is stable if for all $\epsilon > 0$ there exists $\delta > 0$ such that for all $(\tau,q,x) \in \mathcal{H}_{(q_0,x_0)}$ with $\|x_0\| < \delta, \|x(t)\| < \epsilon$ for all $t \in \tau$.

Definition 5.8. Let $x = 0 \in \mathbb{R}^n$ be an equilibrium point of $\mathcal{H}$. $x = 0$ is asymptotically stable if it is stable and there exists $\delta > 0$ such that for all $(\tau,q,x) \in \mathcal{H}^{\infty}_{(q_0,x_0)}$ with $\|x_0\| < \delta$, $\lim_{t \to \tau_\infty} x(t) = 0$.

Definition 5.9 (Quadratic Stability)**.** A linear system

$$\dot{x} = Ax, \tag{5.2}$$

is said to be quadratically stable in $\mathbb{R}$ if there exists a positive definite matrix $P \in \mathbb{R}^{n \times n}$ such that,

$$A^T P + PA < 0.$$

In particular, t^{-a} stability will thus be used to refer to the asymptotic stability of fractional systems. The fact that the components of the state $x(t)$ decay slowly towards 0 following t^{-a} leads to fractional systems sometimes being treated as long memory systems.

Definition 5.10 (t^{-a} Stability)**.** The trajectory $x(t) = 0$ of the system $\frac{d^{\alpha}x(t)}{dt^{\alpha}} = f(t, x(t))$ is t^{-a} asymptotically stable if the uniform asymptotic stability condition is met and if there is a positive real a such that :
$\forall \left\|x\left(t\right)\right\|, t \leq t_0 \ \exists \ N\left(x\left(t\right), t \leq t_0\right), \ t_1\left(x\left(t\right), t \leq t_0\right)$ such that $\forall t \leq t_0, \ \left\|x\left(t\right)\right\| \leq N\left(t - t_1\right)^{-a}$.

Let us consider a fractional-order linear time invariant (FO-LTI) system as:

$$D^{\alpha}x = Ax, x \in \mathbb{R}^n \tag{5.3}$$

where α is the fractional-order.

Theorem 5.11 ([74])**.** *A fractional system given by (5.3) with order α, $1 \leq \alpha < 2$, is t^{-a} asymptotically stable if and only if there exists a matrix $P = P^T > 0$, $P \in \mathbb{R}^{n \times n}$, such that*

$$\begin{bmatrix} \left(A^T P + PA\right)\sin\left(\phi\right) & \left(A^T P - PA\right)\cos\left(\phi\right) \\ \left(-A^T P + PA\right)\cos\left(\phi\right) & \left(A^T P + PA\right)\sin\left(\phi\right) \end{bmatrix} < 0, \tag{5.4}$$

where $\phi = \frac{\alpha\pi}{2}$.

Theorem 5.12 ([74])**.** *A fractional-order system given by (5.3) with order α, $0 < \alpha \leq 1$, is t^{-a} asymptotically stable if and only if there exists a positive definite matrix $P \in \mathbb{R}^{n \times n}$ such that*

$$\left(-\left(-A\right)^{\frac{1}{2-\alpha}}\right)^T P + P\left(-\left(-A\right)^{\frac{1}{2-\alpha}}\right) < 0. \tag{5.5}$$

5.1.2 Common Lyapunov theory

Consider a switched system as follows:

$$\dot{x} = Ax, A \in co\left\{A_1, ..., A_L\right\}, \tag{5.6}$$

where "*co*" denotes the convex combination and $A_i, i = 1, ..., L$ is the switching subsystem. According to [133], (5.6) can be alternatively written as:

$$\dot{x} = Ax, A = \sum_{i=1}^{L} \lambda_i A_i, \forall \lambda_i \geq 0, \sum_{i=1}^{L} \lambda_i = 1. \tag{5.7}$$

Theorem 5.13 ([134]). *A system given by (5.7) is quadratically stable if and only if there exists a matrix $P = P^T > 0$, $P \in \mathbb{R}^{n \times n}$, such that*

$$A_i^T P + P A_i < 0, \forall i = 1, ..., L.$$

5.1.3 Multiple Lyapunov Functions

In this section, we discuss Lyapunov stability of hybrid systems via "multiple Lyapunov functions." The idea here is that even if we have Lyapunov functions for each system individually, we need to impose restrictions on switching to guarantee stability. Indeed, it is easy to construct examples of two globally exponentially stable systems and a switching scheme that sends all trajectories to infinity as we saw earlier.

Theorem 5.14 (Multiple Lyapunov Method [3]). *Given N dynamical systems, Σ_1, ..., Σ_N, each with equilibrium point at the origin, and N candidate Lyapunov functions, $V_1, ..., V_N$. If V_i decreases when S_i is active and*

$$V_i\,(\textit{time when } \Sigma_i \textit{ switched in}) \leq V_i\,(\textit{last time } \Sigma_i \textit{ switched in}) \tag{5.8}$$

then the hybrid system is Lyapunov stable.

Below, we say that V is a candidate Lyapunov function if V is a continuous, positive definite function (about the origin, 0) with continuous partial derivatives.

Now, consider the system with following differential inclusion,

$$\mathcal{H}(C, F, D, G) : \begin{cases} \dot{x} = F(x), \ x \in C \\ x^+ = G\,(x)\,, \ x \in D \end{cases}. \tag{5.9}$$

Given the hybrid system $\mathcal{H}$ with data (C, F, D, G) and the compact set $A \subset \mathbb{R}^n$, the function V : dom $V \to \mathbb{R}$ is a Lyapunov-function candidate for $(\mathcal{H}, A)$ if i) V is

continuous and nonnegative on $(C \cup D) \backslash A \subset \text{dom}\, V$, ii) V is continuously differentiable on an open set $\mathcal{O}$ satisfying $C \backslash A \subset \mathcal{O} \subset \text{dom}\, V$, and iii) $\lim_{\{x \to A,\ x \in \text{dom}\ V \cap (C \cup D)\}} V(x) = 0$.

Conditions i) and iii) hold when dom V contains $A \cup C \cup D$, V is continuous and nonnegative on its domain, and $V(z) = 0$ for all $x \in A$. These conditions are typical of Lyapunov-function candidates for discrete-time systems. Condition ii) holds when V is continuously differentiable on an open set containing $C \backslash A$, which is typical of Lyapunov-function candidates for continuous-time systems. We impose continuous differentiability for simplicity, but it is possible to work with less regular Lyapunov functions and their generalized derivatives. When $x = (\xi, q) \in \mathbb{R}^n \times Q$, where Q is a discrete set, it is natural to define V only on $\mathbb{R}^n \times Q$. To satisfy condition ii), the definition of V can be extended to a neighborhood of $\mathbb{R}^n \times Q$, with $V(\xi, q) = V(\xi, q_0)$ for all q near $q_0 \in Q$. We now state a hybrid Lyapunov theorem.

Theorem 5.15 (Hybrid Lyapunov Stability [3])**.** *Consider hybrid system $\mathcal{H}(C, F, D, G)$. If there exists a Lyapunov-function candidate $V(x)$ such that*

$$\begin{aligned} \langle \nabla V(x), f \rangle &< 0, \text{ for all } x \in C \backslash A, f \in F(x), \\ V(g) - V(x) &< 0, \text{ for all } x \in D \backslash A, g \in G(x) \backslash A, \end{aligned} \tag{5.10}$$

then there exists a left-continuous function $x(t)$ satisfying (5.9) for all $t \geq 0$, and the equilibrium point $x = 0$ is globally uniformly asymptotically stable.

5.2 Stability of fractional-order switching systems

Our objective hereafter is to establish stability conditions for fractional-order switching systems. In this section, we firstly present the asymptotic stability of such systems by common Lyapunov functions, which have been previously generalized to fractional-order switching systems, and further its equivalence in frequency domain.

5.2.1 Common Lyapunov theory

Consider a fractional-order switching system of the form (5.6) as

$$D^{\alpha} x = Ax, A \in co\{A_1, ..., A_L\}. \tag{5.11}$$

Theorem 5.16. *A fractional system described by (5.11) with order α, $1 \leq \alpha < 2$, is stable if and only if there exists a matrix $P = P^T > 0$, $P \in \mathbb{R}^{n\times n}$, such that*

$$\begin{bmatrix} \left(A_i^T P + P A_i\right)\sin\phi & \left(A_i^T P - P A_i\right)\cos\phi \\ \left(-A_i^T P + P A_i\right)\cos\phi & \left(A_i^T P + P A_i\right)\sin\phi \end{bmatrix} < 0, \forall i = 1, ..., L, \tag{5.12}$$

where $\phi = \frac{\alpha\pi}{2}$.

Proof. System (5.11) can be rewritten as:

$$D^\alpha x = Ax, A = \sum_{i=1}^{L} \lambda_i A_i, \forall \lambda_i \geq 0, \sum_{i=1}^{L} \lambda_i = 1. \tag{5.13}$$

Then, from Theorem 5.11, and (5.11), we have

$$\begin{bmatrix} \left(A^T P + P A\right)\sin\phi & \left(A^T P - P A\right)\cos\phi \\ \left(-A^T P + P A\right)\cos\phi) & \left(A^T P + P A\right)\sin\phi \end{bmatrix}, \forall \lambda_i \geq 0, \sum_{i=1}^{L} \lambda_i = 1 \Leftrightarrow$$
$$\sum_{i=1}^{L} \lambda_i \left(\begin{bmatrix} \left(A_i^T P + P A_i\right)\sin\phi & \left(A_i^T P - P A_i\right)\cos\phi \\ \left(-A_i^T P + P A_i\right)\cos\phi & \left(A_i^T P + P A_i\right)\sin\phi \end{bmatrix} \right), \forall \lambda_i \geq 0, \sum_{i=1}^{L} \lambda_i = 1.$$

Therefore, it is obvious that (5.11) is stable if and only if

$$\begin{bmatrix} \left(A_i^T P + P A_i\right)\sin\phi & \left(A_i^T P - P A_i\right)\cos\phi \\ \left(-A_i^T P + P A_i\right)\cos\phi & \left(A_i^T P + P A_i\right)\sin\phi \end{bmatrix} < 0, \forall i = 1, ..., L.$$

□

Theorem 5.17. *A fractional system given by (5.11) with order α, $0 < \alpha \leq 1$, is stable if and only if there exists a matrix $P = P^T > 0$, $P \in \mathbb{R}^{n\times n}$, such that*

$$\left(-\left(-A_i\right)^{\frac{1}{2-\alpha}}\right)^T P + P\left(-\left(-A_i\right)^{\frac{1}{2-\alpha}}\right) < 0, \forall i = 1, ..., L. \tag{5.14}$$

Proof. Assuming zero initial condition, the fractional-order system (5.11) with order α, $0 < \alpha \leq 1$, can be replaced by the following integer-order system [74]:

$$\dot{z} = A_f z, A_f \in co\{A_{f_1}, ..., A_{f_L}\} \tag{5.15}$$

$$z = C_f x, \tag{5.16}$$

where $A_{f_i} = \begin{bmatrix} 0 & \cdots & 0 & A_i^{1/\alpha} \\ A_i^{1/\alpha} & \cdots & 0 & 0 \\ & \ddots & & \vdots \\ \cdots & 0 & A_i^{1/\alpha} & 0 \end{bmatrix}$ and $C_f = \begin{bmatrix} 0 & \cdots & 0 & 1 \end{bmatrix}$. Writing (5.15) in an alternative way yields:

$$\dot{z} = A_f z, A_f = \sum_{i=1}^{L} \lambda_i A_{f_i}, \forall \lambda_i \geq 0, \sum_{i=1}^{L} \lambda_i = 1. \tag{5.17}$$

Therefore, assuming a positive definite matrix $\mathcal{P} = \begin{bmatrix} P & 0 \\ 0 & P \end{bmatrix}$, with proper dimensions and, based on LMI method, the system (5.11) with order α, $0 < \alpha \leq 1$, is stable if:

$$A_f^T \mathcal{P} + \mathcal{P} A_f < 0 \Rightarrow \tag{5.18}$$

$$\sum_{i=1}^{L} \lambda_i (A_{f_i}^T \mathcal{P} + \mathcal{P} A_{f_i}) < 0 \Rightarrow \tag{5.19}$$

$$A_{f_i}^T \mathcal{P} + \mathcal{P} A_{f_i} < 0, \forall i = 1, ..., L. \tag{5.20}$$

Then, it is obvious that expression (5.20) is satisfied if and only if [74]

$$(A_i^{1/\alpha})^T P + P A_i^{1/\alpha} < 0, \forall i = 1, ..., L. \tag{5.21}$$

In [74] it is shown that condition (5.21) is sufficient but not necessary to guarantee the stability. The necessary and sufficient condition for fractional-order systems is given by Theorem 5.12, i.e.,

$$\left(-(-A_i)^{\frac{1}{2-\alpha}}\right)^T P + P\left(-(-A_i)^{\frac{1}{2-\alpha}}\right) < 0, \forall i = 1, ..., L. \tag{5.22}$$

□

5.2.2 Frequency domain approach

Next, frequency domain stability conditions will be given for fractional-order switching systems based on results in [41].

Consider a stable pseudo-polynomial of order $n\alpha$ of system (5.3) as

$$d(s) = s^{n\alpha} + d_{n-1}s^{(n-1)\alpha} + \cdots + d_1 s^{\alpha} + d_0, \tag{5.23}$$

and a polynomial of order n of system $\dot{\tilde{x}} = \tilde{A}\tilde{x}$ as

$$c(s) = s^{n} + c_{n-1}s^{(n-1)} + \cdots + c_1 s + c_0, \tag{5.24}$$

where matrices A and $\tilde{A}$ are given by

$$A = \begin{bmatrix} -d_{n-1} & -d_{n-2} & \cdots & -d_1 & -d_0 \\ 1 & 0 & \cdots & 0 & 0 \\ 0 & 1 & \cdots & 0 & 0 \\ \vdots & \vdots & \ddots & \vdots & \vdots \\ 0 & 0 & \cdots & 1 & 0 \end{bmatrix}, \tilde{A} = \begin{bmatrix} -c_{n-1} & -c_{n-2} & \cdots & -c_1 & -c_0 \\ 1 & 0 & \cdots & 0 & 0 \\ 0 & 1 & \cdots & 0 & 0 \\ \vdots & \vdots & \ddots & \vdots & \vdots \\ 0 & 0 & \cdots & 1 & 0 \end{bmatrix}. \tag{5.25}$$

In the following, the necessary and sufficient condition for the the stability of fractional-order switching system (5.13) when $L = 2$ will be given.

Theorem 5.18. *Consider $d_1(s)$ and $d_2(s)$, two stable pseudo-polynomials of order n corresponding to the switching systems with subsystems $D^{\alpha}x = A_1 x$ and $D^{\alpha}x = A_2 x$ and order α, $1 \leq \alpha < 2$, respectively, then the following statements are equivalent:*

1. $\left|\arg\left(\det((A_1^2 - \omega^2 I) - 2j\omega A_1 \sin\phi)\right) - \arg\left(\det((A_2^2 - \omega^2 I) - 2j\omega A_2 \sin\phi)\right)\right| < \frac{\pi}{2}, \forall\omega$, *being I the identity matrix with proper dimensions.*

2. *$\tilde{A}_1$ and $\tilde{A}_2$ are stable and therefore A_1 and A_2 are t^a asymptotically stable, which means that $\exists P = P^T > 0 \in \mathbb{R}^{n\times n}$ such that*

$$\begin{bmatrix} \left(A_i^T P + P A_i\right)\sin\phi & \left(A_i^T P - P A_i\right)\cos\phi \\ \left(-A_i^T P + P A_i\right)\cos\phi & \left(A_i^T P + P A_i\right)\sin\phi \end{bmatrix} < 0, \forall i = 1, 2.$$

Proof. Consider $c_1(s)$ and $c_2(s)$ are the characteristic polynomials corresponding to $\dot{\tilde{x}} = \tilde{A}_1\tilde{x}$ and $\dot{\tilde{x}} = \tilde{A}_2\tilde{x}$, respectively, with $\tilde{A}_i = \begin{bmatrix} A_i \sin\phi & A_i \cos\phi \\ -A_i \cos\phi & A_i \sin\phi \end{bmatrix}$, $i = 1, 2$. According to Theorem 4.1, the following statements are equivalent:

a) $\frac{c_1(s)}{c_2(s)}$ and $\frac{c_2(s)}{c_1(s)}$ are SPR, where $c_i(s) = \det(sI - \tilde{A}_i)$, $i = 1, 2$.

b) $|\arg(c_1(j\omega)) - \arg(c_2(j\omega))| < \frac{\pi}{2}$, $\forall\ \omega$.

c) $\tilde{A}_1$ and $\tilde{A}_2$ are stable, which means that $\exists \mathcal{P} = \mathcal{P}^T > 0 \in \mathbb{R}^{2n\times 2n}$ such that $\tilde{A}_1^T\mathcal{P} + \mathcal{P}\tilde{A}_1 < 0$, $\tilde{A}_2^T\mathcal{P} + \mathcal{P}\tilde{A}_2 < 0$.

Now, consider $d_1(s)$ and $d_2(s)$ are the characteristic pseudo-polynomials corresponding to the fractional-order systems $D^\alpha x = A_1 x$ and $D^\alpha x = A_2 x$ with order α, $1 \le \alpha < 2$, respectively. From (b), we have

$$|\arg(c_1(j\omega)) - \arg(c_2(j\omega))| = \left|\arg(j\omega I - \tilde{A}_1) - \arg(j\omega I - \tilde{A}_2)\right| < \frac{\pi}{2}, \Leftrightarrow$$
$$\left|\arg\left(\det((A_1^2 - \omega^2 I) - 2j\omega A_1 \sin\phi\right) - \arg\left(\det((A_2^2 - \omega^2 I) - 2j\omega A_2 \sin\phi\right)\right| < \frac{\pi}{2}, \forall\omega.$$

And from (c) choosing $\mathcal{P} = \begin{bmatrix} P & 0 \\ 0 & P \end{bmatrix}$,

$$\tilde{A}_i^T\mathcal{P} + \mathcal{P}\tilde{A}_i = \begin{bmatrix} A_i^T \sin\phi & -A_i^T \cos\phi \\ A_i^T \cos\phi & A_i^T \sin\phi \end{bmatrix}\begin{bmatrix} P & 0 \\ 0 & P \end{bmatrix} + \begin{bmatrix} P & 0 \\ 0 & P \end{bmatrix}\begin{bmatrix} A_i \sin\phi & A_i \cos\phi \\ -A_i \cos\phi & A_i \sin\phi \end{bmatrix} < 0,$$
$$\Leftrightarrow \begin{bmatrix} \left(A_i^T P + P A_i\right)\sin\phi & \left(A_i^T P - P A_i\right)\cos\phi \\ \left(-A_i^T P + P A_i\right)\cos\phi & \left(A_i^T P + P A_i\right)\sin\phi \end{bmatrix} < 0, \forall i = 1, 2.$$

Therefore, the theorem is proved. □

Theorem 5.19. *Consider two stable fractional-order subsystems $D^\alpha x = A_1 x$ and $D^\alpha x = A_2 x$ with order α, $0 < \alpha \le 1$, then the following statements are equivalent:*

1. $|\arg(\det(\mathcal{A}_1 - j\omega I)) - \arg(\det(\mathcal{A}_2 - j\omega I))| < \frac{\pi}{2}$, $\forall\ \omega$.

2. *$\mathcal{A}_1$ and $\mathcal{A}_2$ are stable and therefore A_1 and A_2 are t^a asymptotically stable, which means that $\exists P = P^T > 0 \in \mathbb{R}^{n\times n}$ such that*

$$\mathcal{A}_i^T P + P\mathcal{A}_i < 0, \forall i = 1, 2,$$

where $\mathcal{A}_i = -\left(-A_i\right)^{\frac{1}{2-\alpha}}, \forall i = 1, 2.$

Proof. Let us define $c_i(s) = \det(\mathcal{A}_i - sI)$, $i = 1, 2$. According to Theorem 4.1 and Theorem 5.17, proof is straightforward. □

Although the theory developed in the frequency domain doesn't necessarily prove the SPRness, a relation equivalent to the asymptotic stability was obtained.

5.2.2.1 Stability of switching system with infinite subsystems

As reported in [135, 136], SPRness of the ratio of each pair of polynomials is not sufficient to guarantee their stability. If the three systems are pairwise stable then the region in the space of the coefficients of the polynomials that is stable is presented in the following theorem.

Theorem 5.20 ([136])**.** *Consider $c_1(s)$, $c_2(s)$ and $c_3(s)$, three stable polynomials of order n and A_1, A_2 and A_3, their associated matrix. If the ratio of each pair of polynomials, $\frac{c_1(s)}{c_2(s)}$, $\frac{c_1(s)}{c_3(s)}$ and $\frac{c_2(s)}{c_3(s)}$ is SPR, then the three matrices A_4, A_5 and A_6 associated with the stable polynomials $c_4(s)$, $c_5(s)$ and $c_6(s)$ are stable, where $c_4(s) = \frac{c_1(s)+c_2(s)}{2}$, $c_5(s) = \frac{c_1(s)+c_3(s)}{2}$ and $c_6(s) = \frac{c_2(s)+c_3(s)}{2}$.*

An interesting result in [135, 136] should be noted: N_m stable second order LTI systems are stable if every three-tuple of systems is stable. As we can constrain three systems to be stable, we can constrain N_m second-order systems to be stable.

Reset control systems are a class of HS [28] includes a linear controller which resets some of their states to zero when their input is zero or certain non-zero values. In the next section, the fractional reset control system will be classified as a FDI and the stability of the system will be analyzed using Lyapunov like method studied in this section.

5.3 Stability of Reset Control Systems

Stability of reset controllers has received many attention in the field. Necessary and sufficient conditions for internal stability for a restricted class of systems characterized by a CI and second-order plant were studied in [137]. Stability of a reset control system under constant inputs was analysed in [138, 139] and its experimental application was demonstrated in [140]. BIBO stability and asymptotic tracking of FORE were established on [139, 141]. Likewise, more general reset structures were reported in [46], allowing higher-order controllers and partial-state resetting. In this work, not only a testable necessary and sufficient condition to analyze the stability was given, but also links to both uniform bounded-input bounded-state stability and steady-state performance.

In what concerns the use of fractional calculus in control, the fractional-order integrator has been considered as an alternative reference system for control purposes in order to obtain closed-loop controlled systems robust to gain changes [142, 143]. From another point of view, the fractional-order integrator can be used in feedback control in order to introduce both a constant phase lag and magnitude slope proportional to the integration order. Thus, fractional-order integrators can be used with the same purposes that the reset integrator. Likewise, the fractional-order Clegg integrator (FCI) has been studied in some papers. Thus, its fundamentals can be found in [71, 132], whereas the numerical values for the describing functions with fractional reset control were presented in [144]. In addition, an optimized fractional-order conditional integrator (OFOCI) was also proposed in [145].

Given this context, the purpose of this section is to present the stability conditions of the fractional-order reset control systems by generalizing some of the aforementioned methods.

5.3.1 Stability of Fractional-Order Reset Control

This section concerns stability of fractional-order reset control systems. Firstly, some definitions needed to our main results are given. It should be mentioned that in this section by calling the reset control system (3.40) we refer to the this when $D_r = 0$. It

should be noted that, in the case of having an integer-order controller or an integer-order system, the state space should be realized as an augmented system as follows [108, 146]. Consider the following integer-order system

$$\begin{matrix} \dot{x}(t) = Ax(t) + Bu(t) \\ y(t) = Cx(t) \end{matrix}, \tag{5.26}$$

where $x \in \mathbb{R}^n$ and $y(t)$ are the state vector and the output of the system. The integer-order state space model can be rewritten in the following augmented fractional-order system:

$$\begin{matrix} D^{\alpha}\mathcal{X}(t) = \mathbf{A}\mathcal{X}(t) + \mathbf{B}u(t) \\ y(t) = \mathbf{C}\mathcal{X}(t) \end{matrix}, \tag{5.27}$$

$$\mathbf{A} = \begin{bmatrix} 0 & I & 0 & \cdots & 0 & 0 \\ 0 & 0 & I & \cdots & 0 & 0 \\ \vdots & \vdots & \vdots & \vdots & \vdots & \vdots \\ 0 & 0 & 0 & \cdots & 0 & I \\ A & 0 & 0 & \cdots & 0 & 0 \end{bmatrix}, \ \mathbf{B} = \begin{bmatrix} 0 \\ 0 \\ \vdots \\ 0 \\ B \end{bmatrix}, \mathbf{C} = \begin{bmatrix} C & 0 & 0 & \cdots & 0 & 0 \end{bmatrix}, \tag{5.28}$$

where $\mathcal{X} = [x \ x_{a,1} \ ... \ x_{a,p-1}]^T$ is the vector of augmented states, $p = \frac{1}{\alpha}$, and I is the identity matrix.

Theorem 5.21 (Lyapunov-like theorem [3])**.** *Consider a closed-loop reset system given by (3.40). If there exists a Lyapunov-function candidate $V(x)$ such that*

$$\dot{V}(x(t)) < 0, \ x(t) \notin \mathcal{M}, \tag{5.29}$$

$$\triangle V(x(t)) = V(x(t^+)) - V(x(t)) \leq 0, \ x(t) \in \mathcal{M}, \tag{5.30}$$

then there exists a left-continuous function $x(t)$ satisfying (3.40) for all $t \geq 0$, and the equilibrium point x_e is globally uniformly asymptotically stable.

Definition 5.22. Reset control system (3.40) is said to satisfy the H_β-condition if there exists a $\beta \in \mathbb{R}^{n_\mathcal{R}}$ and a positive-definite matrix $P_\mathcal{R} \in \mathbb{R}^{n_\mathcal{R} \times n_\mathcal{R}}$ such that

$$H_\beta(s) = \begin{bmatrix} \beta C_p & 0_{n_{\bar{\mathcal{R}}}} & P_\mathcal{R} \end{bmatrix} (sI - \mathcal{A})^{-1} \begin{bmatrix} 0 \\ 0_{\bar{\mathcal{R}}}^T \\ I_\mathcal{R} \end{bmatrix}, \tag{5.31}$$

where $\mathcal{A} = \left(-\left(-A_{cl}\right)^{\frac{1}{2-\alpha}} \right)$.

According to [46, 138, 147], an integer-order reset control system of the form of (3.40) –with $\alpha = 1$– is asymptotically stable if and only if it satisfies the H_β-condition. The same idea can be used to prove the stability of fractional-order reset systems.

Now, consider $V(z(t)) = z(t)^T \mathcal{P} z(t),\ \mathcal{P} \in \mathbb{R}^{N \times N}$ as a Lyapunov candidate for the unforced reset system (3.40) ($r = 0$), where $x = [0, \cdots, 0, 1] z(t),\ z(t) \in \mathbb{R}^{N \times N},\ \dot{z} = A_f z(t)$, and $A_f = \begin{bmatrix} 0 & \cdots & 0 & A^{1/\alpha} \\ A^{1/\alpha} & \cdots & 0 & 0 \\ & \ddots & & \vdots \\ 0 & & A^{1/\alpha} & 0 \end{bmatrix}$ (see [74] more details for this transformation, assuming zero initial condition). Then, in accordance with [74], the necessary and sufficient condition to satisfy $\dot{V}(z(t)) < 0$ when $\frac{2}{3} < \alpha \leq 1$ is:

$$\left(A^{\frac{1}{\alpha}}\right)^T P + P \left(A^{\frac{1}{\alpha}}\right) < 0,\ x(t) \notin \mathcal{M}.$$

where $P (\subset \mathcal{P}) \in \mathbb{R}^{n \times n} > 0$. Likewise, based on results stated in Theorem 5.12, the necessary and sufficient condition for $0 < \alpha \leq 1$ is

$$\mathcal{A}^T P + P\mathcal{A} < 0,\ x(t) \notin \mathcal{M}.$$

Transforming the second equation of reset system (3.40), we have

$$z(t^+) = \begin{bmatrix} I_{N-n} & 0 \\ 0 & A_R \end{bmatrix} z(t), \tag{5.32}$$

where I_{N-n} is identity matrix with dimension of $N - n$. Thus, $\triangle V(z(t)) < 0$ if

$$V(z(t^+)) - V(z(t)) =$$

$$z^T(t)\left(\begin{bmatrix} I_{N-n} & 0 \\ 0 & A_R^T \end{bmatrix}\mathcal{P} + \mathcal{P}\begin{bmatrix} I_{N-n} & 0 \\ 0 & A_R \end{bmatrix}\right) z(t) \leq 0. \tag{5.33}$$

Then, (5.33) is satisfied if $V(x(t^+)) - V(x(t)) \leq 0$,

$$x^T(t)(A_R^T P A_R - P \leq 0)x(t) \leq 0,\ x(t) \in \mathcal{M}.$$

Therefore, Theorem 5.21 can be reshaped in the following remark.

Remark 5.23. Choosing $V(z) = z(t)^T \mathcal{P} z(t),\ \mathcal{P} \in \mathbb{R}^{N\times N}$ as a Lyapunov candidate, and applying Theorem 5.12, fractional-order reset system (3.40) is asymptotically stable if and only if:

$$\mathcal{A}^T P + P\mathcal{A} < 0,\ x(t) \notin \mathcal{M}, \tag{5.34}$$

$$A_R^T P A_R - P \leq 0,\ x(t) \in \mathcal{M}. \tag{5.35}$$

Consider a reset system with constant input and let us define $\mathbf{x}(t) = x(t) - x_e = x(t) + A_{cl}^{-1}B_{cl}r$. Thus, reset system (3.40) can be rewritten as:

$$\begin{aligned} D^\alpha \mathbf{x}(t) &= A_{cl}\mathbf{x}(t),\ x(t) \notin \mathcal{M},\ x(0) = x_0 \\ \mathbf{x}(t^+) &= A_R(\mathbf{x}(t) + x_e),\ x(t) \in \mathcal{M} \\ y(t) &= C_{cl}x(t). \end{aligned} \tag{5.36}$$

Choosing a similar Lyapunov function, i.e, $V(z(t)) = z(t)^T \mathcal{P} z(t)$, $\mathbf{x}(t) = [0, \cdots, 0, 1]z(t)$, system (5.36) is stable if conditions (5.29) and (5.30) are satisfied. Comparing (3.40) and (5.36), condition (5.29) is fulfilled if (5.34) is satisfied, and similarly to the unforced system $\triangle V(z(t)) \leq 0$ if $\triangle V(\mathbf{x}(t)) \leq 0$ (see (5.32) and (5.33)). Thus,

$$\triangle V(\mathbf{x}(t)) = V(\mathbf{x}(t^+)) - V(\mathbf{x}(t)) =$$

$$(\mathbf{x}(t) + x_e)^T A_R^T P A_R(\mathbf{x}(t) + x_e) - \mathbf{x}(t)^T P \mathbf{x}(t) < 0 \ \rightarrow$$

$$\mathbf{x}^T(t)(A_R^T P A_R - P)\mathbf{x}(t) < -(M = x_e^T A_R^T P A_R x_e) \ \rightarrow$$

$$\mathbf{x}(t)^T \left(\left(A_R^T P A_R - P\right) < 0\right)\mathbf{x}(t) < 0.$$

Therefore, Remark 5.23 will be also applicable to this special case. Define $\tilde{\mathcal{M}} = \{x \in \mathbb{R}^n : C_{cl}x(t) = r\}$, and let Φ be a matrix whose columns span $\tilde{\mathcal{M}}$. Since $\tilde{\mathcal{M}} \subset \mathcal{M}$, (5.35) is implied by

$$\Phi \left(A_R^T P A_R - P < 0 \right) \Phi \leq 0. \tag{5.37}$$

A straightforward computation shows that inequality (5.37) holds for some positive-definite symmetric matrix P if there exists a $\beta \in \mathbb{R}^{n_\mathcal{R}}$ and a positive-definite $P_\mathcal{R} \in \mathbb{R}^{n_\mathcal{R} \times n_\mathcal{R}}$ such that

$$\begin{bmatrix} 0 & 0_{\bar{\mathcal{R}}} & I_\mathcal{R} \end{bmatrix} P = \begin{bmatrix} \beta C_p & 0_{n_{\bar{\mathcal{R}}}} & P_\mathcal{R} \end{bmatrix}. \tag{5.38}$$

To analyze stability, it suffices to find a positive-definite symmetric matrix P such that (5.34) and (5.38) hold. Taking into account Kalman-Yakubovich-Popov (KYP) lemma [148], such P exists if $\mathrm{H}_\beta(s)$ in (5.31) is strictly positive real (SPR) for some β. In addition, in accordance with [149], it is obvious that the $\mathrm{H}_\beta(s)$ is SPR if

$$|\arg(H_\beta(j\omega))| < \frac{\pi}{2}, \forall \omega. \tag{5.39}$$

Therefore, these results can be stated in the following theorem.

Theorem 5.24. *The closed-loop fractional-order reset control system (3.40) is asymptotically stable if and only if it satisfies the H_β-condition (5.31) or its phase equivalence (5.39).*

5.4 Examples

In this section, some examples are given in order to show the applicability and effectiveness of the stability theories developed for fractional-order hybrid systems. Phase portraits and time responses of the systems will be shown in order to demonstrate their stability.

Example 5.1. *Consider the switching system (5.11) with $L = 2$ with the following parameters:* $A_1 = \begin{bmatrix} -0.1 & 0.1 \\ -2.0 & -0.1 \end{bmatrix}$, $A_2 = \begin{bmatrix} -0.01 & 2.0 \\ -0.1 & -0.01 \end{bmatrix}$ *and order α, $0 < \alpha \leq 1$.*

Applying Theorem 5.19, the phase difference condition should be satisfied for all α, $0 < \alpha \leq 1$, to guarantee the stability –this condition is depicted in Fig. 5.1 for $0 < \alpha \leq 1$ with increments of 0.1. As can be seen, the fractional-order system is stable for $\alpha \in (0, 0.6]$. The phase differences when $\alpha \in [0.7, 1]$ are bigger than $\pi/2$ which indicates unknown stability status, i.e., the system may be stable or unstable. For better understanding of this initial notice on the system stability, its phase portrait is shown in Fig. 5.2 for three values of α –$\alpha = 0.6$, $\alpha = 0.8$ and $\alpha = 0.9$. The green trajectory is an example to show the stability or instability of the switching system. The following conclusions can be stated from these results:

- When $\alpha = 0.6$, it can be observed that the system is stable for arbitrary switching. This can be also confirmed by the fact that a matrix P,

$$P = \begin{bmatrix} 1 & 0.2 \\ 0.2 & 1 \end{bmatrix},$$

satisfies the stability conditions as follows:

$$\left(-\left(-A_1\right)^{\frac{1}{1.4}}\right)^T P + P\left(-\left(-A_1\right)^{\frac{1}{1.4}}\right) = \begin{bmatrix} -1.4716 & -0.6547 \\ -0.8863 & -0.5411 \end{bmatrix} < 0,$$

$$\left(-\left(-A_2\right)^{\frac{1}{1.4}}\right)^T P + P\left(-\left(-A_2\right)^{\frac{1}{1.4}}\right) = \begin{bmatrix} -1.4488 & 0.5894 \\ 0.5894 & -0.4719 \end{bmatrix} < 0.$$

Fig. 5.3 shows the time responses of the system under arbitrary switching around each quadrant and also verifies its stability: the states of the system reach the equilibrium points. The switching region is shown in Fig. 5.6, in which C_1 refers to the zone where only subsystem 1 is active, whereas C_2 is the zone which corresponds to subsystem 2. D is a common region with a random layer where both system can be active. The red lines indicate the switching from subsystem 1 to subsystem 2, whereas the blue lines show the switching in contrary.

- When $\alpha = 0.8$, its phase portrait shows almost the same behaviour as with order $\alpha = 0.6$. Fig. 5.4 also shows that the system is stable under arbitrary switching around each quadrant. However, one can not find a trajectory which leads to unstable switching system, and, consequently, stability of the system under arbitrary switching is in doubt.

- Finally, in the case of $\alpha = 0.9$, the system will be unstable if it switches like the green trajectory shown in Fig. 5.2(c). This fact can be also deduced from the time response plotted in Fig. 5.5.

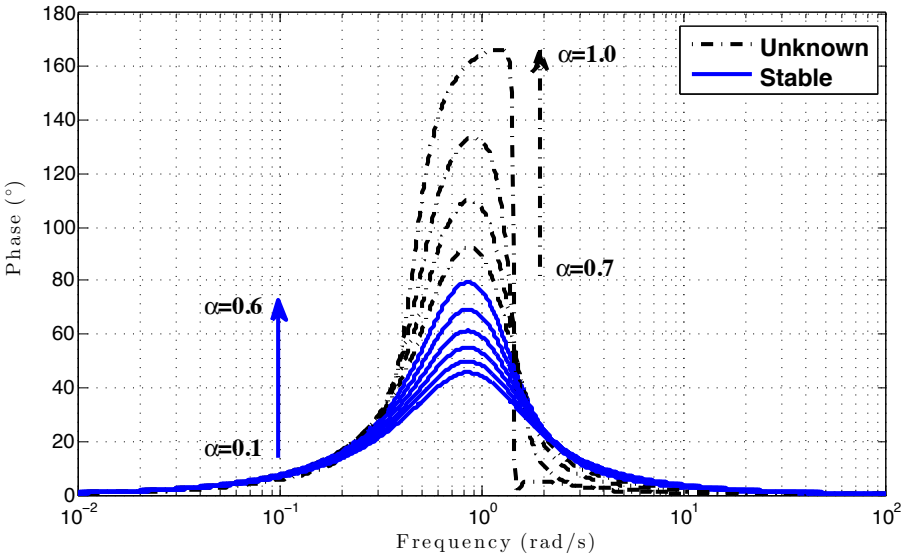

FIGURE 5.1: Phase differences of characteristic polynomials of system in Example 5.1 for different values of its order α, $0 < \alpha \leq 1$

Example 5.2. *Now, consider the switching system given by (5.11) with* $L = 2$ *with the following parameters:* $A_1 = \begin{bmatrix} -0.2 & -1.0 \\ 0.01 & -0.1 \end{bmatrix}$, $A_2 = \begin{bmatrix} -0.3 & 0.01 \\ -1.0 & -0.1 \end{bmatrix}$ *and order* α, $1 < \alpha < 2$.

It is easy to find that the subsystem 1 is stable for $\alpha \in (1, 1.67)$, whereas the subsystem 2 is stable for all values of $\alpha \in (1, 2)$. Therefore, applying Theorem 5.18 when $\alpha \in (1, 1.67)$, the following condition

$$\left| \arg\left(\det\left(\begin{bmatrix} 0.03 - \omega^2 + j0.4\omega \sin\phi & 0.3 + j2\omega \sin\phi \\ -0.003 - j0.02\omega \sin\phi & -\omega^2 + j0.2\omega \sin\phi) \end{bmatrix} \right) \right) - \arg\left(\det\left(\begin{bmatrix} 0.08 - \omega^2 + j0.6\omega \sin\phi & -0.004 - j0.02\omega \sin\phi \\ 0.4 + j2\omega \sin\phi & -\omega^2 + j0.2\omega \sin\phi) \end{bmatrix} \right) \right) \right| < \frac{\pi}{2}, \forall\omega \quad (5.40)$$

should be satisfied, $\forall\ \alpha$, $1 < \alpha < 1.67$. The phase difference (5.40) is depicted in Fig. 5.7(a). In order to make the results clearer, the maximum values of (5.40) are also are plotted in Fig. 5.7(b) versus the order of the system. It can be seen that the

system is stable if $\alpha \in (1, 1.65)$. The stability of the system when $\alpha \in [1.65, 1.67)$ is unknown.

Next, we will see the application developed stability theorems in of the reset control systems.

Example 5.3. *Stability analysis of a fractional-order system controlled by FCI*

Let us consider a plant, $P(s) = 1/s$, controlled by an $\text{FCI}^{0.5}$ in negative feedback without exogenous inputs. Therefore, the closed-loop system can be represented by in augmented state space form as follows (see [108])

$$D^{0.5}x_p(t) = \begin{bmatrix} 0 & 1 \\ 0 & 0 \end{bmatrix} x_p(t).$$

If the state vector is $x(t) = (x_p(t), x_r(t))^T$ with $x_p(t) = (x_{p_1}(t), x_{p_2}(t))^T$ being the plant state and $x_r(t)$, the (reset) controller state, then it results in a reset system like that in (3.40) with

$$A_{cl} = \begin{bmatrix} 0 & 1 & 0 \\ 0 & 0 & 1 \\ -1 & 0 & 0 \end{bmatrix}, \; A_R = \begin{bmatrix} 1 & 0 & 0 \\ 0 & 1 & 0 \\ 0 & 0 & 0 \end{bmatrix}, \; C_{cl} = \begin{bmatrix} 1 & 0 & 0 \end{bmatrix}.$$

In addition, from (5.31), H_β is simply given by (for this case $n_{\mathcal{R}} = 1$ and then $P_{\mathcal{R}} = 1$ without loss of generality):

$$H_\beta(s) = \begin{bmatrix} \beta & 0 & 1 \end{bmatrix} \begin{bmatrix} s + 0.45 & -0.84 & -0.29 \\ 0.29 & s + 0.45 & -0.84 \\ 0.84 & 0.29 & s + 0.45 \end{bmatrix}^{-1} \begin{bmatrix} 0 \\ 0 \\ 1 \end{bmatrix}$$

$$= \frac{(s^2 + 0.9s + 0.45) + \beta(0.29s + 0.84)}{s^3 + 1.35s^2 + 1.35s + 1}.$$

Finally, $Re\left(H_\beta(j\omega)\right) > 0, \forall \omega > 0$ for $-0.53 \leq \beta \leq 0.79$, which means that the system is SPR. The phase equivalence of (5.4) is shown in Fig. 5.8. As observe, $|\arg(H_\beta(j\omega))| < \frac{\pi}{2}$ for all finite $\omega > 0$ and $\beta = 0.3$, which proves the stability of fractional-order reset system studied in this example.

Example 5.4. *Stability analysis of Example 4.4*

Let us go back to Example 4.4 and analyze the stability of the system when applying FORE, CI and FCI. For FORE controller, the integer-order closed-loop system can be given by:

$$\begin{cases} \dot{x} = A_{cl}x = \begin{bmatrix} 0 & 1 & 0 \\ 0 & -0.2 & 1 \\ -1 & -1 & -b \end{bmatrix} x(t) \\ x(t^+) = A_R x = \begin{bmatrix} 1 & 0 & 0 \\ 0 & 1 & 0 \\ 0 & 0 & 0 \end{bmatrix} x(t) \\ y = C_{cl}x = \begin{bmatrix} 1 & 1 & 0 \end{bmatrix} x(t) \end{cases}$$

where $x(t) = [x_{p_1}(t), x_{p_2}(t), x_r(t)]^T$. And, the closed-loop system using FCI can be stated as

$$\begin{cases} D^{0.5}\mathcal{X}(t) = \mathbf{A}_{cl}\mathcal{X}(t) = \begin{bmatrix} 0 & 1 & 0 & 0 & 0 \\ 0 & 0 & 1 & 0 & 0 \\ 0 & 0 & 0 & 1 & 0 \\ 0 & 0 & -0.2 & 0 & 1 \\ -1 & 0 & -1 & 0 & 0 \end{bmatrix} \mathcal{X}(t) \\ \mathcal{X}(t^+) = \mathbf{A}_R\mathcal{X}(t) = \begin{bmatrix} I_4 & 0_{4,1} \\ 0_{1,4} & 0 \end{bmatrix} \mathcal{X}(t) \\ y = \mathbf{C}_{cl}\mathcal{X}(t) = \begin{bmatrix} 1 & 0 & 1 & 0 & 0 \end{bmatrix} \mathcal{X}(t) \end{cases}$$

where $\mathcal{X}(t) = [\mathcal{X}_{p_1}(t), \cdots, \mathcal{X}_{p_4}(t), x_r(t)]^T$, $\mathcal{X}_{p_1}(t) = x_{p_1}(t)$, $\mathcal{X}_{p_3}(t) = x_{p_2}(t)$. According to condition (5.31), H_β corresponding to FORE and FCI are simply given by (for both case FORE and FCI $n_{\mathcal{R}} = 1$ and then $P_{\mathcal{R}} = 1$):

$$H_\beta^{FORE}(s) = \begin{bmatrix} \beta & 0 & 1 \end{bmatrix} (sI - A_{cl})^{-1} \begin{bmatrix} 0 \\ 0 \\ 1 \end{bmatrix} =$$

$$\frac{s^2 + 0.2s + 0.8\beta}{s^3 + (b + 0.2)s^2 + (1 + 0.2b)s + 1}, \tag{5.41}$$

and

$$H_{\beta}^{FCI}(s) = \begin{bmatrix} \beta & 0 & \beta & 0 & 1 \end{bmatrix} \left(sI - \left(-\left(-\mathbf{A}_{cl} \right)^{\frac{2}{3}} \right) \right)^{-1} \begin{bmatrix} 0 \\ 0 \\ 0 \\ 0 \\ 1 \end{bmatrix}. \tag{5.42}$$

Therefore, using Theorem 5.24, the closed-loop systems controlled by FORE and FCI are asymptotically stable if $\mathrm{H}_{\beta}^{FORE}(s)$ and $\mathrm{H}_{\beta}^{FCI}(s)$ are SPR. Substituting $b = 1$ in (5.41), the FORE reset system is asymptotically stable for all $0.42 < \beta \leq 1.46$. With respect to CI (similarly to FORE with $b = 0$), stability cannot be guaranteed with this theorem. And applying FCI, it can be easily stated that the system is asymptotically stable for $\beta \leq 0.62$. In addition, the phase equivalences corresponding to (5.41) and (5.42) are shown in Fig. 5.9 for $\beta = 0.5$ and $b = 1$. It can be seen that both phases verifies condition (5.39), which has concordance with the theoretical results.

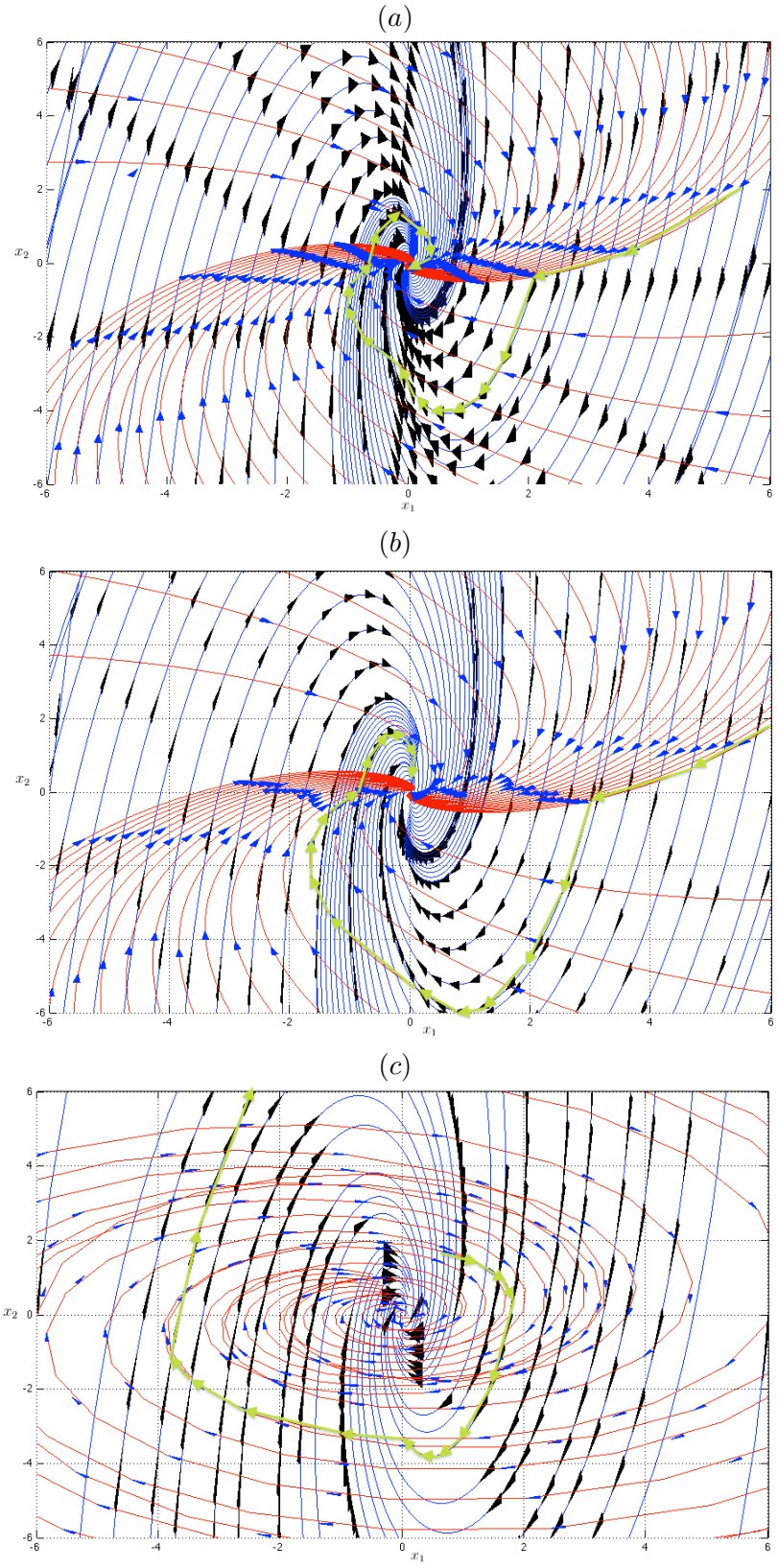

FIGURE 5.2: "Phase portrait of system in Example 5.1 when: (a) $\alpha = 0.6$ (b) $\alpha = 0.8$ (c) $\alpha = 0.9$. The blue trajectory is related to subsystem 1, whereas the red one refers to subsystem 2

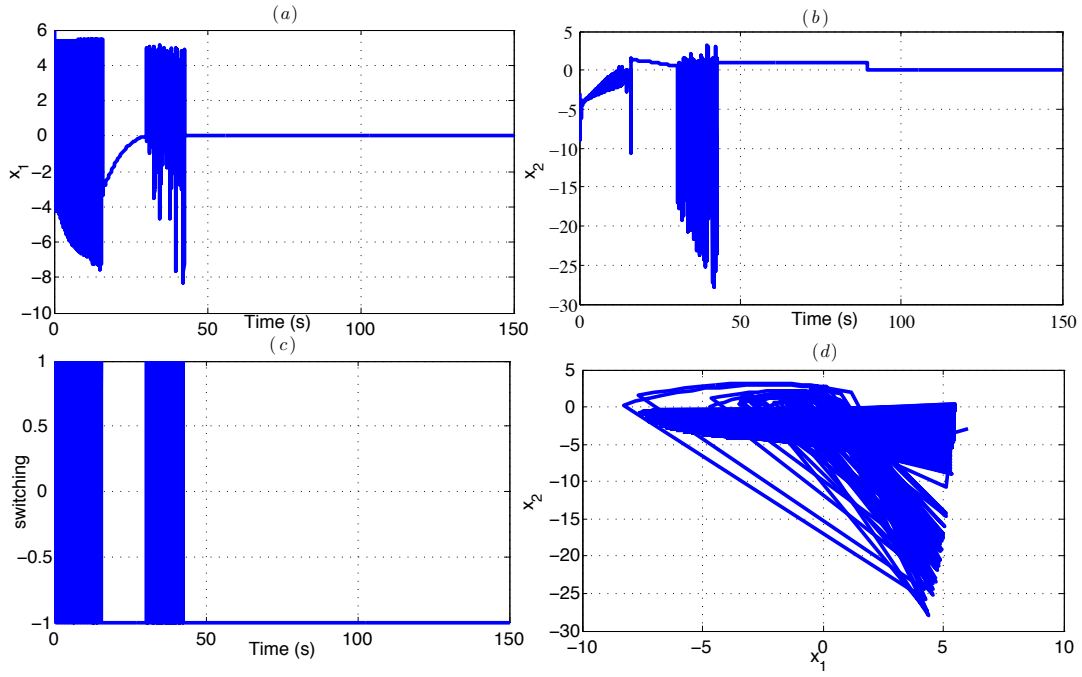

FIGURE 5.3: Response of system in Example 5.1 when $\alpha = 0.6$: (a) Time response of subsystem 1 (b) Time response of subsystem 2 (c) Switching (1 means subsystem 1 is active and -1 means subsystem 2 is active) (d) Phase plane

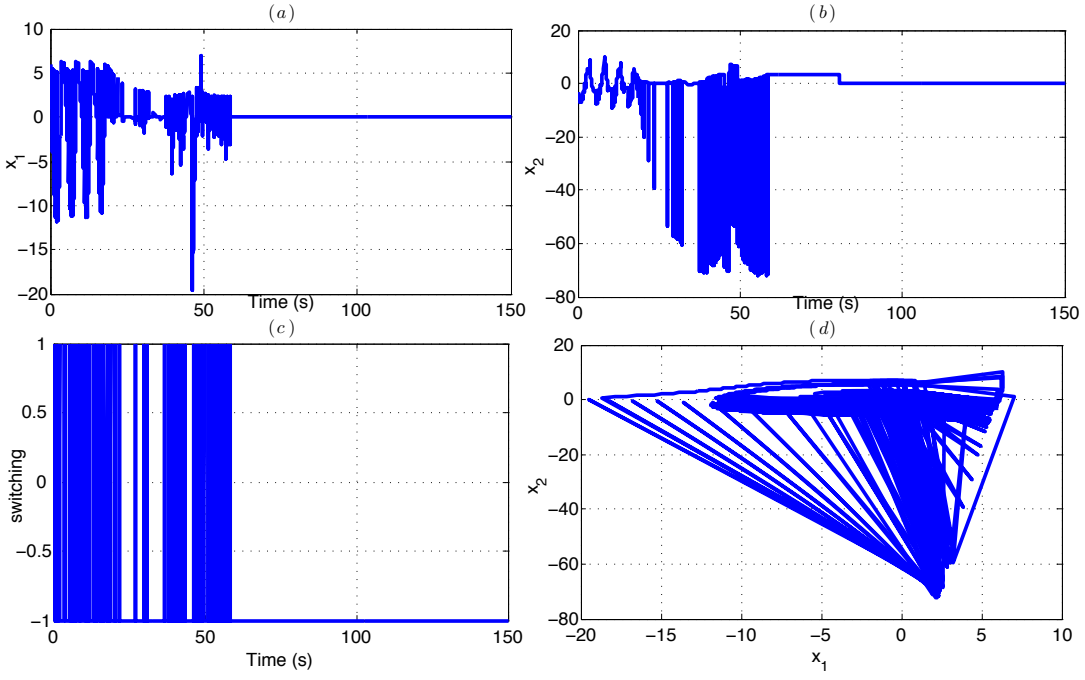

FIGURE 5.4: Response of system in Example 5.1 when $\alpha = 0.8$: (a) Time response of subsystem 1 (b) Time response of subsystem 2 (c) Switching (1 means subsystem 1 is active and -1 means subsystem 2 is active) (d) Phase plane

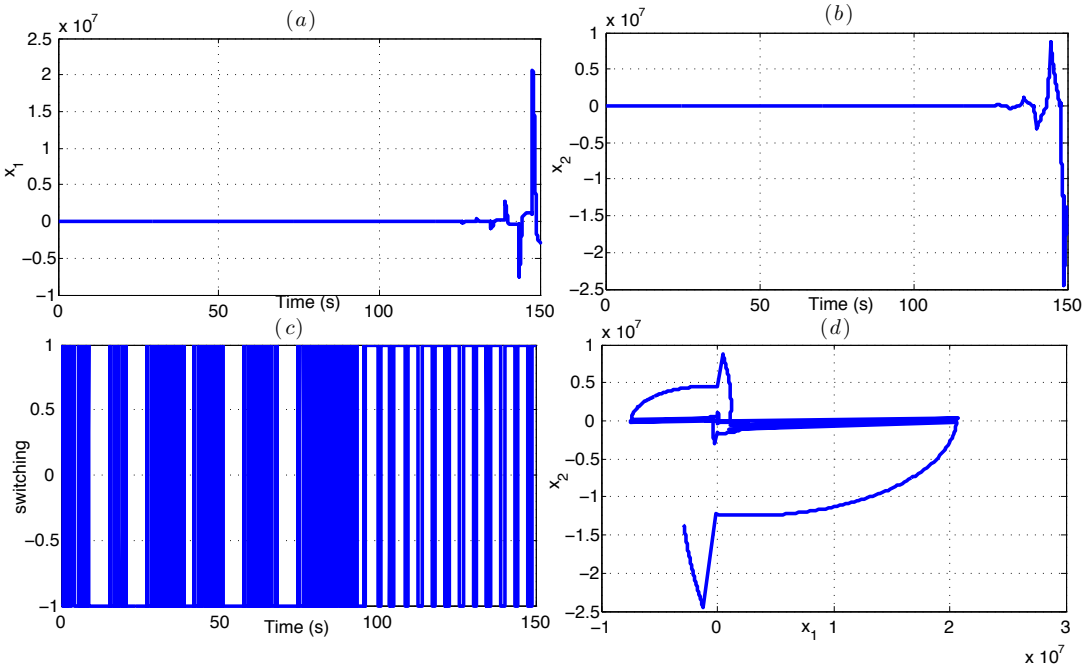

FIGURE 5.5: Response of system in Example 5.1 when $\alpha = 0.9$: (a) Time response of subsystem 1 (b) Time response of subsystem 2 (c) Switching (1 means subsystem 1 is active and -1 means subsystem 2 is active) (d) Phase plane

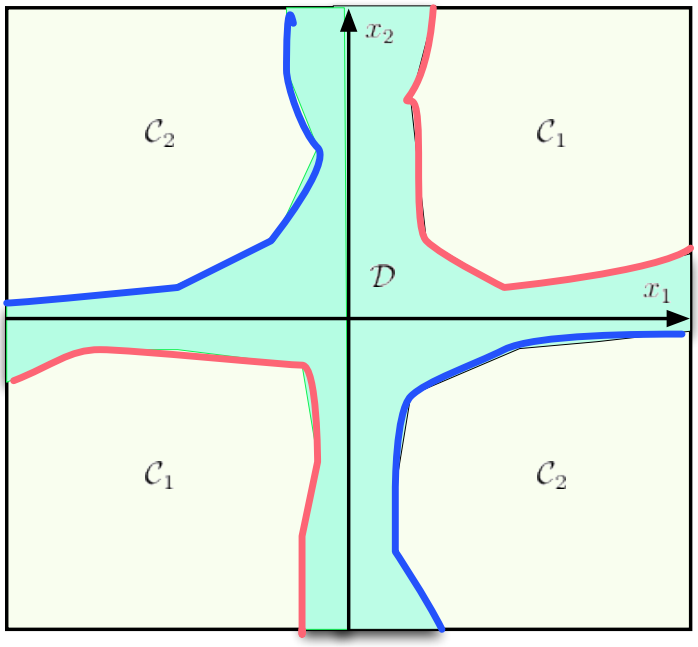

FIGURE 5.6: Switching region for random switching of system in Example 5.1

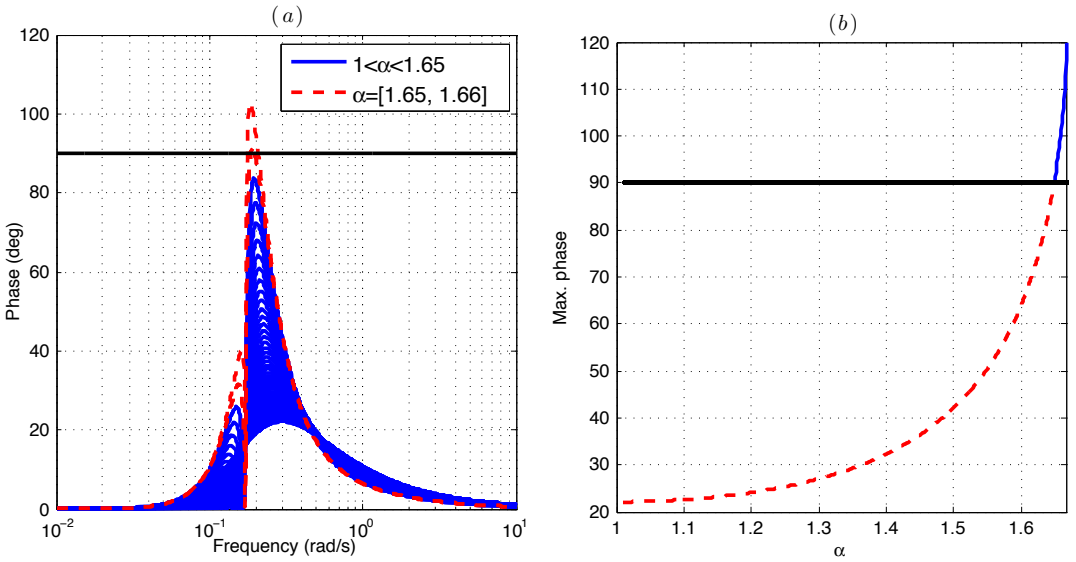

FIGURE 5.7: Stability of the system in Example 5.2 for different values of its order α, $1 < \alpha \leq 2$: (a) Phase difference of condition (5.40) (b) Maximum value of (5.40) versus α

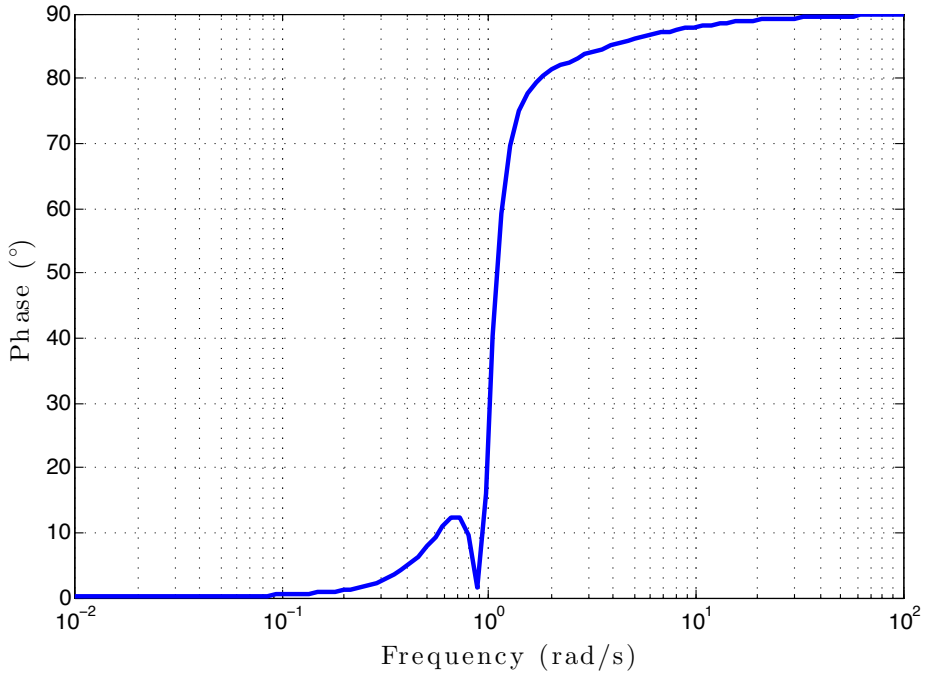

FIGURE 5.8: Phase equivalence of H_β (5.4) in Example 5.3

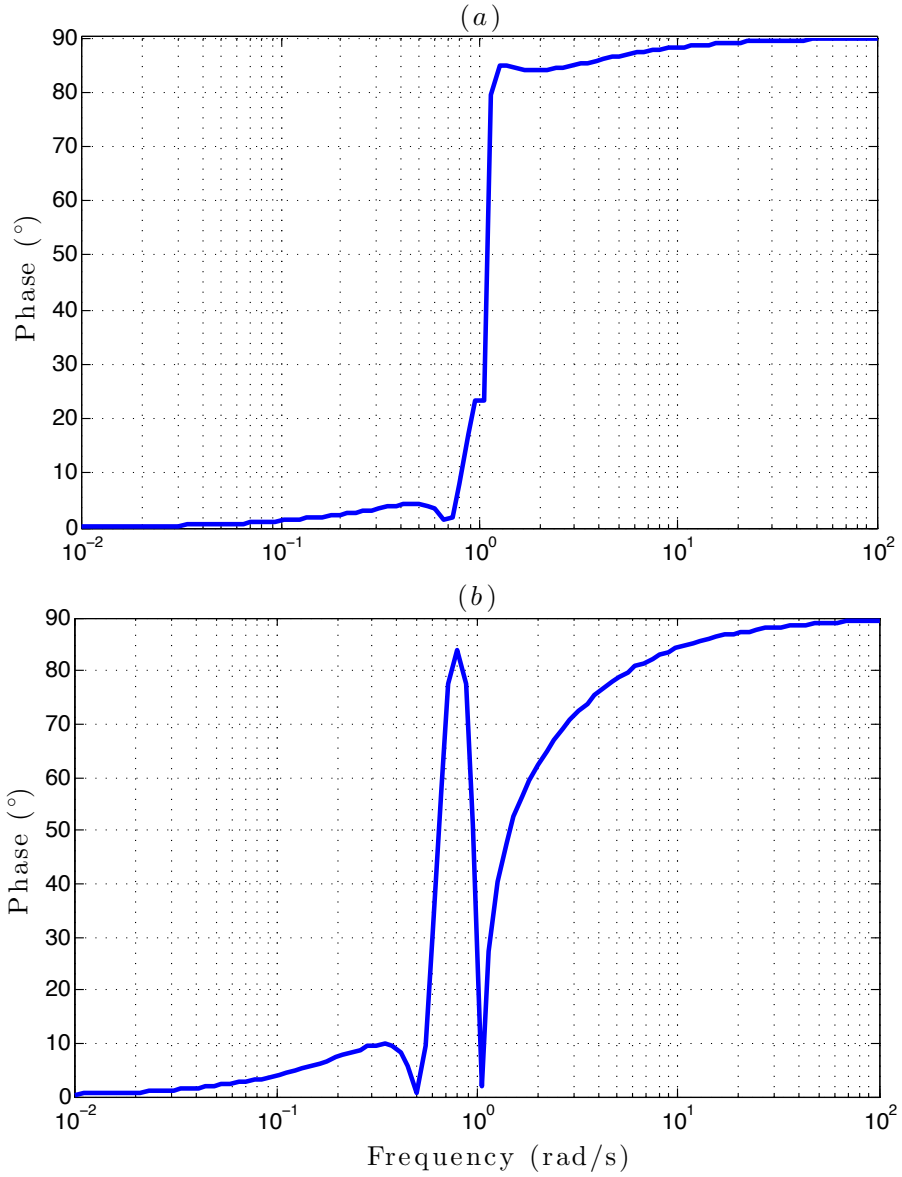

FIGURE 5.9: Phase equivalence of H_β in Example 5.4: (*a*) Applying FCI (*b*) Applying FORE

Chapter 6

Experimental Application of Hybrid Fractional-Order System

6.1 Adaptive Cruise Control at Low Speed

Road transport has virtually absorbed all the growth mobility in recent decades. The considerable increase in the number of vehicles for transportation of people or goods have caused an increase in the number of road fatalities. So governments and automotive manufactures have joined their efforts to try to reduce these figures. Since more than 80% of road accidents are due to the human factor [150], it turns road transport into a suitable candidate to the application of autonomous or semi-autonomous control systems to avoid –or reduce– driver errors. In this context, the development of aid system to advice the driver in advance or even to autonomously manage vehicle's actuators for accident reduction or mitigation is an open field of research.

During last years, significant advances have been carried out in this field. Most of commercial vehicles have included cameras or radars to detect pedestrians [151] or a leading vehicle [152] respectively or even ultrasound sensors for parking assistance [153]. Although these vehicles have included warning devices as head-up displays or audible signals, the last decision remains on the driver. So next step is to turn from warning to automatic devices. Concerning vehicle's automation, one can distinguish between lateral –associated to the steering wheel– or longitudinal –associated to the

brake and throttle pedals– actions. The work presented in this section is focused in the latter.

Automatic speed control –well-known as cruise control (CC) in the literature– was one of the first autonomous system implemented on a vehicle. It involves in regulating the action over the throttle pedal to try to follow a desired speed. A review about first implemented systems with mean errors of 15 km/h with respect to the reference speed can be found in [154]. Subsequent step was the inclusion of the brake pedal in the speed control system. Based on this inclusion and the use of radar system for detecting the leading vehicle, adaptive CC (ACC) systems were implemented for freeways driving [155]. Current research line in speed control is based on vehicle-to-vehicle (V2V) communications in order to reduce the distance between vehicles. These control systems, called cooperative ACC (CACC) [156–158], have been experimentally tested with prototype vehicles (see e.g. [159]).

Controlling the speed of a vehicle is a classic application of control system theory and, as a matter of fact, most of the commercial systems are based on PID controllers because of the proper vehicle's behaviour versus their easy implementation. A review of automated vehicle control techniques can be found in [160]. Although PID can achieve adequate results, advanced control techniques capable of improving their benefits are required in the automotive field. Given this context, in the past few years fractional-order PID controllers, i.e., the generalization of traditional PID to non-integer orders, are recognized to guarantee better closed-loop performance and robustness with respect to the latter controllers –refer to e.g. [71, 161] for fundamentals and benefits of fractional-order control (FOC).

One of the key issues in the longitudinal control is the cooperation and commutation between throttle and brake pedals due to the significant differences between accelerating and braking dynamics of the vehicle. In this context, hybrid control, which is based on the switching between different controllers, can be an accurate approach to achieve stability and provide an effective mechanism to deal with these highly complex systems by combining the advantages of different controllers [10, 14, 162]. Examples of hybrid controllers in the automotive field include applications for automated highway systems [163], motion planning (see e.g. [164–166]), collision avoidance [167], trajectory tracking [15, 168], etc. Even though research in hybrid control has been the object of

an intense and productive research effort in the recent years in the automotive field, from our best knowledge, this is the first time that benefits of fractional hybrid control are used for ACC manœuvres.

Synthesizing hybrid controllers which satisfy multiple control objectives plays an important role in real-time applications, mainly since the switching mechanism has a large influence of the properties of the closed-loop. This problem is discussed in e.g. [34, 169, 170]. Our approach introduces practical restrictions to prevent fast switching between both accelerating and braking modes, as will be explained. Obviously, experimental implementation of fractional-order controllers is also an important consideration (for a current survey on implementation techniques, e.g. refer to [71]). Among them, fractional order controllers will be implemented as digital IIR filters in the experiments.

With these premises, the purpose of this part is threefold. Firstly, to design two fractional-order PI controllers capable of the proper and independent control of the throttle and brake pedals; secondly, to design and implement a hybrid control law for commutation between both pedals in a safe and robust way, including some remarks about hybrid fractional controllers and their application to CC; and finally, to show its experimental feasibility for ACC applications considering two different rules for generating the safe inter-distance between vehicles.

6.1.1 Automatic Vehicle

As commented previously, a production vehicle –a convertible Citroën C3 Pluriel of the AUTOPIA Program at the Center for Automation and Robotics (CAR)– was used to check the CC and ACC manœuvres in practice. This section briefly summarizes the modifications performed in the vehicle to act autonomously on the throttle and brake pedals, as well as its dynamic longitudinal model when accelerating and braking at very low speeds.

6.1.1.1 Description

The vehicle control system for automatic driving follows the classical perception-reasoning-action paradigm [2, 171]. The first stage is in charge of localizing as precisely

and robustly as possible the vehicle. To that end, the following subsystems are embedded in the vehicle:

- A double-frequency global positioning system (GPS) receiver running in real-time kinematic (RTK) carrier phase differential mode that supplies 2 cm of resolution positioning at a refresh rate of 5 Hz.
- A wireless local area network (IEEE 802.11) support, which allows the GPS to receive both positioning error corrections from the GPS base station and vehicle and positioning information from the preceding vehicle.
- An inertial measurement unit (IMU) Crossbow IMU 300CC placed close to the centre of the vehicle to provide positioning information during GPS outages.
- Car odometry supplied by a set of built-in sensors in the wheels, whose measurements can be read by accessing the controller area network (CAN) bus of the vehicle. This is implemented by means of a CAN Card 2.6.

Thereafter, an on-board computer is in charge of requesting values from each of the on-board sensors with which to compute the controller's input values.

Finally, the devices that make possible to act on the throttle and brake of the car are an electrohydraulic system capable of injecting pressure into the car's anti-block braking system (ABS), and an analogue card which can send a signal to the car's internal engine computer to demand acceleration or deceleration. The electro-hydraulic braking system is mounted in parallel with the original one. Two shuttle valves are installed connected to the input of the anti-lock braking system (ABS) in order to keep the two circuits independent. A pressure limiter tube set at 120 bars is installed in the system to avoid damage to the circuits. Two more valves are installed to control the system: a voltage-controlled electro-proportional pilot to regulate the applied pressure, and a spool directional valve to control the activation of the electrohydraulic system by means of a digital signal. These two valves are controlled via an I/O digital-analogue CAN card. The voltage for the applied pressure is limited to 4 V (greater values correspond to hard braking and are not considered). More details can be found in [172].

6.1.1.2 Dynamic longitudinal model

To design the controllers for CC and ACC manœuvres at very low speeds, a model of the automatic vehicle was obtained experimentally when accelerating and braking. However, although obtaining its exact dynamics is impossible, because of the kind of manœuvres planned in this work, there was no need to use a complex model of the vehicle for the circuit in which the experimental manœuvres will be performed. As a result, simple linear models were considered –similar models have been also used in [96, 173]. On the one hand, the vehicle speed when accelerating was simplified as

$$G_1(s) \simeq \frac{4.39}{s + 0.1746}. \tag{6.1}$$

On the other, the vehicle dynamics when braking can be given by an uncertain first order transfer function that depends on the voltage applied to the brake pedal [172]:

$$G_2(s) \simeq \frac{1}{\tau s + 1}, \tag{6.2}$$

where the time constant τ varies with the action over the brake in the interval $\tau \in [1.6, 3.1]$ s. The validation of these models can be found in [110, 112, 116] (for more details see Appendix).

6.1.2 Cruise Control

This section presents the hybrid CC of the vehicle at low speeds based on the different vehicle's dynamics when accelerating and braking. The design of the fractional-order controllers for the throttle and the brake is firstly given and then, the hybrid modelling, control and stability analysis of the system.

6.1.2.1 Design of the fractional-order-Controllers

The most important mechanical and practical requirement of the vehicle to take into account during the design process is to obtain a smooth vehicle's response so as to guarantee its acceleration to be less than the well-known comfort acceleration, i.e., less than 2 m/s^2.

In our previous works [112, 116, 174], some classical and fractional-order PI controllers were designed for CC manœuvres. In this work, the fractional-order PI controller designed in [112] will be used for the throttle action –it was designed to control the throttle and brake pedals, but neglecting the dynamics during braking–, whereas the brake will be controlled by a robust fractional-order PI due to the system uncertainty described previously. The motivation of improving that design by considering a hybrid model of the vehicle mainly arises from its application to ACC manœuvres, in which commutation between pedals plays a key role for the success of the whole –longitudinal and lateral– control.

Consider a fractional-order PI controller of the form

$$C(s) = k_p + \frac{k_i}{s^\alpha}. \tag{6.3}$$

Specifications related to phase margin, gain crossover frequency and output disturbance rejection are going to be considered. Let assume that the gain and phase crossover frequency of the open-loop system are given by ω_{cp} and ω_{cg}, the phase and the gain margins are denoted by ϕ_m and M_g and the output disturbance rejection is defined by a desired value of a sensitivity function $S(s)$ for a desired frequencies range. The three specifications to be fulfilled to achieve stability and robustness are the following:

1. Phase margin specification:

$$\arg\left(C(j\omega_{cp})G(j\omega_{cp})\right)] = -\pi + \phi_m \tag{6.4}$$

$$\arg\left(C(j\omega_{cg})G(j\omega_{cg})\right) = -\pi \tag{6.5}$$

2. Gain crossover frequency specification:

$$|C(j\omega_{cp})G(j\omega_{cp})| = 1 \tag{6.6}$$

$$|C(j\omega_{cg})G(j\omega_{cg})|_{dB} = 1/M_g \tag{6.7}$$

3. Output disturbance rejection:

$$\left|\frac{1}{1 + C(j\omega)G(j\omega)}\right|_{dB} \leq -20 \text{ dB}, \ \omega \leq \omega_s. \tag{6.8}$$

To tune the fractional-order PI controller (6.3) for the throttle, the set of equations (6.4)-(6.6)-(6.8) were solved with the Matlab function *fsolve* for the following specifications: $\phi_m = 90°$, $\omega_{cp} = 0.45$ rad/s and $\omega_s = 0.035$ rad/s. The controller parameters were: $k_p = 0.09$, $k_i = 0.025$ and $\alpha = 0.8$ –the full design of this controller can be found in [112].

With respect to the control of the brake, a fractional-order PI controller robust to variations in the system time constant was required. In accordance with [101], the set of equations (6.4) to (6.7) turned into the following set of four nonlinear equations with four unknown variables –k_p, k_i, α and ω_{cg}–:

$$\tan^{-1}\left(\frac{k_p\omega_{cp}^{\alpha}\sin\frac{\alpha\pi}{2}}{k_i + k_p\omega_{cp}^{\alpha}\cos\frac{\alpha\pi}{2}}\right) - \tan^{-1}(\tau\omega_{cp}) + \frac{(2-\alpha)\pi}{2} - \phi_m = 0, \tag{6.9}$$

$$\tan^{-1}\left(\frac{k_p\omega_{cg}^{\alpha}\sin\frac{\alpha\pi}{2}}{k_i + k_p\omega_{cg}^{\alpha}\cos\frac{\alpha\pi}{2}}\right) - \tan^{-1}(\tau\omega_{cg}) + \frac{(2-\alpha)\pi}{2} = 0, \tag{6.10}$$

$$20\log\left(\frac{\sqrt{(k_i + k_p\omega_{cp}^{\alpha}\cos\frac{\alpha\pi}{2})^2 + (k_p\omega_{cp}^{\alpha}\sin\frac{\alpha\pi}{2})^2}}{\omega_{cp}^{\alpha}\sqrt{(\tau\omega_{cp})^2+1}}\right) = 0, \tag{6.11}$$

$$20\log\left(\frac{\sqrt{(k_i + k_p\omega_{cg}^{\alpha}\cos\frac{\alpha\pi}{2})^2 + (k_p\omega_{cg}^{\alpha}\sin\frac{\alpha\pi}{2})^2}}{\omega_{cg}^{\alpha}\sqrt{(\tau\omega_{cg})^2+1}}\right) - \frac{1}{M_g} = 0. \tag{6.12}$$

In this case, the Matlab function *fmincon* was used to reach out its solution, which finds the constrained minimum of a function of several variables. Actually, (6.11) was considered as the main function to optimize with (6.9), (6.10) and (6.12) as its constraints. Considering $\phi_m = 90°$, $\omega_{cp} = 0.7$ rad/s and $M_g = 4$ dB as specifications, the obtained controller parameters for the brake control were: $k_p = 0.07$, $k_i = 0.11$ and $\alpha = 0.45$. Figure 6.1 shows the Bode diagrams of the vehicle when braking with the designed PI$^{\alpha}$ controller. It can be observed that $\omega_{cp} = 0.7$ rad/s and $\phi_m = 93°$, which fulfil the design specifications with robustness to variations of system time constant τ.

6.1.2.2 Hybrid Control

In a hybrid dynamic system, state sometimes flows (continuously) while at other times it makes jumps. Whether a flow or a jump occurs, the state of the system depends on its location in the state space. Thus, a hybrid dynamic system is usually described by two functions, f and g, and two sets, C and D. The function f generates a differential

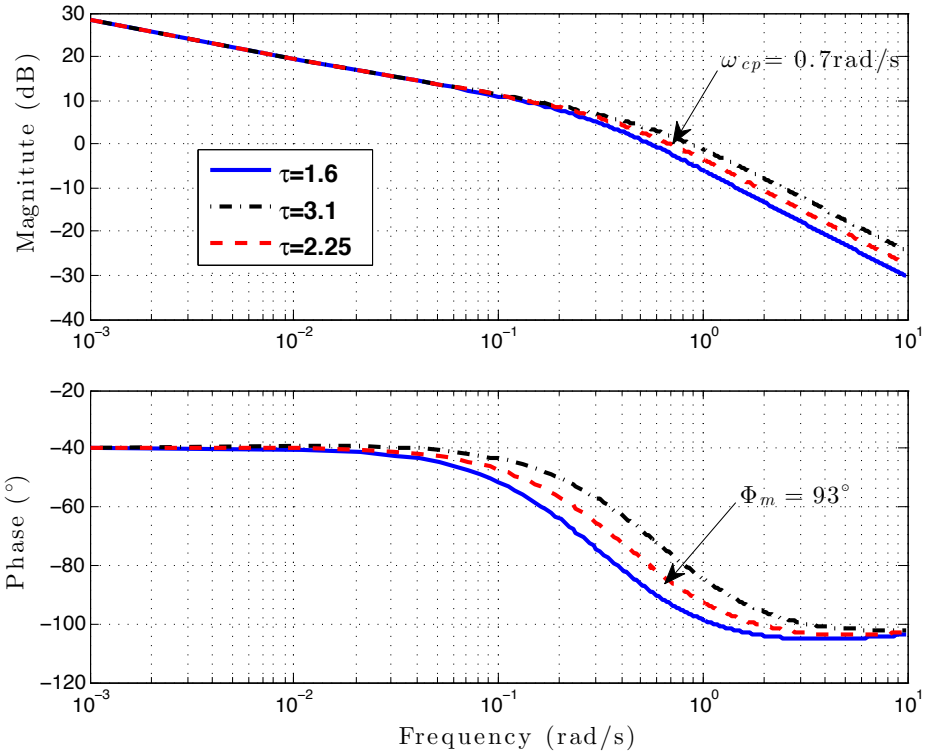

FIGURE 6.1: Bode diagrams of the vehicle controlled by applying the designed PI^{α} brake controller with different values of the time constant τ for the brake

equation that governs the flow, and the function g generates a reset equation that governs jumps. The function f is often only specified for variables that can flow, whereas the function g is often only specified for variables that can jump. The set C indicates where flow may occur in the state space, whereas the set D refers to the same for jumps. Where these sets overlap, both flowing and jumping may be possible.

To model the control of the vehicle as a hybrid system, let describe both the system and the controllers by their transfer functions as follows:

$$G_q(s) = \frac{K_q}{s + T_q}, \tag{6.13}$$

$$C_q(s) = k_{p_q} + \frac{k_{i_q}}{s^{\alpha_q}}, \tag{6.14}$$

where q, $q = 1, 2$, refers to the throttle and the brake actions, respectively, and with the parameters given in Table 6.1. Thus, the closed-loop transfer function of the system can be written as:

$$\frac{Y(s)}{R(s)} = \frac{\gamma_q s^{\alpha_q} + \beta_q}{s^{\alpha_q+1} + (T_q + \gamma_q)s^{\alpha_q} + \beta_q}, \ q = 1, 2, \tag{6.15}$$

where $\gamma_q = K_q k_{p_q}$ and $\beta_q = K_q k_{i_q}$. Using an approximation of order n for the term s^{α_q} as $s^{\alpha_q} = \frac{a_n^q s^n + \cdots + a_1^q s + a_0^q}{b_n^q s^n + \cdots + b_1^q s + b_0^q}$, transfer function (6.15) can be rewritten as:

$$\frac{Y(s)}{R(s)} = \frac{\mathbf{a}_n^q s^n + \cdots + \mathbf{a}_1^q s + \mathbf{a}_0^q}{s^{n+1} + \mathbf{b}_n^q s^n + \cdots + \mathbf{b}_1^q s + \mathbf{b}_0^q}, q = 1, 2, \tag{6.16}$$

where $\mathbf{a}_n^q = \gamma_q + \beta_q \frac{b_n^q}{a_n^q}$ and $\mathbf{b}_n^q = \frac{a_{n-1}^q}{a_n^q} + (T_q + \gamma_q) + \beta_q \frac{b_n^q}{a_n^q}$.

TABLE 6.1: Parameters of the transfer functions of the system –throttle and brake– and the controllers

	K_q	T_q	k_{p_q}	k_{i_q}	α_q
Throttle ($q = 1$)	4.39	0.175	0.09	0.025	0.8
Brake ($q = 2$)	$1/\tau$	$1/\tau$	0.07	0.11	0.45

TABLE 6.2: Coefficients of the characteristic polynomials $c_q(s)$

	$b_7 \times 10^3$	$b_6 \times 10^5$	$b_5 \times 10^5$	$b_4 \times 10^5$	$b_3 \times 10^5$	$b_2 \times 10^4$	b_1	b_0
Throttle ($q = 1$)	1.206	1.064	6.292	5.293	1.715	1.366	132.5	0.088
Brake ($q = 2$)	1.266	1.737	15.77	13.43	3.48	1.463	56.41	0.015

Therefore, (6.16) can be represented in state space formulation as follows:

$$\dot{x} = \mathbf{A}_q x + \mathbf{B}_q r(t),$$

$$y = \mathbf{C}_q x, \tag{6.17}$$

being $\mathbf{A}_q = \begin{bmatrix} -\mathbf{b}_n & -\mathbf{b}_{n-1} & \cdots & -\mathbf{b}_1 & -\mathbf{b}_0 \\ 1 & 0 & \cdots & 0 & 0 \\ 0 & 1 & \cdots & 0 & 0 \\ \vdots & \vdots & \ddots & \vdots & \vdots \\ 0 & 0 & \cdots & 1 & 0 \end{bmatrix}$, $\mathbf{B}_q = \begin{bmatrix} 1 \\ 0 \\ 0 \\ \vdots \\ 0 \end{bmatrix}$, $\mathbf{C}_q = \begin{bmatrix} \mathbf{a}_N^q & \mathbf{a}_{N-1}^q & \cdots & \mathbf{a}_0^q \end{bmatrix}$

and $x = \begin{bmatrix} x_1 & x_2 & \cdots & x_n \end{bmatrix}^T$.

Let denote $V_{ref}(t)$ and $V(t)$ as the reference and actual velocities of the vehicle –will be referred to as $r(t)$ and $y(t)$, respectively– and e as the velocity error, i.e., $e = r(t) - y(t)$. Now assume that the controller C_1 will be activated if $e > -\varepsilon$ and the other controller

C_2, when $e =< \varepsilon$. Thus, the flow set and the flow map are taken to be, respectively,

$$\begin{bmatrix} \dot{x} \\ \dot{q} \end{bmatrix} = \begin{bmatrix} \mathbf{A}_q x + \mathbf{B}_q r_q(t) \\ 0 \end{bmatrix}, \tag{6.18}$$

$$\mathcal{C} := \left\{ (x, q) \in \mathbb{R}^{\alpha_q + 1} \times \{1, 2\} \, | q = 1 \& \; y(t) < r(t) + \varepsilon \text{ or } q = 2 \; \& \; y(t) > r(t) - \varepsilon \right\}.$$

Likewise, the jump set is

$$\mathcal{D} := \left\{ (x, q) \in \mathbb{R}^{\alpha_q + 1} \times \{1, 2\} \, | q = 1 \; \& \; y(t) = r(t) + \varepsilon \text{ or } q = 2 \; \& \; y(t) = r(t) - \varepsilon \right\}.$$

In what concerns the jump map, since the role of jump changes is to toggle the logic mode and the state component x does not change during jumps, it will be

$$\begin{bmatrix} x \\ q \end{bmatrix}^+ = \begin{bmatrix} x \\ 3 - q \end{bmatrix}. \tag{6.19}$$

Figure 6.2 shows the switching between throttle and brake actions corresponding to $\varepsilon = 0$, in which S_1 and S_2 represent the region when the throttle and the brake is active, respectively. It can be seen that the system is stable during switching between throttle and brake actions.

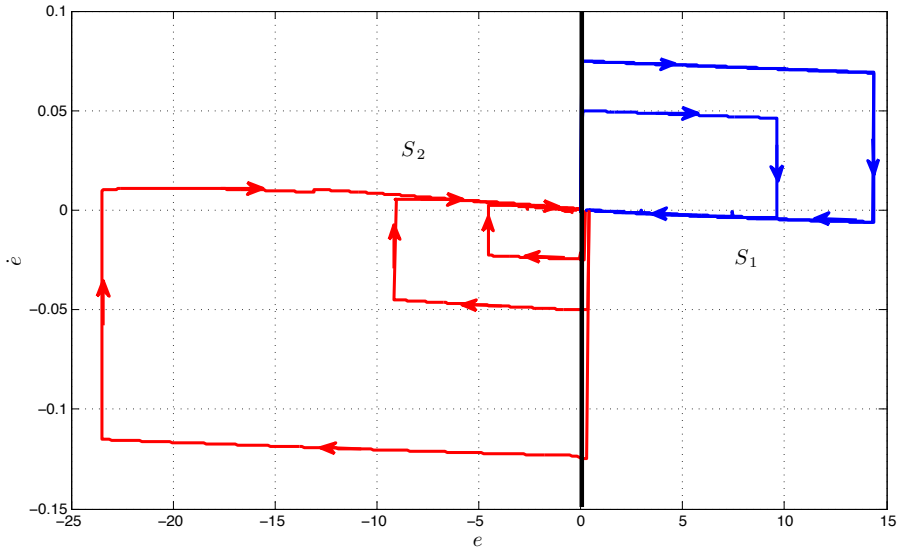

FIGURE 6.2: Switching phases for the throttle and brake actions

In order to analyse the stability of the hybrid system, the frequency domain method

proposed in [41] is going to be used. To this respect, the system has to be described as a switching system. So, let us represent hybrid system (6.17) as switching as follows:

$$\dot{x} = \mathbf{A}x, \;\; \mathbf{A} \in co\left\{\mathbf{A}_1, \mathbf{A}_2\right\}, \tag{6.20}$$

where *co* denotes a convex combination, $\mathbf{A_q}$ are the switching subsystems, and its characteristic polynomials of order $n+1$ as:

$$c_q(s) = s^{n+1} + \mathbf{b}_n^q s^n + \cdots + \mathbf{b}_1^q s + \mathbf{b}_0^q. \tag{6.21}$$

A system described by (6.20) is quadratically stable if and only if there exists a matrix $P = P^T > 0$, $P \in \mathbb{R}^n \times n$, such that $\mathbf{A}_q^T P + P\mathbf{A}_q < 0$, $\forall q = 1, ..., L$ [134]. And, equivalently in the frequency domain, system (6.20) is quadratically stable if and only if

$$|\arg(c_1(j\omega)) - \arg(c_2(j\omega))| < \frac{\pi}{2}, \forall\omega, \tag{6.22}$$

where $c_1(s)$ and $c_2(s)$ are two stable polynomials of order $n+1$ corresponding to the subsystems $\dot{x} = \mathbf{A_1}x$ and $\dot{x} = \mathbf{A_2}x$, respectively [41].

For the vehicle, the coefficients of the characteristic polynomials for the closed-loop system (6.16) are given in Table 6.2. Figure 6.3 shows the phase difference of the previous polynomials when applying condition (6.22) for different values of the time constant τ in the brake dynamics. As observed, the phase difference is less than 90° independently of τ, which prove the quadratic stability of the controlled system taking into account the uncertainty in the brake dynamics. Note that $s^{(\alpha_q)}$, $q = 1, 2$, were approximated by 8th integer-order polynomials using the modified Oustaloup's method in the frequency range $[0.001, 1000]$ rad/s (see e.g. [71]).

6.1.3 Adaptive Cruise Control

This section addresses ACC manœuvres with two different distance policies considering two cooperating vehicles –one manual, the leader, and another automatic– at very low speeds (see a scheme in Figure 6.4). The objective is to act the throttle and the brake of the automatic vehicle to track as precisely as possible both a desired distance between the two vehicles (inter-distance) and a target relative velocity. Actually, a

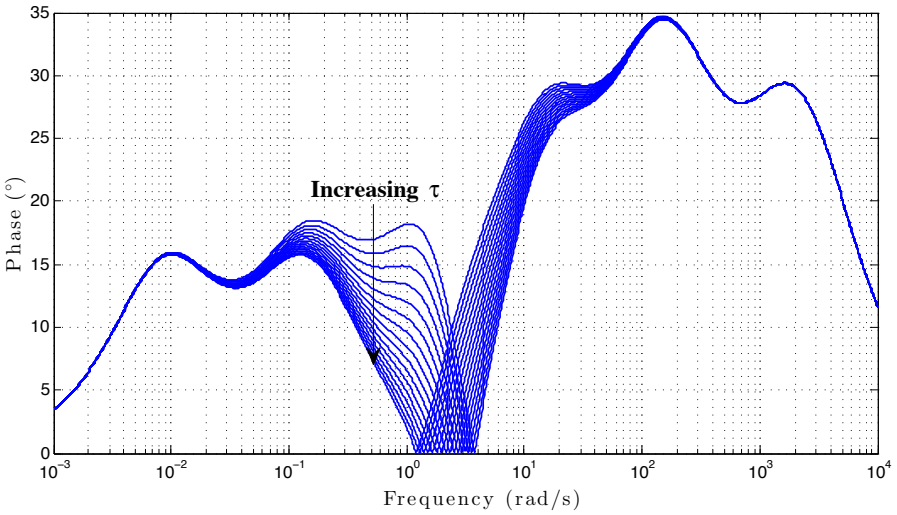

FIGURE 6.3: Phase differences between the characteristic polynomials of the closed-loop system

classical PD controller will be designed to perform the inter-distance control, whereas the previously designed hybrid fractional-order control will be used for the longitudinal control of the automatic vehicle. Thus, at least two control law regimes are needed: one for the desired velocity tracking (problem studied in Section 6.1.2) and the other which tracks a desired following distance between the leader vehicle and a detected lead vehicle.

6.1.3.1 Inter-distance Policies

In ACC, it is necessary to set the inter-distance in a safe distance, which is called safe inter-distance, d_r, and will be the reference distance for the control. Although different strategies have been proposed in the literature to obtain d_r, we will focus on the distance policies reported in [175] and [1] mainly due to their success.

In accordance with [175], d_r has been calculated as the minimal distance to avoid a collision if the preceding vehicle were to act unpredictably:

$$d_r = hV + d_c + l_v, \tag{6.23}$$

which is known as constant-time headway policy, where l_v is the vehicle length, d_c is the minimal inter-distance to avoid collision, V is vehicle velocity and h is the constant-time headway, which is specified by the driver. No collision can occur if the following

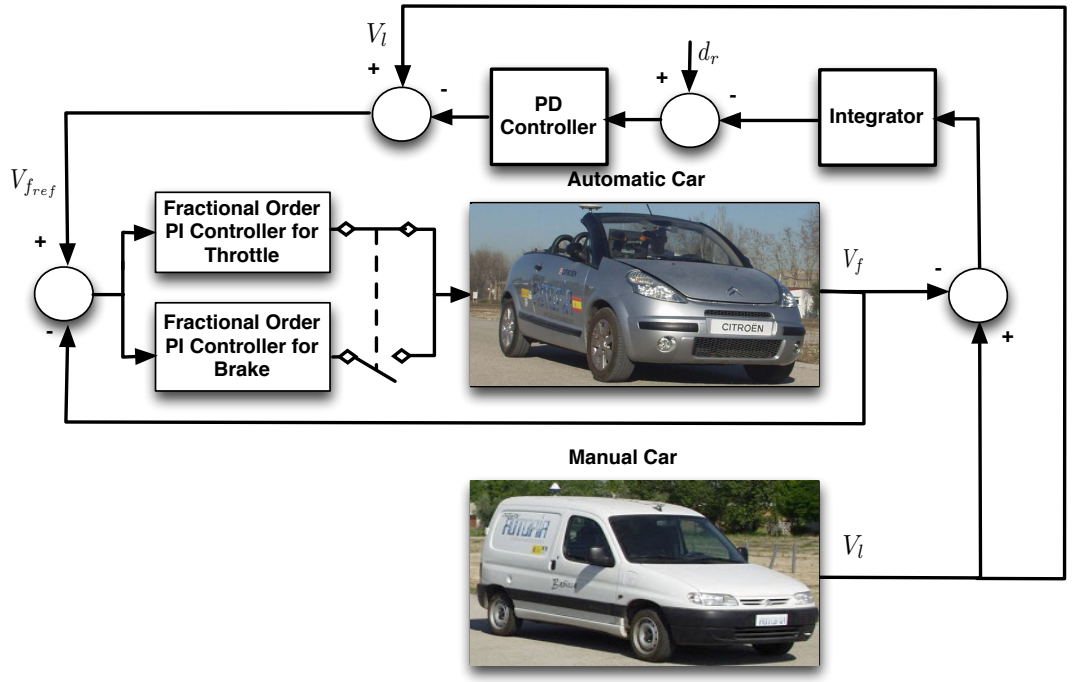

FIGURE 6.4: Scheme of ACC manœuvres with the two Citroën vehicles

condition is satisfied [176]:

$$h \geq \frac{2\gamma_{max}}{J_{max}}, \tag{6.24}$$

where γ_{max} and J_{max} are the maximum attainable vehicle's acceleration and the maximum driver desired jerk, respectively.

On the other hand, a safe inter-distance policy is proposed in [1] in such a way control could be designed independently of the vehicle's model, permitting the additional control loop only be responsible of the model-matching between the actual system and the desired reference dynamics. As shown in Fig. 6.5, the dynamic reference model will provide a reference inter-distance less than the 2-s headway rule if the allowed maximum acceleration is high enough. In particular, the inter-distance reference model describes the virtual dynamics of a vehicle which is positioned at a reference distance d_r from the leading vehicle as follows:

$$\begin{aligned} \dot{d}_r &= c(d_0 - d_r)^2 + x_q(t) - \beta, \\ \beta &= \dot{x}_f(0) + c(d_0 - d_r(0))^2, \end{aligned} \tag{6.25}$$

where d_0 is the nominal safe inter-distance, c plays the role of a damping constant – from a nonlinear model–, x_l is the position of the leading vehicle and $\dot{x_f}$ is the velocity of the follower. Note that all l and f subscripts refer to leading and following vehicles, respectively.

It should be remarked that both inter-distance policies (6.23) and (6.25) satisfy the following comfort and safety constraints: (i) $d_r \geqslant d_c$, (ii) $|V_f| \leqslant \gamma_{max}$ and (iii) $\left|\ddot{V_f}\right| \leqslant J_{max}$. They are taken to represent the worst case scenario in an emergency and limitations on the response of the traction and braking systems in the vehicle, as well as what is physiologically tolerable for the occupants.

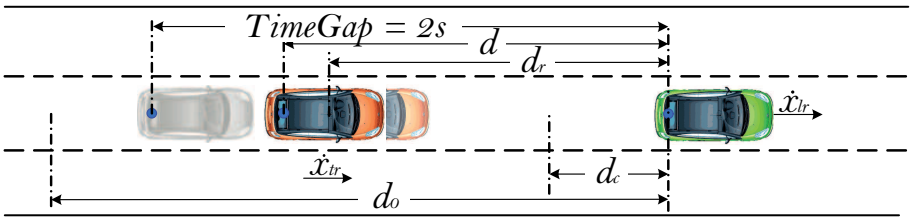

FIGURE 6.5: Stop & go scheme (reproduced from [1])

6.1.3.2 Design of the Inter-distance Controller

In this section, a classical PD controller is going to be designed in order to obtain the reference speed for the following vehicle and guarantee the tracking of d_r, which will be generated with the aforementioned policies.

A block diagram of the closed-loop control to be performed in the vehicle is illustrated in Figure 6.6. The inner loop system can be expressed as:

$$F(s) = C_d(s)G_c(s)G_d(s),$$

where C_d, G_c and G_d denote the transfer functions of PD controller, the closed-loop longitudinal control and a traditional integrator, respectively, i.e.,

$$C_d(s) = k_p + k_d s, \tag{6.26}$$

$$G_c(s) = \frac{C_q(s)G_q(s)}{1 + C_q(s)G_q(s)}, \tag{6.27}$$

$$G_d(s) = \frac{1}{s}. \tag{6.28}$$

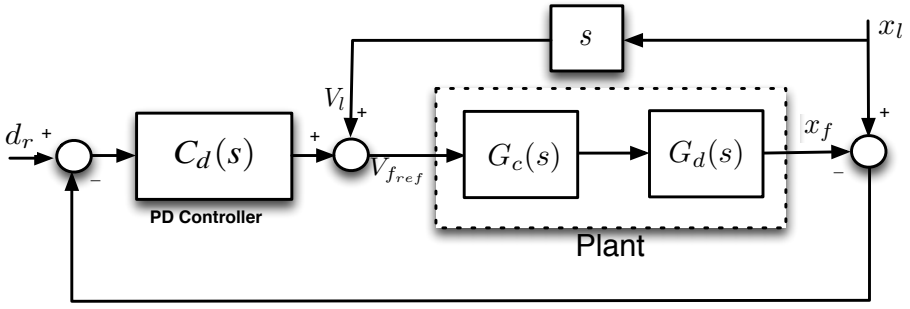

FIGURE 6.6: Scheme of the closed-loop control of the automatic vehicle for ACC manœuvres

In order to design a unique PD for the two inner-loop systems because of the brake and throttle dynamics, the system with lower phase margin was considered: the dynamics when throttle is active. Considering the following design specifications for the inner loop:

$$\arg\left(F(j\omega_{cp})\right) = -\pi + \phi_m, \tag{6.29}$$

$$|F(j\omega_{cp})| = 0 \text{ dB}, \tag{6.30}$$

with $\phi_m > 80°$ and $0.6 < \omega_{cp} < 1$ rad/s, the obtained parameters of PD controller were: $k_p = 0.7$ and $k_d = 1.2$. Bode diagrams depicted in Fig. 6.7 correspond to the closed-loop systems. As seen, both systems fulfil the previous specifications –the controlled throttle and brake systems have phase margins equal to 86° measured at $\omega_{cp} = 0.94$ rad/s and 81° at $\omega_{cp} = 0.62$ rad/s, respectively.

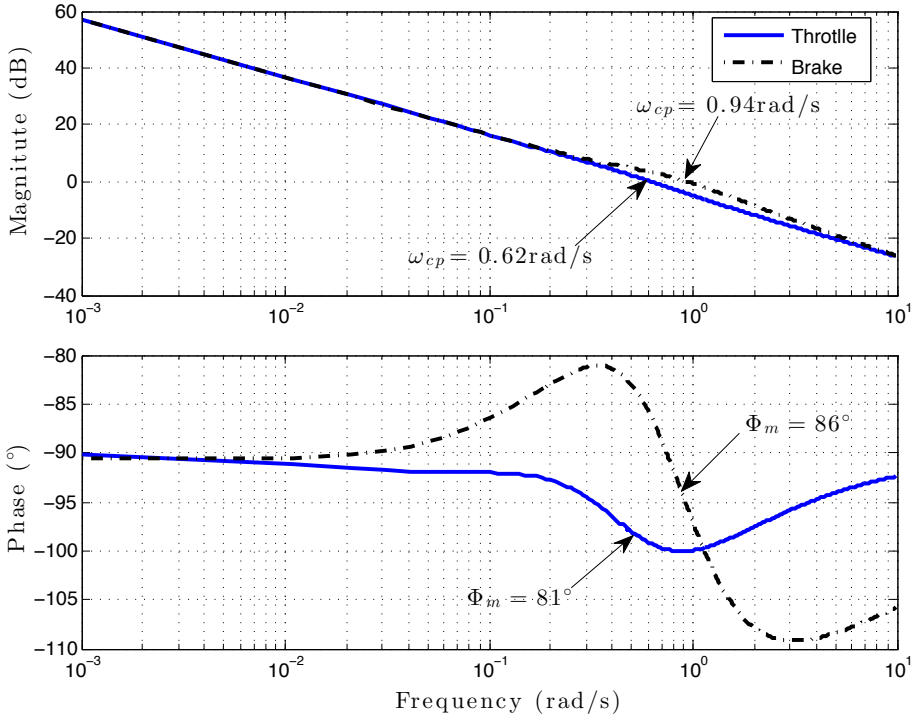

FIGURE 6.7: Bode diagrams of $F(s)$

6.1.4 Simulation and Experimental Results

The real experiments were carried out on the real vehicle in the CAR's private driving circuit, which was designed with scientific purposes, so only experimental vehicles were driven in this area. Two vehicles were used for the experimental phase: a fully-automated vehicle and a manually driven one. As commented, the former is a convertible Citroën C3 Pluriel and is equipped with automatic driving capabilities with hardware modifications made to the throttle and the brake pedal actions. The latter vehicle is an electric Citroën Berlingo van also equipped with automatic driving capabilities. For the purpose of this work, it was driven by a human driver making the leading car's behaviour as close to a real traffic situation as possible. Both vehicles were equipped with RTK-DGPS working at 5 Hz as the main sensor.

This section shows the goodness of the proposed fractional hybrid strategy through simulation and experimental results, grouped into CC and ACC manœuvres. Firstly, the details of how to implement the fractional-order controllers digitally are given. Digital implementation of the fractional-order controller is stated in Appendix.

6.1.4.1 Results for CC Manœuvres

The designed hybrid controller for CC manœuvres was tested by Matlab/Simulink simulations and on the real automatic vehicle for different low velocity references between 5 and 20 km/h. In simulation, a random noise with mean 0.85 was added to the nominal value of $\tau = 2.25$ in order to show the efficiency of the robust controller.

Figure 6.8 shows the behaviour of the vehicle when applying the designed fractional-order hybrid controller; more precisely, velocity tracking, acceleration and normalized control action are included. In Fig. 6.8(a), the solid and dash-dotted lines refer to the experimental and simulated responses, whereas the dotted lines is the velocity reference. Firstly, it is worth mentioning that both the experimental and the simulated behaviours are quite similar, so the considered longitudinal dynamics of the vehicle is good enough for the manœuvres at low speeds. Furthermore, the simulated and experimental vehicle responses are stable and smooth and track the desired reference. In Fig. 6.8(c), both the velocity and the brake control inputs were normalized to the interval $[-1, 1]$, where positive values mean throttle actions –solid line– and the negative, brake ones –dotted line. It can be seen that the acceleration and control action are met the desired intervals. One can also appreciate the soft action over vehicle's actuators obtaining a good comfort for car's occupants-this is reflected in the acceleration values.

To sum up, the fractional-order hybrid control may be useful for autonomous vehicles at low speeds to control both the brake and the throttle actions, specially due to its possibility of obtaining more adjustable time and frequency responses and allowing the fulfilment of more robust performances.

6.1.4.2 Results for ACC Manœuvres

To compare the control with the two inter-distance policies in conditions as equal as possible, a pre-defined route was recorded. This route was first travelled over with the manually driven vehicle, and all the relevant variables to perform the control-position, speed and acceleration were stored. In this way, the human influence in two consecutive trials was removed. The distance between vehicles at the beginning of the test was set

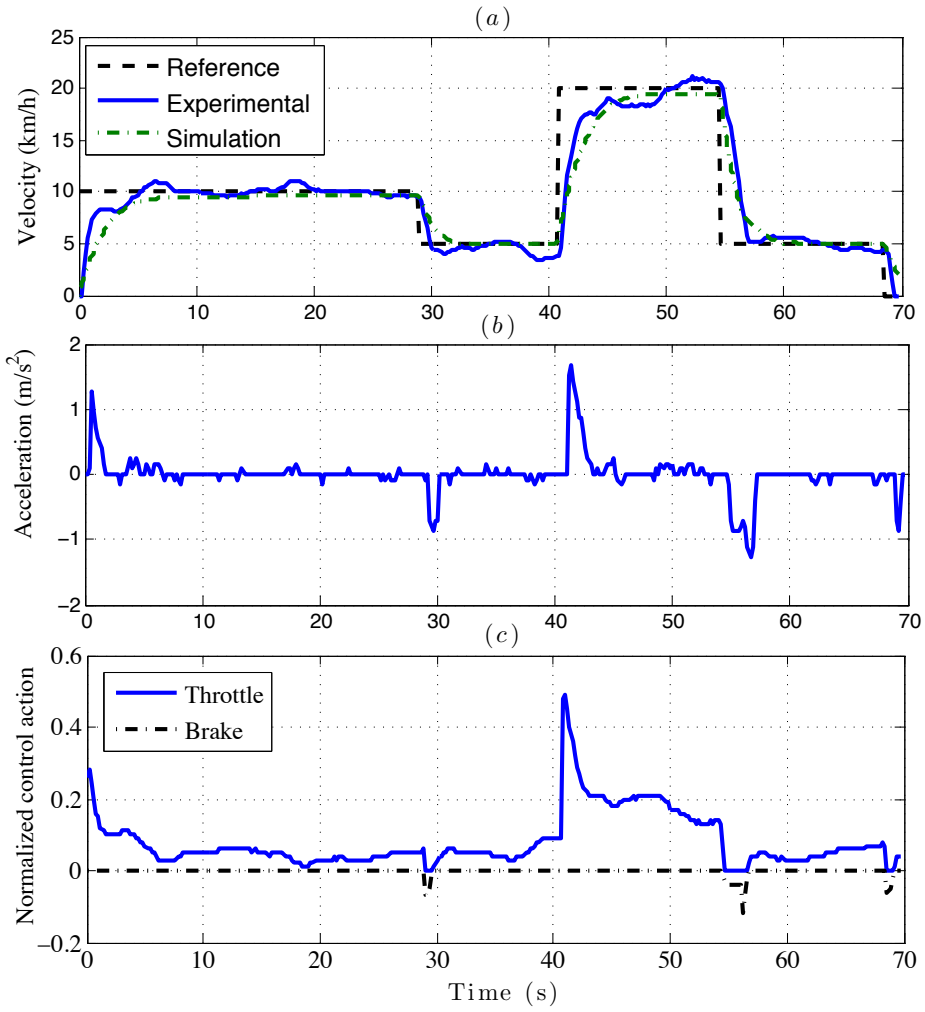

FIGURE 6.8: CC results: (*a*) Velocity (*b*) Acceleration (*c*) Normalized control action

to 6 m. Once this distance was achieved with 1-centimetre accuracy using the RTK-DGPS positioning system, the test was initiated. The inter-distance dynamic models were parametrized to provide: a maximum speed of $V_{max} = 50$ km/h, a maximum acceleration of $\gamma_{max} = 2$ m/s^2, a maximum jerk of $J_{max} = 5$ m/s^3 and a constant-time headway of $h = 0.8$ s.

Figures 6.9 and 6.10 illustrate the behaviour of the automatic vehicle when using the reference inter-distance given by (6.23) –with $d_c + l_v = 6$ m– and (6.25) for ACC manœuvres, respectively. Figure 6.9 and 6.10(a) depict the simulated –thinner red lines– and experimental –thicker blue lines– velocity of the following vehicle with respect to the leading one, which is considered as reference for the former. Only slight differences can be observed between the velocity of the leader and the follower, especially in simulation. In Fig. 6.9 and 6.10(b), the desired and the experimental inter-distances

are represented. As observe, the actual inter-distance tracks the reference inter-distance adequately. Automatic vehicle's acceleration and jerk are shown in Fig. 6.9 and 6.10(c) and (d), whose values are lower than the aforementioned pre-requisites. And finally, Fig. 6.9 and 6.10(e) show the normalized control action. As can be seen, the vehicle behaves efficiently during both acceleration and deceleration, even when the leading car reduces its speed significantly –at time 64 s, the following car properly follows the reference inter-distance as well as the time it increases the speed.

In order to compare the results for the different inter-distance policies, an error function was defined as:

$$J = \frac{1}{T}\int_0^T (|e_{nd}| + |e_v| + u_s)dt, \tag{6.31}$$

where $e_{nd} = d/d_r - 1$ is the normalized inter-distance error (in m), $e_v = V_{f_{ref}} - V_f$ is the velocity error (in km/h) and $u_s = \left|\frac{du}{dt}\right|$ is the control smoothness. Table 6.5 gives the results obtained by both strategies. As can be seen, the inter-distance policy given by (6.25) causes smoother inter-distance and, consequently, the vehicle's behaviour is smoother. On the contrary, using the rule (6.23), the vehicle's performance is poor in comparison with the previous strategy, but may be acceptable for a range of speeds.

For comparison purposes with other strategies reported in the literature, the experimental results in [159] will be taken into account, in which the same route was used for the tests. In that work, it was shown that the maximum value of e_{nd} was obtained at time around 64 s, with a value of 2.56 m. On the contrary, when applying the hybrid controller proposed in this work, the maximum inter-distance error is 0.93 m, which proves the improvement which can be obtained with the designed fractional-order strategy. Moreover, the performance of the automatic vehicle when applying the fractional hybrid controller is significantly better when the leading car's speed is drastically reduced to 0 and then increased, at about time 85 s. Concerning vehicle's acceleration, another advantage of using this fractional strategy is to produce smooth velocity changes and, consequently, small accelerations are attained. To summarize, the tracking error is smaller when applying the fractional-order hybrid controller in comparison with the obtained by the strategies in [159], especially when the desired inter-distance is generated by using the rules suggested in [175]. It is also worth mentioning that the control actions may be soften, but they can be neglected from a perspective of the comfort of the car's occupants.

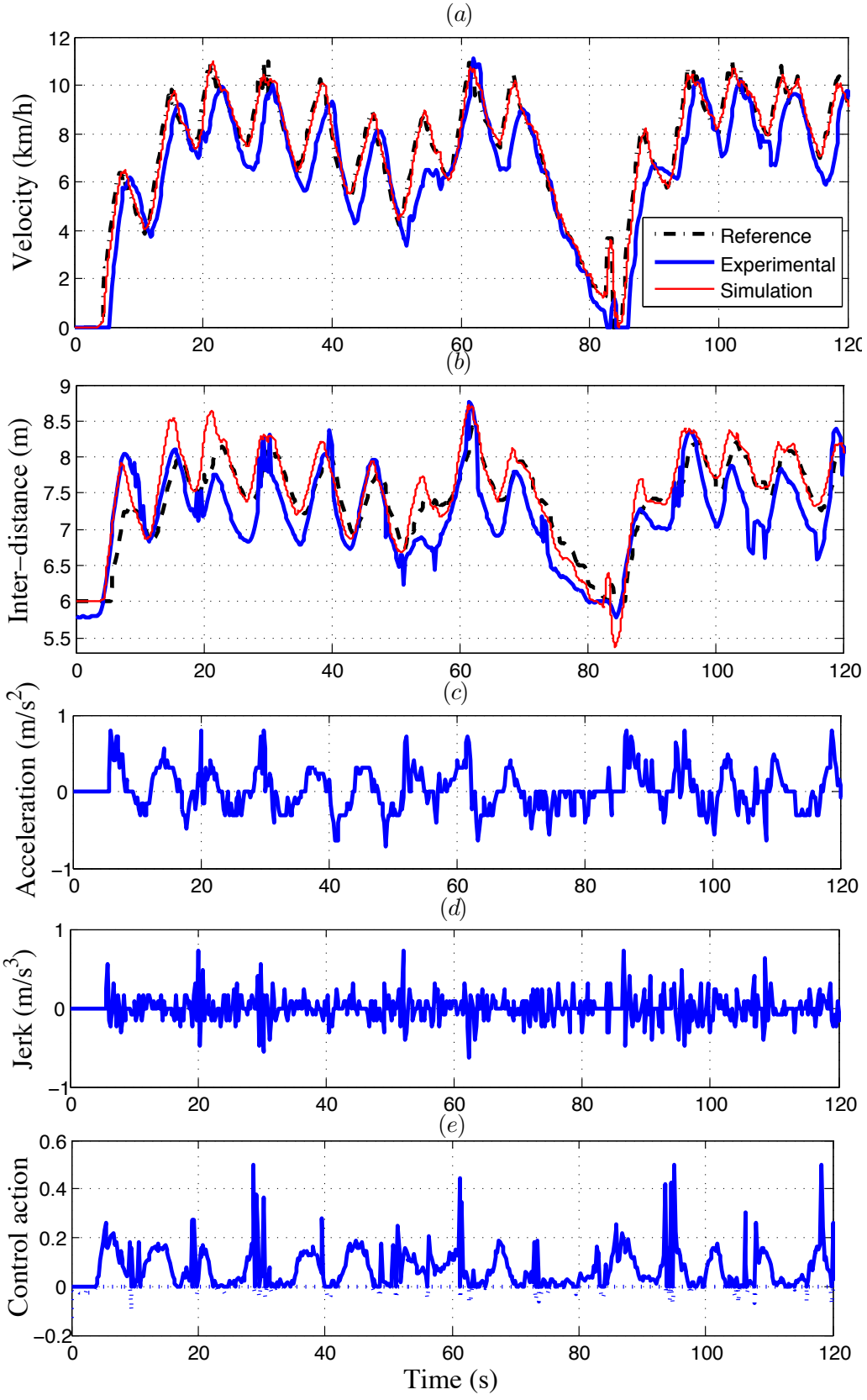

FIGURE 6.9: ACC results using (6.23) as the reference inter-distance ($d_c + l_v = 6$ m): (a) Velocity (b) Inter-distance (c) Acceleration (d) Jerk (e) Normalized control action

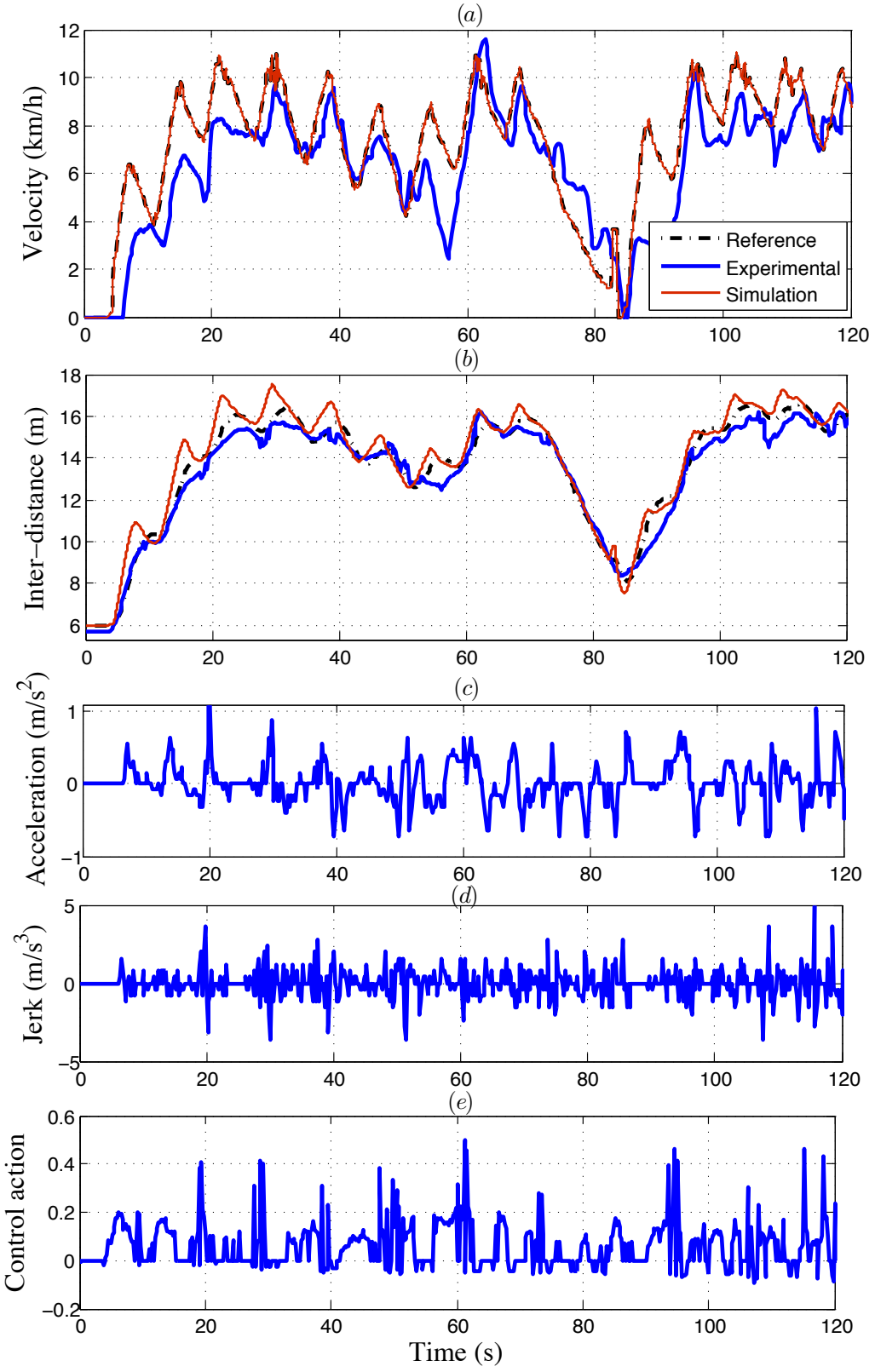

FIGURE 6.10: ACC results using (6.25) as the reference inter-distance: (*a*) Velocity (*b*) Inter-distance (*c*) Acceleration (*d*) Jerk (*e*) Normalized control action

TABLE 6.3: ACC results when using the reference inter-distance given by (6.23) and (6.25)

Controller	e_{n_d}	e_v	u_s	J
Inter-distance (6.23)	0.049	1.011	0.216	1.584
Inter-distance (6.25)	0.032	0.331	0.279	0.902

6.2 Fractional-Order Reset Control of the Servomotor

This section concerns applying a reset fractional-order proportional-Clegg integrator controller for the velocity control of a servomotor and this strategy is compared with integer-order reset controllers.

6.2.1 Experimental application to control a servomotor

The aim of this section is to design and compare fractional- and integer-order reset strategies for the velocity control of a servomotor. It contains the description of the experiments performed in the MATLAB/Simulink environment and the stability analysis of the controlled system. Details of the implementation of the controllers are included in Appendix.

6.2.1.1 Design of the controllers

In reset control systems, it is a common practice to firstly design the linear controller which will be used as base linear system in reset control. In this application, three base controllers, of integer- and fractional-order, i.e., a PI, a PID and a fractional-order PI (FPI), were tuned considering the following specifications related to phase margin ϕ_m and gain crossover frequency ω_{cp}: $\phi_m \simeq 45°$ at $\omega_{cp} \simeq 5.5$ rad/s. The parameters of each controller which allow to fulfil these specifications are given in the Table 6.4. However, these base controllers can make the controlled system fast but very underdamped, so reset controllers are required to reduce overshoot and increase phase margin (e.g. refer to [28, 49]). Thus, replacing traditional integrators in the base controllers by CI or FCI, the following reset controllers were also obtained: a proportional CI (PCI), a proportional Clegg integro-differentiator (PCID) and a FPCI. It should be remarked that up to three design specifications can be fulfilled with the FPCI –there exists

one more degree of freedom due to its order α. Since only two specifications have to be fulfilled, the performance of the system was analyzed for different values of α were considered for the FPCI –$0.5 \leq \alpha \leq 1$ with steps of 0.05– causing the following features on the system response: the higher the value of α, the faster response and, on the contrary, the lower the value of α, the smaller the oscillation in steady state. Taking into account both issues, an intermediate value of α was chosen for the FPCI for this application: $\alpha = 0.75$.

Figure 6.11 shows the Bode diagram of the controlled system by applying the designed base and reset controllers –solid and dotted lines, respectively. As can be seen, the specifications are fulfilled in all cases and the speed of the system is similar with all controllers. It is worth remarking that we are interested on reset controllers which make the system behaves identically in terms of speed of the response. In addition, it can be observed that phase margin can be increased not only by using the reset controllers, but also by fractional-order controllers due to their order α. It should be remarked that the DF of the CI and the FCI were used to get the frequency responses for the reset controllers.

TABLE 6.4: Parameters of the base controllers

	K_p	K_i	K_d	α
PI	1.6	18.5	-	-
PID	1.528	23.16	0.152	-
FPI	0.067	13.4	-	0.75

6.2.1.2 Stability analysis

In this section, stability of the system controlled when applying the FPCI will be analyzed using the theory presented in the previous section. Only the system stability for the proposed controller is of interest for this paper in order to show the applicability of the developed theory. The analysis when applying the rest of the controllers is skipped, but the same procedure could be applied.

Consider transfer function of the servomotor as (see the appendix for the model),

$$G_s(s) = \frac{K}{Ts+1} = \frac{0.93}{0.61s+1}, \tag{6.32}$$

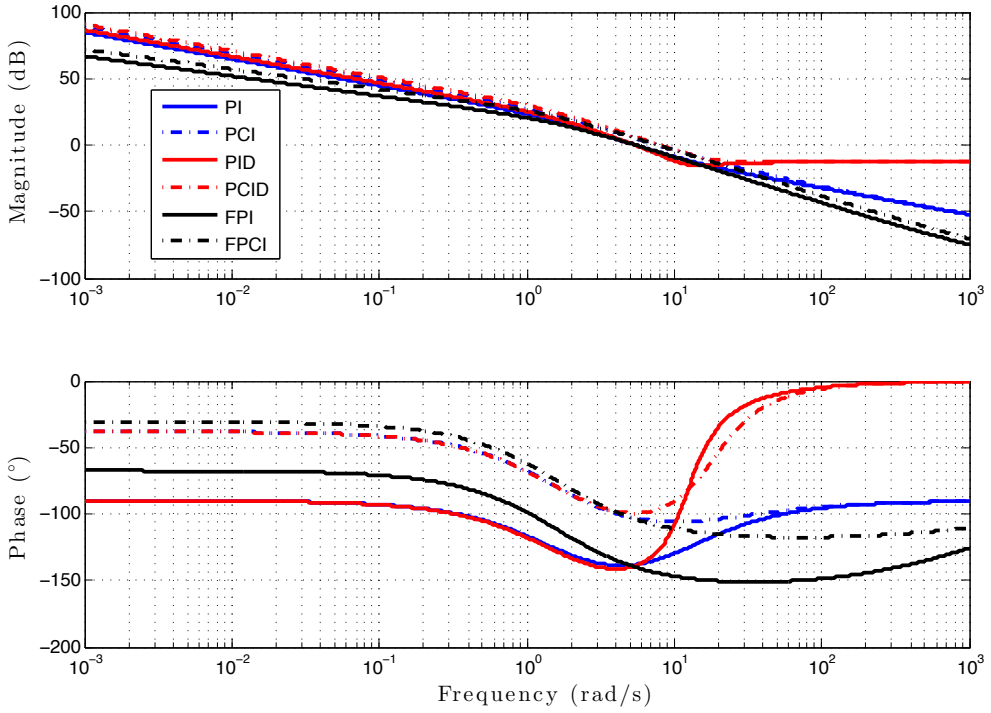

FIGURE 6.11: Bode diagram of the controlled system by applying the designed controllers. Solid lines correspond to base linear controllers, whereas dotted lines refer to reset controllers

controlled by the FPCI. Denote the state vector as $x(t) = (x_p(t), x_r(t))^T$ and the plant and controller states as $x_p(t)$ and $x_r(t)$, respectively. Thus, the reset control system can be expressed of the form of (3.40) as follows:

$$\begin{bmatrix} \dot{x}_p(t) \\ D^\alpha x_r(t) \end{bmatrix} = A_{cl}x(t) = \begin{bmatrix} -1.7415 & 20.4295 \\ -1 & 0 \end{bmatrix} x(t) + \begin{bmatrix} 1.5246 \\ 1 \end{bmatrix} r, \tag{6.33}$$

$$x(t^+) = A_R x(t) = \begin{bmatrix} 1 & 0 \\ 0 & 0 \end{bmatrix} x(t), \; y(t) = C_{cl}x(t) = \begin{bmatrix} 1 & 0 \end{bmatrix} x(t). \tag{6.34}$$

Taking into account that $\alpha = 0.75 = \frac{3}{4}$, let consider $\mathcal{X}_{p_i}(t) = D^{\frac{i-1}{4}} x_p(t), i = 1, \cdots, 4$ and $\mathcal{X}_{r_i}(t) = D^{\frac{i-1}{4}} x_r(t), i = 1, \cdots, 3$ and define the state vector of the augmented system as $\mathcal{X}(t) = (\mathcal{X}_{p_1}(t), \cdots, \mathcal{X}_{p_4}(t), \mathcal{X}_{r_1}(t), \mathcal{X}_{r_2}(t), \mathcal{X}_{r_3}(t))$, the augmented system can be represented as:

$$D^{\frac{1}{4}}\mathcal{X}(t) = A\mathcal{X}(t) + Br =$$

$$\begin{bmatrix} O_{3,1} & I_{3,3} & O_{3,1} & O_{3,2} \\ -1.7415 & O_{1,3} & 20.4295 & O_{1,2} \\ O_{2,1} & O_{2,3} & O_{2,1} & I_{2,2} \\ -1 & O_{1,3} & 0 & O_{1,2} \end{bmatrix} \mathcal{X}(t) + \begin{bmatrix} O_{3,1} \\ 1.5246 \\ O_{2,1} \\ 1 \end{bmatrix} r, \tag{6.35}$$

$$\mathcal{X}(t^+) = \begin{bmatrix} I_{6,6} & O_{6,1} \\ O_{1,6} & 0 \end{bmatrix} \mathcal{X}(t), \; y(t) = \begin{bmatrix} 1 & O_{(1,6)} \end{bmatrix} \mathcal{X}(t), \tag{6.36}$$

where $O_{l,m}$ denotes a matrix of zeros with dimension of $l \times m$. In addition, according to (5.31), H_β is simply given by (for this case $n_{\mathcal{R}} = 1$, then $P_{\mathcal{R}} = 1$ without loss of generality and $C_p = \begin{bmatrix} 1 & 0 & 0 & 0 \end{bmatrix}$):

$$H_\beta(s) = \begin{bmatrix} \beta & 0_{1,5} & 1 \end{bmatrix} \left(sI + (-A)^{\frac{1}{2-\alpha}} \right)^{-1} \begin{bmatrix} 0 \\ 0_{5,1} \\ 1 \end{bmatrix}. \tag{6.37}$$

Therefore, using Theorem 5.24, the closed-loop controlled system is asymptotically stable if $\mathrm{H}_\beta(s)$ is SPR. This is fulfilled for all $-0.1 \leq \beta \leq 0.93$. The phase equivalence of condition (6.37) is shown in Fig. 6.12 for $\beta = 0.5$. It can be seen that the controlled system is asymptotically stable since the phase equivalence of $\mathrm{H}_\beta(s)$ is less than 90°, which means that SPRness is verified.

6.2.1.3 Results

Next, the simulated and experimental responses were arranged in two groups: the obtained by the designed base controllers and the results corresponding to the reset controllers. All tests were carried out for a velocity reference of 3 rad/s.

The results obtained applying the base controllers are shown in Fig. 6.13, where solid, dotted and dash-dotted lines refer to PI, PID and FPI, respectively. From this figure, it can be stated that: (i) the experimental results are identical to the simulated ones; (ii) all responses are stable but have a undesirable value of overshoot.

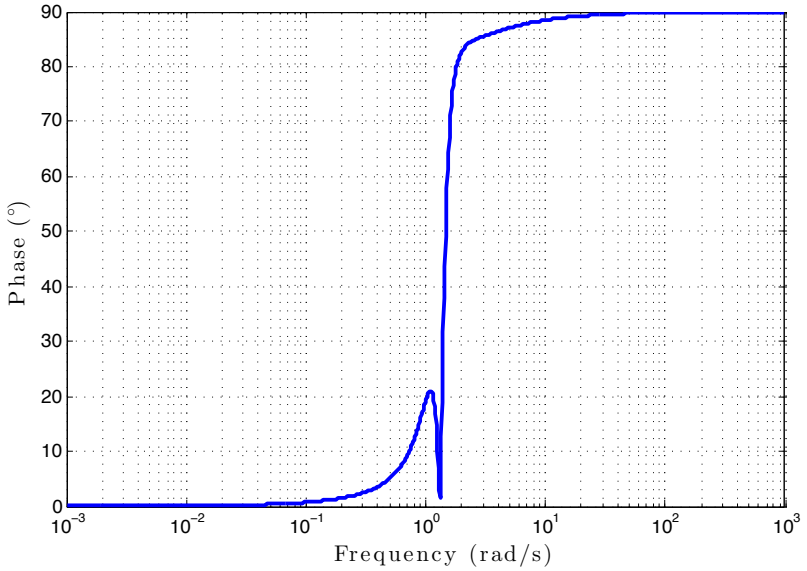

FIGURE 6.12: Phase equivalence of H_β-condition for the servomotor

Figure 6.14 shows the simulation and experimental results corresponding to the PCI, PCID and FPCI –solid, dotted and dash-dotted lines, respectively. As observed, simulated and experimental results are quite similar, as shown with the previous controllers. Moreover, the overshoot is reduced for all cases. It can be also seen that both the simulated and the experimental responses using PCI and PCID are stable but have a permanent oscillation in steady state due to a limit cycle –also in control efforts. On the contrary, one can see that there is no oscillation applying the FPCI.

In order to preserve the integral effect, the integrators $s^{-\alpha}$ of all reset controllers were implemented in Simulink as $s^{-\alpha} = s^{-n}s^{n-\alpha}$, with $n-1 \leq \alpha \leq n$, where the derivative part $s^{n-\alpha}$ is an integer-order transfer function of fifth order that fits the frequency response in the range $\omega \in (10^{-3}, 10^{3})$ rad/s, obtained by the modified Oustaloup's method (e.g. refer to [71] for continuous-time implementations of fractional-order operators). On the other hand, the implementation of FCI in Simulink was carried out as shown in Fig. 6.15, in which the fractional-order differentiator block was obtained by the Grünwald–Letnikov definition (e.g. see [58]).

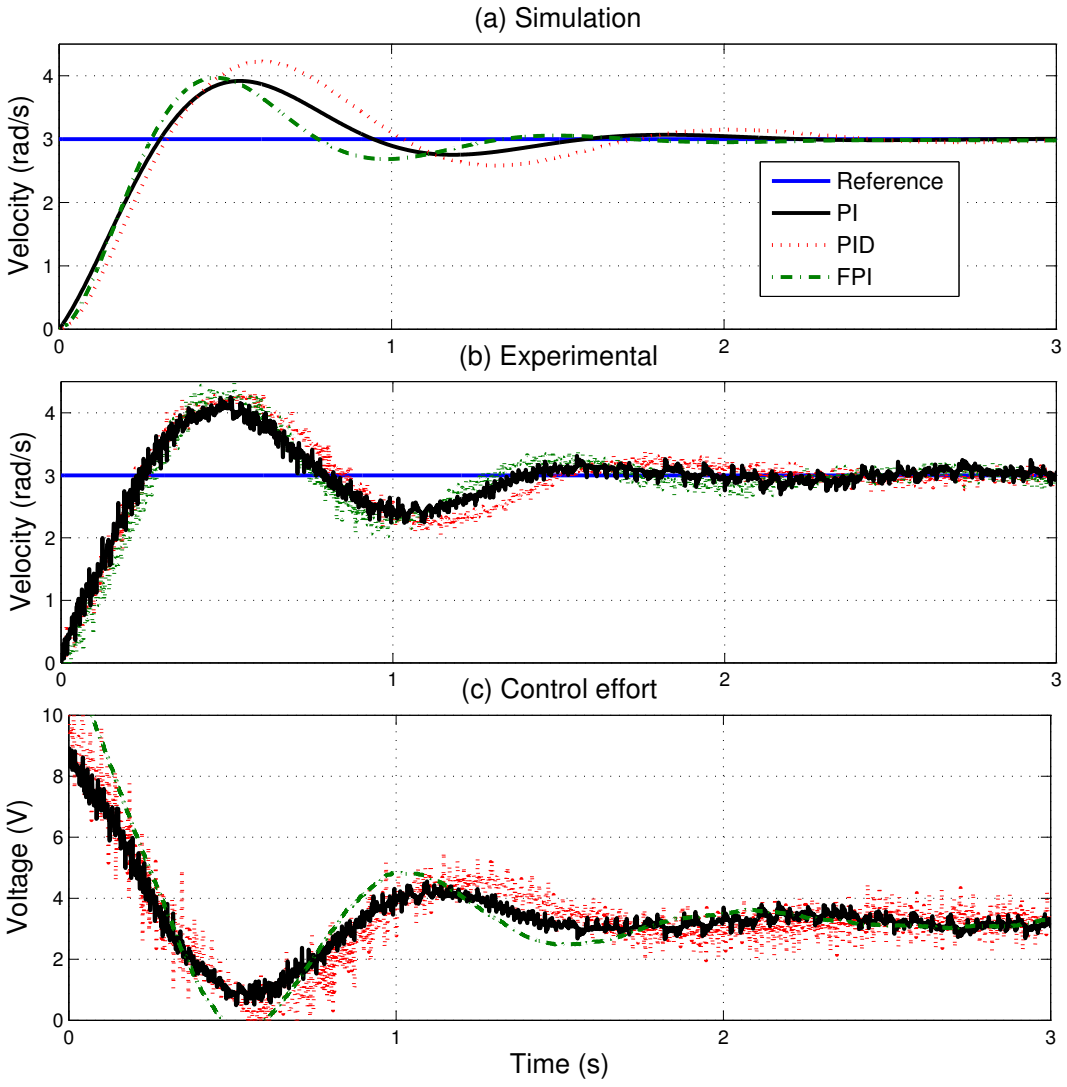

FIGURE 6.13: Response of the servomotor when applying the designed base controllers: (a) Simulated step responses (b) Experimental step responses (c) Experimental control efforts. (Solid line: PI, dotted line: PID, dash-dotted: FPI)

6.3 Stability Analysis of Smart Wheel

In the literature, NCS are commonly treated as hybrid and/or switching systems [177], so the stability problem of such systems can be analyzed on the basis of switching systems. A smart wheel shown in Fig. 6.16 is controlled with gain and order scheduling controller in [97, 106]. In this controller gain scheduling and networked control lead to the consideration of time-varying switching systems, where the system and the controllers can be represented as follows:

$$G_j(s) = \frac{0.1484}{0.045s + 1} e^{-(0.592+\tau_j)s}, \tag{6.38}$$

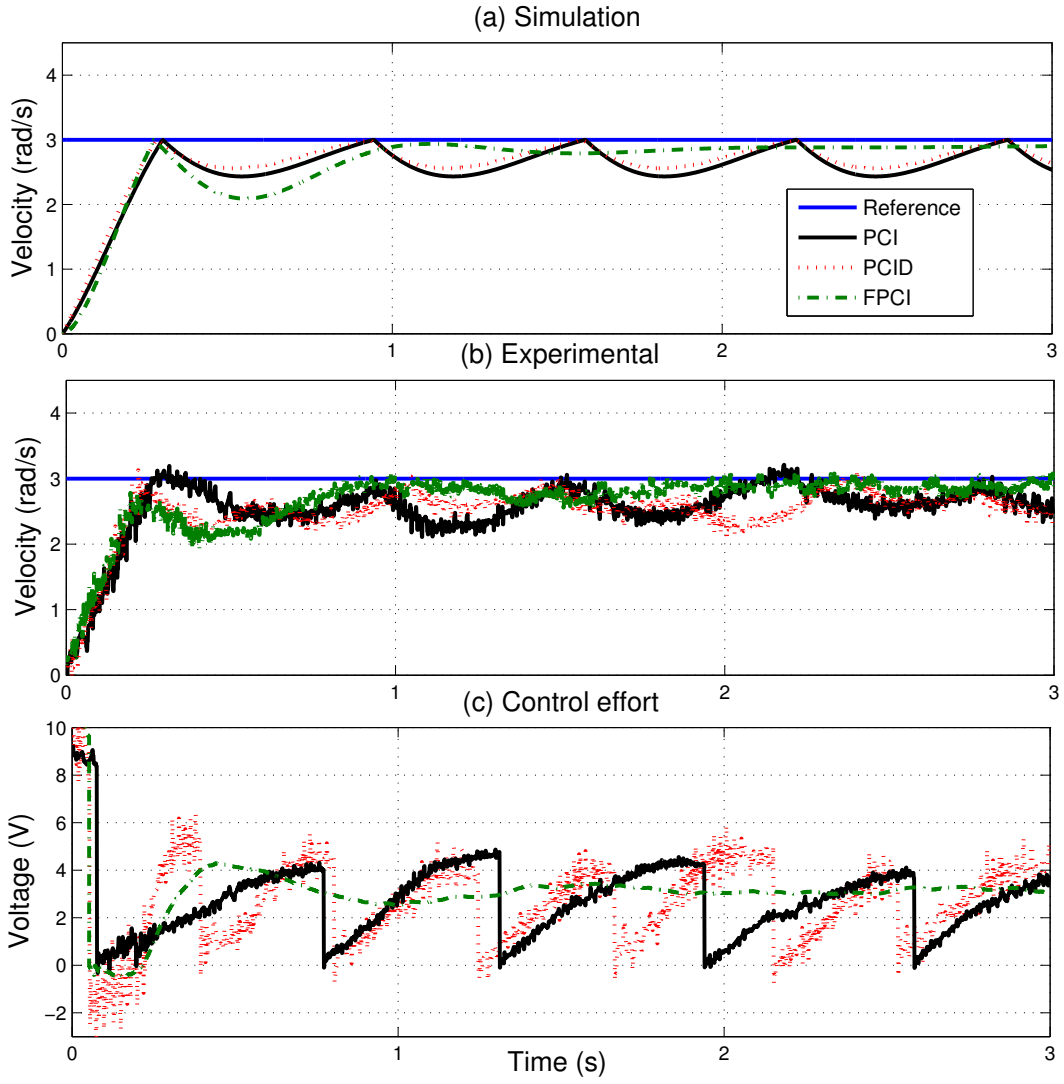

FIGURE 6.14: Response of the servomotor when applying the designed reset controllers: (a) Simulated step responses (b) Experimental step responses (c) Experimental control efforts. (Solid line: PCI, dotted line: PCID, dash-dotted: FPCI)

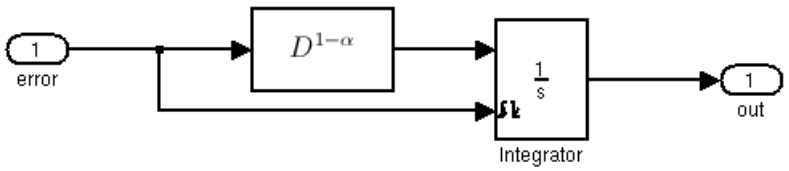

FIGURE 6.15: Implementation of FCI in Simulink

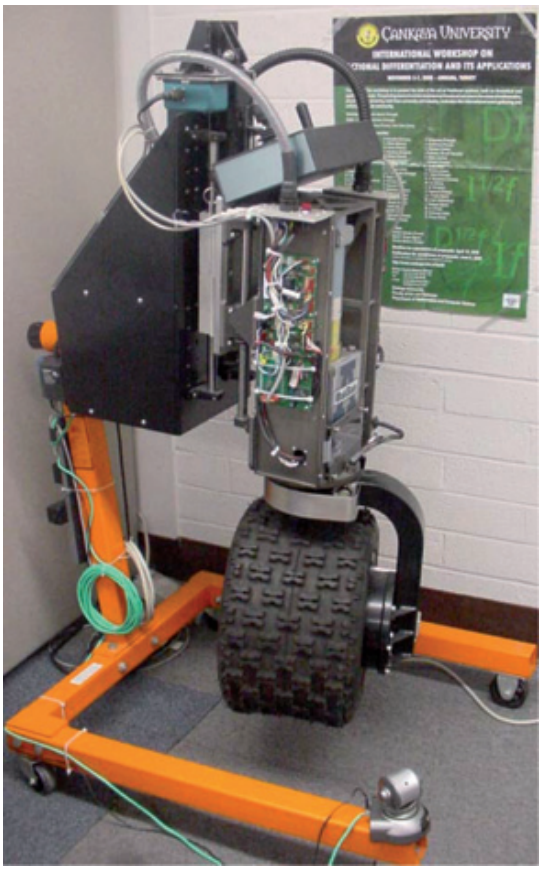

FIGURE 6.16: Photo of the SmartWheel NCS Testbed at CSOIS, Utah State University (USA)

$$C_j(s) = \beta_j \left(2.1586 + \frac{5.9853}{s^{1.1}}\right), \; j = 1, 2, ..., 13, \tag{6.39}$$

where τ_j refers to the network delay $\tau_{network}$ and β_j is the gain scheduler with the switching parameters given in Table 6.5. Hence, there are 13 subsystems to be considered.

TABLE 6.5: System and controller parameters for each switching

j	1	2	3	4	5	6	7	8	9	10	11	12	13
τ	0	0.1	0.2	0.3	0.4	0.5	0.6	0.7	0.8	0.9	1.0	1.1	1.2
β	1.6	1.35	1.3	1.15	1	0.9	0.8	0.7	0.65	0.6	0.55	0.5	0.45

Let assume that switching between the controllers is not arbitrary and happens between each pair separately –step by step. Thus, regarding to Theorem 4.1 the following 12 conditions should be satisfied to guarantee the quadratic stability of the controlled

system given by (6.38) and (6.39):

$$|\arg(c_1(j\omega)) - \arg(c_2(j\omega))| < \frac{\pi}{2}, \forall\omega,$$

$$|\arg(c_2(j\omega)) - \arg(c_3(j\omega))| < \frac{\pi}{2}, \forall\omega,$$

$$\vdots$$

$$|\arg(c_{12}(j\omega)) - \arg(c_{13}(j\omega))| < \frac{\pi}{2}, \forall\omega,$$

where c_j, $j = 1, 2, ..., 13$, denotes the closed-loop polynomial of the system. It is important to remark that, due to the fact that the controller parameters and network delay are time varying, the stability analysis of the closed-loop system is difficult to establish for all possible cases of process switching. As a matter of fact, it is a common practice to assume slow variations of the operating conditions and, consequently, suppose that the scheduled variable, the external gain β in this case, vary slowly [178] or step by step. Therefore, the stability method used here makes sense.

Figure 6.17 shows the phase difference between each pair of characteristic polynomials of the closed-loop system for step by step switching. It can be observed that the system is quadratically stable, with the maximum phase difference equal to 30°, less than 90°. It should be remarked that the delay was approximated by using a third order Padé approximation in the frequency range of $[0.01, 100]$ rad/s, so the results are valid in this range of frequencies.

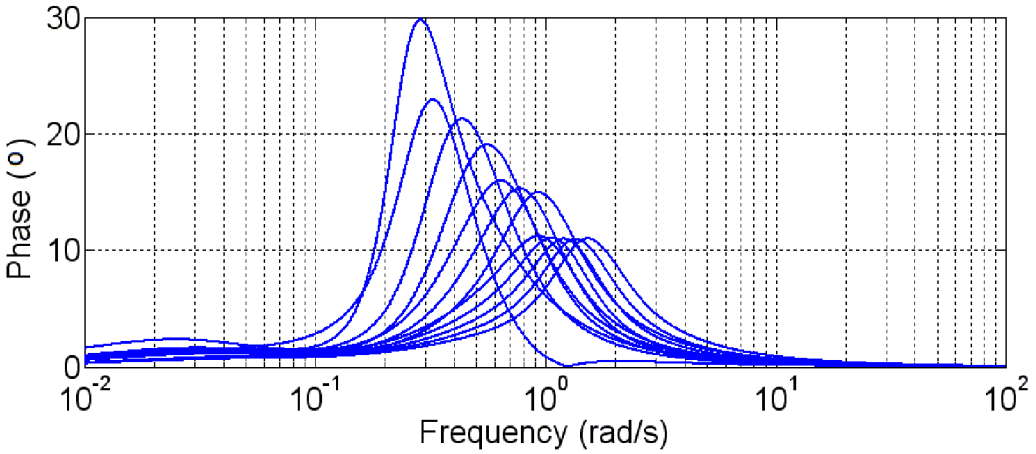

FIGURE 6.17: Phase difference between each pair of characteristic polynomials of the closed-loop system, i.e., (c_1, c_2), (c_3, c_4), $\cdots$, and (c_{12}, c_{13}) for step by step switching

Chapter 7

Conclusions and Future Works

This thesis is devoted to the fractional-order hybrid systems in particular switching systems, and reset control systems. An important conclusion which may be drawn from the laboratory tests is that presented fractional-order hybrid controllers can yield a substantial improvement in performance compared to integer-order one. This is of course not to say that fractional-order hybrid controllers are always better, what one classifies as better depends on the case. Simulation and experimental results obtained from a Citröen C3 vehicle, a servomotor, and the CSOIS Smart Wheel showed the effectiveness of the proposed strategies.

Chapter 4 addressed the design of robust controllers for switching systems in frequency domain considering specifications regarding performance and robustness and ensuring the quadratic stability of the controlled system. In particular, different integer and fractional-order controllers were designed to fulfill a set of desired specifications ensuring the stability of the switching systems. Simulation results show the effectiveness of the proposed tuning method to be fulfilled for serval specifications and for different kinds of switching systems.

Special attention has been given in this thesis to the fractional-order reset controllers. On the other section of chapter 4, some traditional reset control strategies were compared with the fractional-order Clegg integrator. It has been demonstrated that the FCI has better performance in compensating the phase of the system. Likewise, it has been shown that FCI may be capable of reducing the overshoot in a proper and better way. Thereafter, the particular features of several modified reset control strategies, of

integer and fractional-order are investigated to improve the performance of a system, especially in terms of prevention of Zeno solutions and traditional time domain specifications. It was focused on fractional-order reset systems and the possibilities of use of a new fractional-order proportional-Clegg integrator to avoid Zeno phenomena. A general advanced reset control has been proposed by combining the particular features of the previous controllers, allowing not only to avoid the occurrence of Zeno solutions but also to reduce, or even eliminate, the overshoot. It has been concluded that,

- The FPCI are able to avoid the Zeno solution tuning the parameter α.
- The PI$^{\alpha}$+CI$^{\alpha}$ as well as the prevention of Zeno solution, are able to improve time time domain specification (specially reducing the overshoot) comparing the PI+CI controller.
- Advanced reset controller are able to avoid the Zeno solution and eliminate the overshoot for the first order system.
- Although advanced reset controller reduces overshoots in the higher order system but not completely eliminate it, so that using (i) fractional-order advanced reset controller and (ii) advanced reset controller with periodic resets, can significantly reduce overshoots or eliminate it.

As a future work, tuning of the PI$^{\alpha}$+CI$^{\alpha}$ can be good challenged in order to obtain the less overshoot and better performance.

In chapter 5, the stability of a class of fractional-order switching system and fractional-order reset control systems has been studied. A theoretical framework was developed to prove their stability in terms of common Lyapunov functions, which were generalized to such fractional-order systems, and equivalent frequency-domain conditions. In addition, Lyapunov stability has been generalized for fractional-order reset systems, presenting its phase equivalence in the frequency domain. The results have shown the applicability of the proposed method to prove the stability of such fractional-order systems. The theorems developed are applicable for the commensurate fractional-order system which can be developed for in-commensurate order as future work.

In chapter 6 experimental results were presented to extensively validate the fractional-order strategies developed in this Thesis. In particular: a fractional-order hybrid

strategy has been designed to control both the throttle and the brake pedals for cruise control (CC) and adaptive cruise control (ACC) manœuvres at very low speeds of Citröen C3 vehicle. Simulated and experimental results, obtained for real vehicles in a real circuit, were given to demonstrate the effectiveness of the proposed fractional hybrid control law. Since the vehicle has different dynamics during accelerating and decelerating, two fractional-order PI controllers were designed for controlling the throttle and the brake for CC manœuvres. A hybrid model of the controlled system was obtained and its quadratic stability was analyze by means of a frequency domain method, modeling the system as a switching (hybrid) system. ACC manœuvres were performed by two different distance policies using two cooperating vehicles –one manual, the leader, and another automatic–, in which the desired inter-distance between the leader and follower is maintained by an additional PD controller.

As another application, integer- and fractional-order reset strategies were designed and compared for the velocity control of a servomotor. It was shown that fractional-order integrators can modify the dynamics of the reset action and improve the performance of the system, avoiding Zeno solution. Finally, as a multi-controller, the gain and order scheduling control of smart wheel reported in [97, 106] is recalled and the stability of this switching system is analyzed.

Conclusiones y trabajo futuro

Esta tesis está dedicada a los sistemas híbridos de orden fraccionario, en particular a los sistemas conmutados y a los sistemas de control reset. Una importante conclusión que puede extraerse de las pruebas de laboratorio es que los controladores híbridos de orden fraccionario propuestos pueden aportar una mejora sustancial en el rendimiento de los sistemas en comparación con los de orden entero. Esto, por supuesto, no quiere decir que los controladores híbridos de orden fraccionario siempre sean mejores, lo que se clasifica como mejor depende del caso. Los resultados de simulación y experimentales obtenidos en un vehículo Citröen C3, un servomotor, y la smart wheel del Center for Self Organizing and Intelligent Systems (Utah State University, USA) muestran la efectividad de las estrategias propuestas.

El capítulo 4 se ha dedicado al diseño de controladores robustos para sistemas de conmutación en el dominio de la frecuencia teniendo en cuenta las especificaciones sobre el rendimiento y la robustez y asegurando la estabilidad cuadrática del sistema controlado. En particular, varios controladores de orden fraccionario y orden entero fueron diseados para cumplir un conjunto de especificaciones deseadas para asegurar la estabilidad de los sistemas de conmutación. Los resultados de simulación muestran la efectividad del método de sintonización propuesto para cumplir diferentes especificaciones y para diferentes tipos de sistemas conmutados.

Especial atención se ha dado en esta tesis a los controladores reset de orden fraccionario. En otra sección del capítulo 4, algunas de las estrategias tradicionales de control reset se compararon con el integrador Clegg de orden fraccionario (FCI). Se ha demostrado que el FCI tiene un mejor rendimiento en la compensación de la fase del sistema. Asimismo, se ha demostrado que el FCI puede ser capaz de reducir el sobreoscilacion de una manera adecuada y eficaz. Despus de eso, las características particulares de

varias estrategias de control reset modificado, de orden entero y fraccionario, se investigan para mejorar el rendimiento de un sistema, especialmente en prevención de las soluciones tipo Zeno y mejora de especificaciones en el dominio de tiempo. Se centró el trabajo en los sistemas reset de orden fraccionario y las posibilidades de uso de un nuevo controlador de orden fraccionario proporcional-Clegg integrador para evitar fenómenos tipo Zeno. Un control reset avanzado ha sido propuesto combinando las características particulares de los controladores anteriores, lo que permite no sólo evitar la aparición de soluciones tipo Zeno sino tambin reducir, o incluso eliminar, el sobreoscilacion. Se ha concluido que,

- El controlador FPCI es capaz de evitar la solución tipo Zeno ajustando el parámetro α.
- El controlador PI$^{\alpha}$+CI$^{\alpha}$, aparte de prevenir las soluciones tipo Zeno, es capaz de mejorar los especificaciones en el dominio tiempo (especialmente la reducción del sobreoscilacion) en comparación el controlador PI+CI.
- El controlador reset avanzado es capaz de evitar la solución tipo Zeno y eliminar la sobreoscilacion para sistemas de primer orden.
- Aunque el controlador reset avanzado reduce la sobreoscilacion en sistemas de orden más que uno, pero no lo elimina completamente, el uso (i) del controlador reset avanzado de orden fraccionario y (ii) del controlador reset avanzado con reseteo periódico, pueden reducir significativamente la sobreoscilacion o eliminarla.

Como trabajo futuro, la sintonización de los controladores PI$^{\alpha}$+CI$^{\alpha}$ puede ser un buen reto para obtener el menos sobreoscilacion y mejor rendimiento.

En el capítulo 5 se ha estudiado la estabilidad de una clase de sistemas conmutados de orden fraccionario y de sistemas de control reset de orden fraccionarios. Se ha desarrollado un marco teórico para probar su estabilidad en trminos de las funciones comunes de Lyapunov, generalizadas para sistemas de orden fraccionario, y condiciones equivalentes en el dominio de la frecuencia. Además, la estabilidad de Lyapunov se ha generalizado para los sistemas reset de orden fraccionario, presentando su equivalencia en fase en el dominio de la frecuencia. Los resultados han mostrado la aplicabilidad del mtodo propuesto para probar la estabilidad de tales sistemas de orden fraccionario. Los

teoremas desarrollados son aplicables para sistema de orden conmensurable, aunque se pueden desarrollar para orden no conmensurable como trabajo futuro.

En el capítulo 6 se han presentado los resultados experimentales para validar ampliamente las estrategias de orden fraccionario desarrolladas en esta tesis. En particular: una estrategia de control híbrido de orden fraccionario ha sido diseada para controlar los pedales del acelerador y del freno para maniobras del control de crucero (CC) y de control de crucero adaptativo (ACC) a velocidades muy bajas de un vehículo Citröen C3. Los resultados simulados y experimentales, obtenidos para los vehículos reales en un circuito real, se dan para demostrar la efectividad de la propuesta de control híbrido de orden fraccionario. Por tener diferentes dinámicas durante la aceleración y deceleración, dos controladores PI de orden fraccionario fueron diseados para controlar el acelerador y el freno para las maniobras de CC. Se ha obtenido un modelo híbrido del sistema controlado y su estabilidad cuadrática se analiza por medio de un mtodo en el dominio de la frecuencia, modelando el sistema como una sistema conmutado. Las maniobras ACC se realizaron para dos políticas de distancia diferentes utilizando dos vehículos cooperantes –uno manual, el líder, y otro automático–, utilizando un controlador PD adicional para mantener la distancia deseada entre el líder y el seguidor.

Como otra aplicación, se disearon y compararon estrategias de control reset de orden entero y fraccionario para el control de la velocidad de un servomotor. Se demostró que los integradores de orden fraccionario puede modificar la dinámica de la acción de reseteo y mejorar el rendimiento del sistema, evitando soluciones tipo Zeno. Finalmente, como caso de multicontrolador, se ha revisado y analizado la estabilidad del controlador con planificación de ganancias y ordenes de una smart wheel presentado en [97, 106].

Appendix A

Description of the Experiments

This appendix briefly describes the experimental platforms which were used in this Thesis to validate the proposed controllers, including their physical descriptions, dynamic models, and experimental set-ups. In particular, the three experimental platforms are: a servomotor, and a Citroën C3 vehicle.

A.1 Servomotor

With respect to the servomotor description, the information included in this section can be found in the *Feedback's* User Manual [179].

A.1.1 Description

The *Servo Fundamentals Trainer (33-001)* by *Feedback* was designed to investigate the fundamental principles of servo control, i.e., it allows investigation of open- and closed-loop control for speed and position (see Fig. A.1).

The system comprises three units:

- A Mechanical Unit (33-100), which is the servo strictly speaking. It consists of an open-board format assembly carrying the mechanics of the system plus its

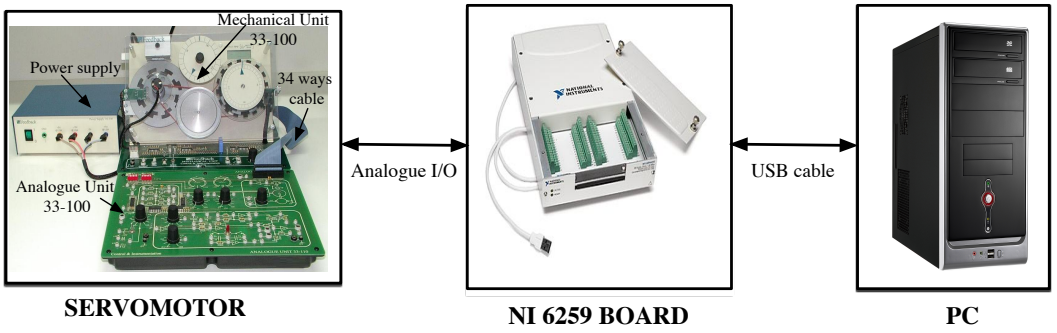

FIGURE A.1: Connection scheme for the velocity control of the servomotor

supporting electronics as shown in Fig. A.2 (a). The electromechanical components comprise DC motor, an analogue tachogenerator, analogue input and output potentiometers, absolute and incremental digital encoders, and magnetic brake. It includes the following supporting electronics: power amplification; a low frequency sine, square, and triangle waveform generator for testing purposes; encoder reading circuitry; and LCD speed display.

- An Analogue Unit (33-110), which connects to the mechanical unit through a 34-way ribbon cable which carries all power supplies and signals, enabling the normal circuit interconnections to be made on this unit (see its scheme in Fig. A.2 (b)). It carries a four input error amplifier, a controller with independent P, I, and D channels, and facilities for single amplifier compensation circuits.

- A Power Supply (01-100), which provides all of the necessary DC voltage supplies required by the system.

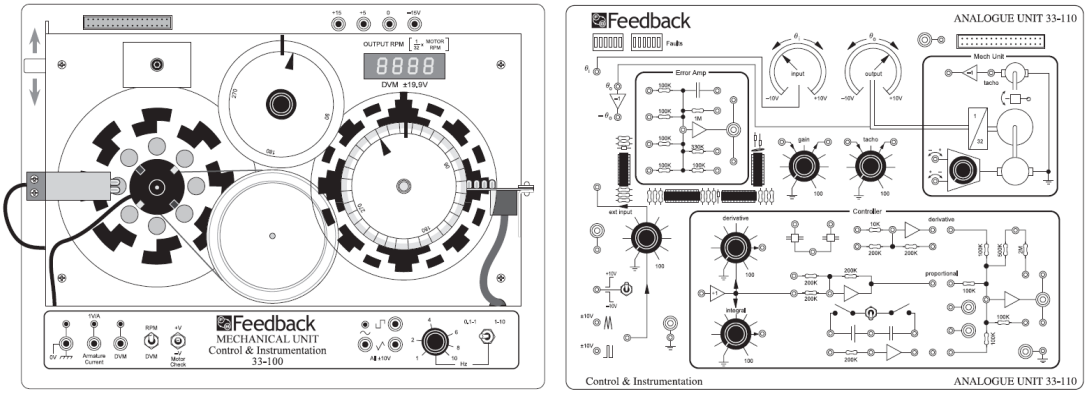

(a) (b)

FIGURE A.2: Appearance of servo units: (a) Mechanical Unit 33-100 (b) Analogue Unit 33-110

The mechanical unit has a brake whose position changes the gain and the time constant of the system, i.e., the break acts as a load to the motor. The analogue unit allows speed and position control of the servomotor.

A.1.2 Dynamic model

Figure A.3 illustrates the experimental open loop response, represented as a solid line in red colour, of the servo speed for a step input with a value of $4V$. From this response, the servo dynamic model for its speed can be given by the following first order plus delay transfer function:

$$G_s(s) = \frac{K}{Ts+1} = \frac{0.93}{0.61s+1}. \tag{A.1}$$

The simulated open loop response of the servo speed (**??**) is also included in Fig. A.3 (dashed blue line). As can be observed, only slight differences can be found between the two responses, experimental and simulated, this validating the dynamic model (**??**).

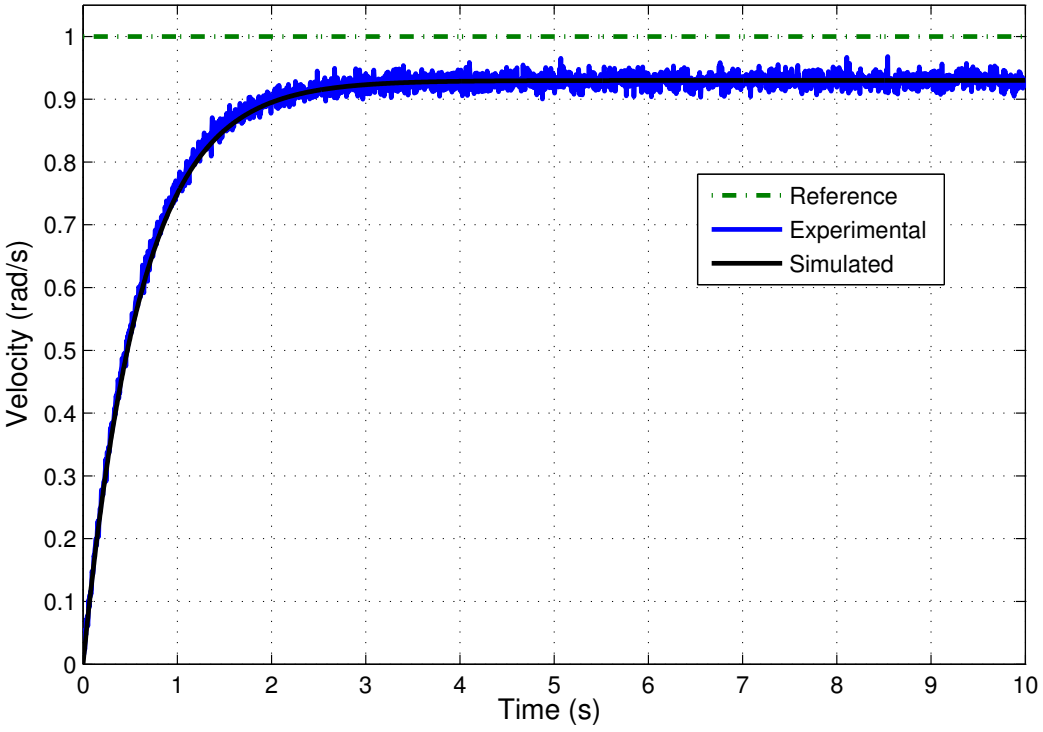

FIGURE A.3: Open loop response of the servo speed (experimental and simulated)

In the experimental set-up to control the servomotor, as shown in Fig. A.4, a data acquisition board *NI DAQPad-6259* by *National Instruments* is also used (see Fig. A.5).

This board implements high-performance data acquisition hardware, with some key features being the following (refer to [180] for detailed information about this board):

a) 32 analogue inputs (AI), 4 analogue outputs (AO), and 48 digital input/outputs (DI/DO);

b) flexible AI and AO sample and convert timing;

c) many triggering modes;

d) independent AI, AO, DI, and DO FIFOs;

e) seamless interface to signal conditioning accessories;

f) two flexible 32-bit counter/timer modules with hardware gating;

g) easy and friendly software interface.

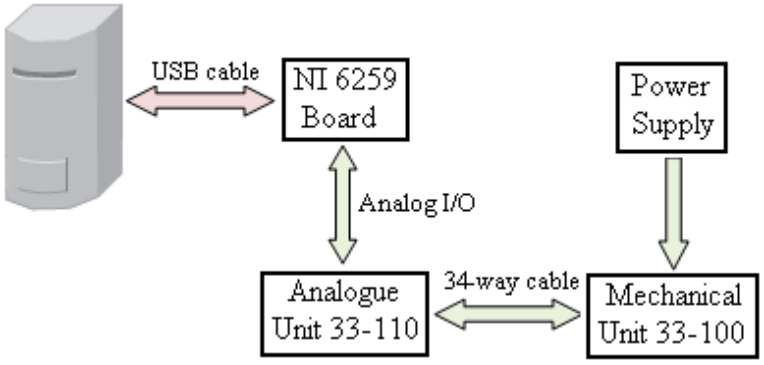

FIGURE A.4: Experimental set-up scheme to control the servomotor

A.2 Citroën C3 vehicle

AUTOPIA group has been working on the development of autonomous vehicles for the last 15 years at the *Center for Automation and Robotics* (CAR) (see more information at http://www.iai.csic.es/users/autopia/). Currently, AUTOPIA is working towards traffic control of cooperating vehicles. To this end, several commercial vehicles were modified to permit autonomous guidance.

For longitudinal control applications at low speeds, the experimental vehicle is a commercial convertible Citroën C3 Pluriel (see Fig. A.6). Here, some information about

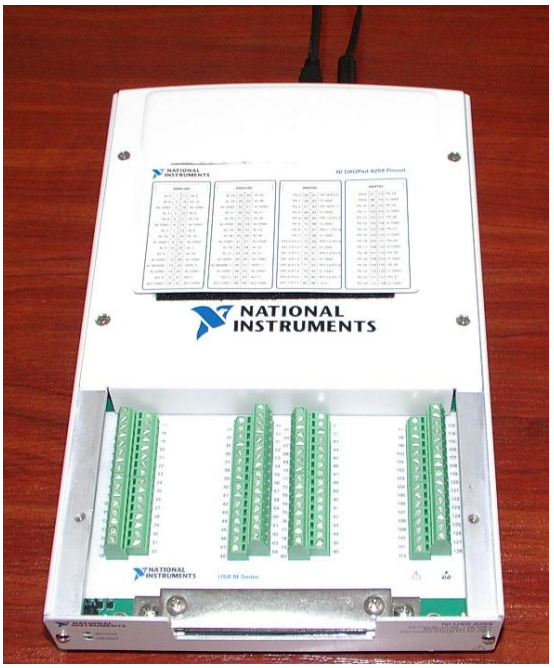

FIGURE A.5: Picture of *NI 6259* Data Acquisition Board

it and its modifications to act autonomously on the throttle and brake pedals –i.e., longitudinal control– are provided. For detailed information, refer to [2] (see Fig. A.7).

FIGURE A.6: Picture of the Citroën C3 vehicle at CAR

A.2.1 Description

The vehicle equipment consists principally of [181]:

- A double-frequency global positioning system (GPS) receiver running in real-time kinematic (RTK) carrier phase differential mode that supplies 2cm of resolution positioning at a refresh rate of 5Hz.

- A wireless local area network (IEEE 802.11) support, which allows the GPS to receive positioning error corrections from the GPS base station.

- An inertial measurement unit (IMU) Crossbow IMU 300CC placed close to the centre of the vehicle.

- Car odometry supplied by a set of built-in sensors in the wheels, whose measurements can be read by accessing the controller area network (CAN) bus of the vehicle. This is implemented by means of a CAN Card 2.6. Specifically, we read the car's wheel-speed data.

- An on-board computer, which is able to request values from each of the input devices with which to compute the controller's input values. The devices that make it possible to act on the throttle and brake of the car are an electrohydraulic system capable of injecting pressure into the car's anti-block braking system (ABS), and an analogue card which can send a signal to the car's internal engine computer to demand acceleration or deceleration.

- The electro-hydraulic braking system is mounted in parallel with the original one. Two shuttle valves are installed connected to the input of the anti-lock braking system (ABS) in order to keep the two circuits independent. A pressure limiter tube set at 120 bars is installed in the system to avoid damage to the circuits. Two more valves are installed to control the system: a voltage-controlled electro-proportional pilot to regulate the applied pressure, and a spool directional valve to control the activation of the electrohydraulic system by means of a digital signal. These two valves are controlled via an I/O digital-analogue CAN card. The voltage for the applied pressure is limited to 4V (greater values correspond to hard braking and are not considered).

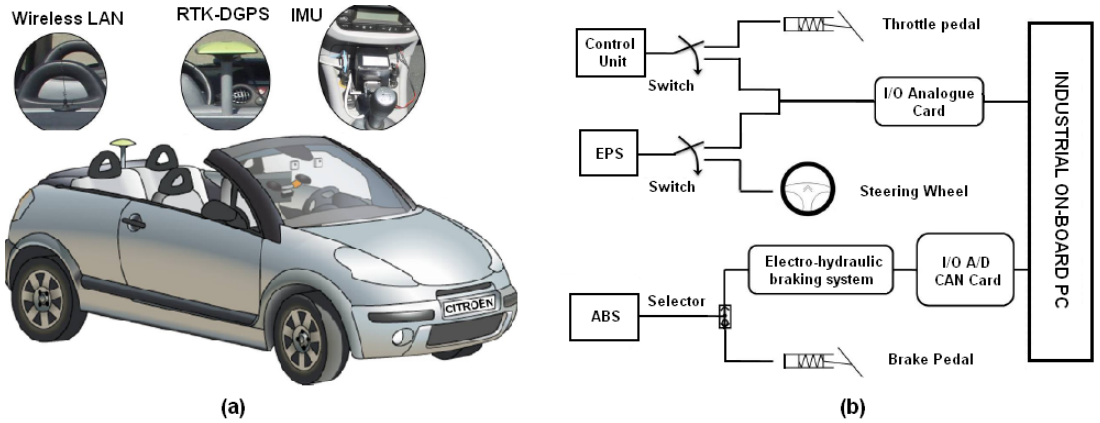

FIGURE A.7: Some details of Citroën C3 vehicle (reproduced from [2]): (a) On-board sensors (b) Automation of the vehicle's actuators

A.2.2 Dynamic longitudinal model

Due to the impossibility of obtaining the exact dynamics that describes the vehicle, in this work the idea is to obtain a simple linear model of the vehicle for the circuit on which the experimental manœuvres will be performed.

To do so, we use a chirp signal as the input signal of the vehicle throttle, as shown in Fig. A.8 (solid blue line), where the dashed red line corresponds to the slope angle of the circuit. In this case, the experimental vehicle response is plotted in Fig. A.9 (solid blue line), which includes the vehicle's inherent dynamics and the environment and circuit perturbations, such as the slope of the circuit. Including the vehicle's interaction with the terrain during the identification of vehicle dynamics is commonly used in the vehicle automation literature (see [96] and references therein). The identification process is carried out by means of the *Identification Toolbox* of MATLAB based on the frequency domain, considering the mentioned input and experimental response and selecting a second order model for the approximation. The transfer function obtained is given by:

$$G_v(s) = \frac{K}{s^2 + 2\delta\omega_n s + \omega_n^2}, \tag{A.2}$$

where $K = 7.8473{\cdot}10^4$, $\delta = 160$, and $\omega_n = 55.87$, which corresponds to the dashed red line in Fig. A.9. However, the poles of (A.2) are $p_1 = -0.1746$ and $p_2 = -1.7878{\cdot}10^4$, so it is evident that the vehicle dynamics will be given by the smaller pole. As a result,

the transfer function (A.2) can be reduced to first order as follows:

$$G_v(s) \simeq \frac{K_1}{s+p_1} = \frac{4.39}{s+0.1746}. \tag{A.3}$$

Simple linear longitudinal models were also used in [96] and [173]. Figure A.10 shows the comparison of the step responses of the second and first order models of the vehicle, transfer functions (A.2) and (A.3), respectively. As observed, the system response is almost the same, hence we shall henceforth use the first order model given by (A.3) to describe the longitudinal vehicle dynamics due to its simplicity. It has the same form as a servo speed.

It is important to remark that the identification process is carried out only by acting on the throttle. The identification of vehicle dynamics when braking is neglected for two reasons: (1) since target speeds are set lower than 15km/h, the vehicle always remains in first gear (with a high engine braking force); (2) since the automated braking system (see [172]) was designed for emergency braking situations at high speeds, a minimal action on the brake at lower speeds causes significant deceleration. Bearing this in mind, for simplicity, a controller for the brake is not needed for our tests.

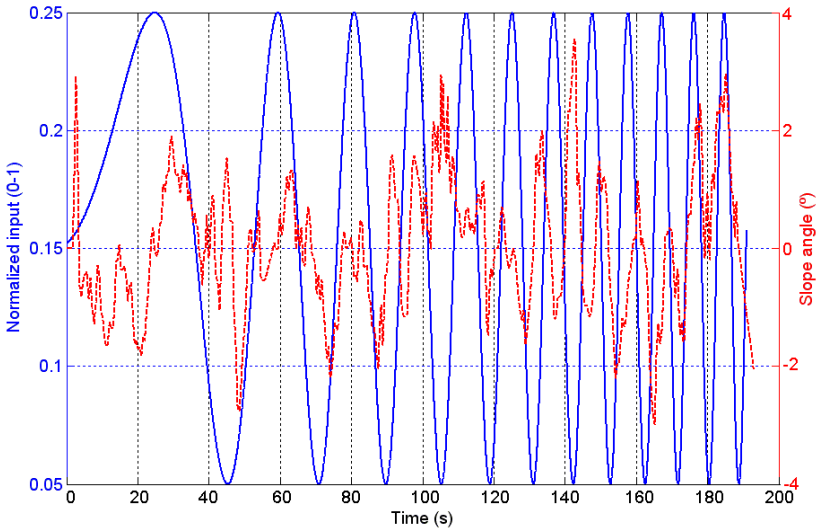

FIGURE A.8: Normalized throtlle input to vehicle's longitudinal model. The variation of the circuit slope is also illustrated

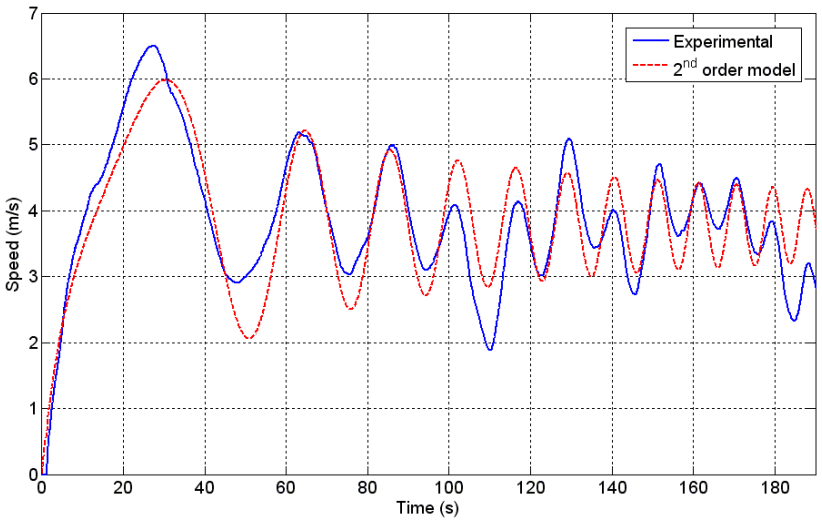

FIGURE A.9: Comparison of vehicle's responses (experimental and second order model)

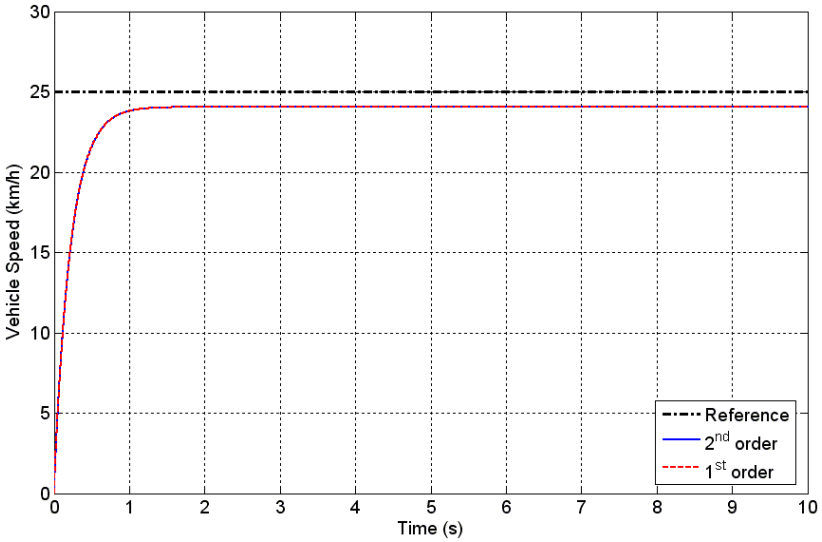

FIGURE A.10: Step responses of the second and first order model of the vehicle

A.2.3 Set-up

Manœuvres were performed on CAR's private driving circuit illustrated in Fig. A.11. It was designed with scientific purposes, so that only experimental vehicles are driven in this area. The circuit includes 90^o bends and different slopes so as to validate the controllers in different circumstances as close to a real environment as possible. For each test, we selected the same starting point on the circuit.

FIGURE A.11: Aerial view of the private driving circuit at CAR

It is important to remark that, for networked control tests, network delays were added manually by software in order to validate the proposed controllers in worse network conditions. Induced delays in a Wi-Fi network are of the order of milliseconds [177], which is not really suitable for our purposes.

A.2.4 Digital Implementation of fractional-order Controllers

TABLE A.1: Coefficients of the approximations $P_q(z)$ of the fractional-order controllers

	b_0	b_1	b_2	b_3	b_4	b_5	b_6	b_7
Throttle ($q=1$)	0.157	0.133	−0.439	−0.366	0.406	0.334	−0.124	−0.101
Brake ($q=2$)	0.353	0.188	−1.027	−0.538	0.996	0.513	−0.321	−0.162
		a_1	a_2	a_3	a_4	a_5	a_6	a_7
Throttle ($q=1$)		−0.866	−2.746	2.339	2.507	−2.095	−0.760	0.621
Brake ($q=2$)		−0.540	−2.881	1.505	2.766	−1.395	−0.885	0.430

Theoretically, a fractional-order controller is an infinite-dimensional linear filter, and that all existing implementation schemes are based on finite-dimensional approximations. In practice, we use a digital method, specifically the indirect discretization method, which requires two steps: firstly obtaining a finite-dimensional continuous approximation for the integral part $s^{-\alpha}$, and secondly discretizing the resulting s-transfer function. In our case, in order to preserve the integral effect, $s^{-\alpha}$ was implemented as $s^{-\alpha} = s^{-1}s^{1-\alpha}$; actually, only the fractional part $P(s) = s^{1-\alpha}$ was approximated by the modified Oustaloup's method (see e.g. [71]). Thus, an integer-order transfer function that fits the frequency response of $P(s)$ in the range $\omega \in (10^{-3}, 10^{3})$ was obtained with 7 poles and 7 zeros. Later, the discretization of this continuous approximation was carried out by using the Tustin rule with a sampling period $T_s = 0.2$ s –GPS

sampling period. Considering both the throttle and the brake controllers, 8th-order digital IIR filters of the form:

$$C_q(z) = k_{p_q} + k_{i_q} \left(\frac{2}{T_s} \frac{1 - z^{-1}}{1 + z^{-1}} \right)^{-1} P_q(z)$$

were obtained, where

$$P_q(z) = \frac{\sum_{k=0}^{7} b_k z^{-k}}{1 + \sum_{k=1}^{7} a_k z^{-k}},$$

and with the coefficients given in Table A.1.

Bibliography

[1] J.J. Martinez and C. Canudas de Wi. A safe longitudinal control for adaptive cruise, control and stop-and-go scenarios. *IEEE Transaction on Control Sytem Technology*, 15(2):246–258, 2007.

[2] V. Milanés, D. Llorca, B. Vinagre, C. González, and M. Sotelo. Clavileño: Evolution of an autonomous car. In *Proceedings of the 13th International IEEE Conference on Intelligent Transportation Systems*, 2010.

[3] R. Goebel, R. Sanfelice, and A. Teel. Hybrid dynamical systems. *Control Systems Magazine, IEEE*, 29(2):28–93, 2009.

[4] R. Alur, C. Belta, F. Ivančić, V. Kumar, M. Mintz, G. Pappas, H. Rubin, and J. Schug. Hybrid modeling and simulation of biomolecular networks. *Hybrid Systems: Computation and Control*, pages 19–32, 2001.

[5] P. Lincoln and A. Tiwari. Symbolic systems biology: Hybrid modeling and analysis of biological networks. *Hybrid Systems: Computation and Control*, pages 147–165, 2004.

[6] H. Witsenhausen. A class of hybrid-state continuous-time dynamic systems. *Automatic Control, IEEE Transactions on*, 11(2):161–167, 1966.

[7] J. Ezzine and AH Haddad. On the controllability and observability of hybrid systems. In *Proceedings of the American Control Conference, 1988*, pages 41–46. IEEE, 1988.

[8] A. Gollu and P. Varaiya. Hybrid dynamical systems. In *Proceedings of the 28th IEEE Conference on Decision and Control*, pages 2708–2712. IEEE, 1989.

[9] M.S. Branicky. Studies in hybrid systems: Modeling, analysis, and control. Technical report, DTIC Document, 1995.

[10] R. Fierro and F.L. Lewis. A framework for hybrid control design. *Systems, Man and Cybernetics, Part A: Systems and Humans, IEEE Transactions on*, 27(6): 765–773, nov 1997. ISSN 1083-4427. doi: 10.1109/3468.634640.

[11] P.J. Antsaklis and A. Nerode. Hybrid control systems: An introductory discussion to the special issue. *Automatic Control, IEEE Transactions on*, 43(4): 457–460, 1998.

[12] JM Schumacher et al. *Introduction to hybrid dynamical systems*. Springer-Verlag, 1999.

[13] P.J. Antsaklis. A brief introduction to the theory and applications of hybrid systems. In *IEEE, Special Issue on Hybrid Systems: Theory and Applications*. Citeseer, 2000.

[14] N.H. McClamroch and I. Kolmanobsky. Performance benefits of hybrid control design for linear and nonlinear systems. *Proceedings of the IEEE*, 88(7):1083 –1096, jul 2000. ISSN 0018-9219. doi: 10.1109/5.871310.

[15] C. Altafini, A. Speranzon, and K.H. Johansson. *Hybrid Systems: Computation and Control*, volume 2289 of *Lecture Notes in Computer Science*, chapter Hybrid Control of a Truck and Trailer Vehicle, pages 439–469. Springer Berlin / Heidelberg, 2002.

[16] P.J. Antsaklis and X.D. Koutsoukos. Hybrid systems: review and recent progress. *Software-Enabled Control*, pages 273–298, 2003.

[17] R. Goebel, J. Hespanha, A.R. Teel, C. Cai, and R. Sanfelice. Hybrid systems: generalized solutions and robust stability. In *Proceedings of the 6th IFAC symposium in nonlinear control systems*, pages 1–12. Citeseer, 2004.

[18] R.G. Sanfelice, M.J. Messina, S. Emre Tuna, and A.R. Teel. Proceedings of the robust hybrid controllers for continuous-time systems with applications to obstacle avoidance and regulation to disconnected set of points. In *American Control Conference, 2006*, pages 6–pp. IEEE, 2006.

[19] R. Sanfelice, R. Goebel, and A. Teel. A feedback control motivation for generalized solutions to hybrid systems. *Hybrid Systems: Computation and Control*, pages 522–536, 2006.

[20] Ricardo G. Sanfelice. *Robust Hybrid Control Systems*. PhD thesis, UNIVERSITY of CALIFORNIA Santa Barbara, 2007.

[21] R.G. Sanfelice and A.R. Teel. A throw-and-catch hybrid control strategy for robust global stabilization of nonlinear systems. In *Proceedings of the American Control Conference, 2007. ACC'07*, pages 3470–3475. IEEE, 2007.

[22] R.G. Sanfelice, R. Goebel, and A.R. Teel. Generalized solutions to hybrid dynamical systems. *ESAIM: Control, Optimisation and Calculus of Variations*, 14 (04):699–724, 2008.

[23] R.W. Sinnet, M.J. Powell, R.P. Shah, and A.D. Ames. A human-inspired hybrid control approach to bipedal robotic walking. In *Proceedings of the 18th IFAC World Congress*, pages 6904–11, 2011.

[24] M. Yamaguchi, I. Muramoto, and N. Takahashi. Control system for hybrid vehicle. *Asian Journal of Control*, 14(1):12–22, January 11 2012. EP Patent 1,199,205.

[25] Kai Wulf. *Quadratic and Non-Quadratic Stability Criteria for Switched Linear Systems*. PhD thesis, National University of Ireland, 2004.

[26] R. N. Shorten. *A Study of hybrid dynamical systems with application to automotive control*. PhD thesis, Dept. of Electrical and Electronic Engineering, University College Dublin, Republic of Ireland, 1996.

[27] Douglas Leith, Robert Shorten, William Leithead, Oliver Mason, and Paul Curran. Issues in the design of switched linear control systems: A benchmark study. *International Journal of Adaptive Control and Signal Processing*, 17(2):103–118, 2003.

[28] A. Baños and A. Barreiro. *Reset Control Systems*. Springer Verlag, 2011.

[29] K.S. Narendra and J. Balakrishnan. Adaptive control using multiple models. *Automatic Control, IEEE Transactions on*, 42(2):171–187, 1997.

[30] Hai Lin and Panos J. Antsaklis. Stability and stabilizability of switched linear systems: A short survey of recent results. *IEEE Transactions on Automatic Control*, 54(2):24 –29, 2009.

[31] Robert Shorten, Fabian Wirth, Oliver Mason, Kai Wulff, and Christopher King. Stability criteria for switched and hybrid systems. *SIAM Review*, 49(4):545–592, 2007.

[32] Wen-An Zhang and Li Yu. Stability analysis for discrete-time switched time-delay systems. *Automatica*, 45(10):2265–2271, 2009. ISSN 0005-1098.

[33] Chien-Hua Lee. Robust stabilization of linear continuous systems subjected to time-varying state delay and perturbations. *Journal of the Franklin Institute*, 333(5):707–720, 1996. ISSN 0016-0032.

[34] Daniel Liberzon. *Switching in Systems and Control*. Birkäuser, 2003.

[35] Jinxing Lin, Shumin Fei, and Zhifeng Gao. Stabilization of discrete-time switched singular time-delay systems under asynchronous switching. *Journal of the Franklin Institute*, 349(5):1808–1827, 2012. ISSN 0016-0032.

[36] Vu N. Phat. Switched controller design for stabilization of nonlinear hybrid systems with time-varying delays in state and control. *Journal of the Franklin Institute*, 347(1):195–207, 2010. ISSN 0016-0032.

[37] K. S. Narendra and J. Balakrishnan. A common lyapunov function for stable lti system with commuting a-matrices. *IEEE Trans. Automat. Control*, 39(12): 2469–2471, 1994.

[38] Y. Mori, T. Mori, and Y. Kuroe. On a class of linear constant systems which have a common quadratic lyapunov function. In *Proceedings of the 37th IEEE Conference on Decision and Control*, 1998.

[39] H. Shim, D.J. Noh, , and J.H. Seo. Common lyapunov function for exponentially stable nonlinear systems. In *Proceedings of the 4th SIAM Conference on Control and its Applications*, 1998.

[40] A. P. Molchanov and E. S. Pyatnitskii. Criteria of asymptotic stability of differential and difference inclusions encountered in control theory. *Systems and Control Letters*, 1989.

[41] M. Kunze, A. Karimi, and R. Longchamp. Frequency domain controller design by linear programming guaranteeing quadratic stability. In *Proceedings of the 47th Conference on Decision and Control (CDC'08)*, pages 345–350, 2008.

[42] J. Clegg. A nonlinear integrator for servomechanism. *AIEE Transactions Part II, Application and Industry*, 77:41–42, 1958.

[43] KR Krishnan and IM Horowitz. Synthesis of a nonlinear feedback system with significant plant-ignorance for prescribed system tolerances. *International Journal of Control*, 19(4):689–706, 1974.

[44] I. Horowitz and P. Rosenbaum. Nonlinear design for cost of feedback reduction in systems with large parameter uncertainty. *International Journal of Control*, 21(6):977–1001, 1975.

[45] C. Hollot, O. Beker, Y. Chait, and Q. Chen. On establishing classic performance measures for reset control systems. *Perspectives in robust control*, pages 123–147, 2001.

[46] O. Beker, CV Hollot, Y. Chait, and H. Han. Fundamental properties of reset control systems. *Automatica*, 40(6):905–915, 2004.

[47] L. Zaccarian, D. Nesic, and A.R. Teel. First order reset elements and the Clegg integrator revisited. In *Proceedings of the 2005 American Control Conference (ACC'05)*, volume 1, pages 563–568, june 2005.

[48] J. Zheng, Y. Guo, M. Fu, Y. Wang, and L. Xie. Improved reset control design for a PZT positioning stage. In *Proceedings of the IEEE International Conference on Control Applications*, pages 1272–1277, 2007.

[49] J. Zheng, Y. Guo, M. Fu, Y. Wang, and L. Xie. Development of an extended reset controller and its experimental demonstration. *IET Control Theory & Applications*, 2(10):866–874, 2008.

[50] A. Baños and A. Vidal. Design of PI+CI reset compensators for second order plants. In *Proceedings of the IEEE International Symposium on Industrial Electronics (ISIE'07)*, pages 118–123, 2007.

[51] A. Baños and A. Vidal. Definition and tuning of a PI+CI reset controller. In *Proceedings of the 2007 European Control Conference (ECC'07)*, pages 4792–4798, 2007.

[52] Dragan Nesic, Andrew R Teel, and Luca Zaccarian. Stability and performance of SISO control systems with first-order reset elements. *IEEE Transactions on Automatic Control*, 56(11):2567–2582, 2011.

[53] F.S. Panni, D. Alberer, and L. Zaccarian. Set point regulation of an EGR valve using a FORE with hybrid input bias estimation. In *Proceedings of the 2012 American Control Conference (ACC'12)*, pages 4221–4226, 2012.

[54] S. Hassan HosseinNia, Inés Tejado, and Blas M. Vinagre. Fractional-order reset control: Application to a servomotor. *Mechatronics*, -:–, 2013. Accepted.

[55] S. Hassan HosseinNia, Inés Tejado, and Blas M. Vinagre. Basic properties and stability of fractional order reset control systems. In *Proceedings of the 12th European Control Conference (ECC'13)*, 2013. Accepted.

[56] A. Oustaloup. *La Commade CRONE: Commande Robuste d'Ordre Non Entier*. Paris : Hermes, 1991.

[57] P. Lanusse, S. Sabatier, X. Moreau, and A. Oustaloup. Robust control: Crone control. In *Proceedings of the Tutorial Workshop on "Fractional Calculus Applications in Automatic Control and Robotics", 41st IEEE Conference on Decision and Control (CDC'02)*, 2002.

[58] I. Podlubny. Fractional-order systems and $PI^{\lambda}D^{\mu}$ controllers. *IEEE Transactions on Automatic Control*, 44(1):208–214, 1999.

[59] Ramon Vilanova and Antonio Visioli. *PID Control in the Third Millennium: Lessons Learned and New Approaches*. Springer, 2012.

[60] Y.Q. Chen, H. Dou, B.M. Vinagre, and C.A. Monje. A robust tuning method for fractional order pi controllers. *2nd IFAC Workshop on Fractional Differentiation and its Applications, Porto, Portugal*, 2006.

[61] G. Maione and P. Lino. New tuning rules for fractional pi^{α} controllers. *Nonlinear Dynamics*, 49(1):251–257, 2007.

[62] Y. Luo, Y.Q. Chen, C.Y. Wang, and Y.G. Pi. Tuning fractional order proportional integral controllers for fractional order systems. *Journal of Process Control*, 20(7):823–831, 2010.

[63] Y. Luo and Y.Q. Chen. Fractional order [proportional derivative] controller for a class of fractional order systems. *Automatica*, 45(10):2446–2450, 2009.

[64] R. Caponetto, G. Dongola, L. Fortuna, and A. Gallo. New results on the synthesis of fo-pid controllers. *Communications in Nonlinear Science and Numerical Simulation*, 15(4):997–1007, 2010.

[65] Concepción A. Monje, Blas M. Vinagre, Vicente Feliu, and Yang Quan Chen. Tuning and auto-tuning of fractional order controllers for industry applications. *Control Engineering Practice*, 16(7):798–812, 2008. ISSN 0967-0661.

[66] Y.Q. Chen, T. Bhaskaran, and D. Xue. Practical tuning rule development for fractional order proportional and integral controllers. *Journal of Computational and Nonlinear Dynamics*, 3:021403, 2008.

[67] Varsha Bhambhani, Yiding Han, Shayok Mukhopadhyay, Ying Luo, and YangQuan Chen. Hardware-in-the-loop experimental study on a fractional order networked control system testbed. *Communications in Nonlinear Science and Numerical Simulation*, 15(9):2486 – 2496, 2010. ISSN 1007-5704. doi: 10.1016/j.cnsns.2009.10.010. URL http://www.sciencedirect.com/science/article/pii/S1007570409005292.

[68] D. Valério and J. Costa. Tuning rules for fractional pids. *Advances in Fractional Calculus*, pages 463–476, 2007.

[69] S. Dormido, E. Pisoni, and A. Visioli. An interactive tool for loop-shaping design of fractional-order PID controllers. In *Proceedings of the 4th IFAC Workshop on Fractional Differentiation and Its Applications (FDA'10)*, 2010.

[70] E. Pisoni, A. Visioli, and S. Dormido. An interactive tool for fractional order pid controllers. In *Proceedings of the 35th Annual Conference of IEEE Industrial Electronics (IECON '09)*, pages 1468 –1473, 2009.

[71] C. A. Monje, Y. Q. Chen, B. M. Vinagre, D. Xue, and V. Feliu. *Fractional-order Systems and Controls. Fundamentals and Applications*. Springer, 2010.

[72] Riccardo Caponetto, Giovanni Dongola, Luigi Fortuna, and Ivo Petras. *Fractional Order Systems: Modeling and Control Applications*. Series on Nonlinear Science, Series A. World Scientific, 2010.

[73] Mohammad Saleh Tavazoei and Mohammad Haeri. A note on the stability of fractional order systems. *Mathematics and Computers in Simulation*, 79(5):1566–1576, 2009. ISSN 0378-4754.

[74] M. Moze, J. Sabatier, and A. Oustaloup. LMI characterization of fractional systems stability. *Advances in Fractional Calculus*, pages 419–434, 2007.

[75] D. Baleanu, S. J. Sadati, R. Ghaderi, A. Ranjbar, T. Abdeljawad, and F. Jarad. Stability theorem for fractional systems with delay. *Abstract and Applied Analysis*, 2010:9, 2010.

[76] Yang Quan Chen and Kevin L. Moore. Analytical stability bound for a class of delayed fractional order dynamic systems. *Nonlinear Dynamics*, 29:191–200, 2002.

[77] Yan Li, Yang Quan Chen, and Igor Podlubny. Mittag–leffler stability of fractional order nonlinear dynamic systems. *Automatica*, 45(8):1965–1969, 2009. ISSN 0005-1098.

[78] Xiang-Jun Wen, Zheng-Mao Wu, and Jun-Guo Lu. Stability analysis of a class of nonlinear fractional-order systems. *IEEE Transactions on Circuits and Systems II: Express Briefs*, 55(11):1178–1182, 2008.

[79] Chuang Li and Jingcheng Wang. Robust stability and stabilization of fractional order interval systems with coupling relationships: The $0 < \alpha < 1$ case. *Journal of the Franklin Institute*, 349(7):2406–2419, 2012. ISSN 0016-0032.

[80] Zeng Liao, Cheng Peng, Wang Li, and Yong Wang. Robust stability analysis for a class of fractional order systems with uncertain parameters. *Journal of the Franklin Institute*, 348(6):1101–1113, 2011. ISSN 0016-0032.

[81] Hong Sheng Li, Ying Luo, and Yang Quan Chen. A fractional order proportional and derivative (FOPD) motion controller: Tuning rule and experiments. *IEEE Transactions on Control Systems Technology*, 18(2):516–520, 2010. ISSN 1063-6536.

[82] Long ge Zhang, Jun min Li, and Guo pei Chen. Extension of Lyapunov second method by fractional calculus. *Pure and Applied Mathematics*, 3:291–294, 2005.

[83] Abdelghani Ouahab. Some results for fractional boundary value problem of differential inclusions. *Nonlinear Analysis*, 69:3877—3896, 2008.

[84] M. Benchohra, J. Henderson, S. K. Ntouyas, and A. Ouahab. Existence results for fractional functional differential inclusions with infinite delay and applications to control theory. *Fractional Calculus and Applied Analysis*, 11(1):35–56, 2008.

[85] Y.K. Chang and J.J. Nieto. Some new existence results for fractional differential inclusions with boundary conditions. *Mathematical and Computer Modelling*, 49 (3-4):605–609, 2009.

[86] MOUFFAK BENCHOHRA, SAMIRA HAMANI, JUAN JOSE NIETO, and BOUALEM ATTOU SLIMANI. Existence of solutions to differential inclusions with fractional order and impulses. *lectronic Journal of Differential Equations*, 80:1–18, 2010.

[87] B. Ahmad, J.J. Nieto, and J. Pimentel. Some boundary value problems of fractional differential equations and inclusions. *Computers & Mathematics with Applications*, 2011.

[88] T. Kaczorek. Positive fractional 2d hybrid linear systems. *BULLETIN OF THE POLISH ACADEMY OF SCIENCES TECHNICAL SCIENCES*, 56(3):273–277, 2008.

[89] Tadeusz Kaczorek. Realization problem for positive fractional hybrid 2d linear systems. *Fractional Calculus and Applied Analysis*, 11(3):353–368, 2008.

[90] Katica R Hedrih. Main chains and eigen modes of fractional order hybrid multipendulum system dynamics. *Physica Scripta*, 2009.

[91] Saeed Balochian, Ali Khaki-Sedigh, and Asef Zare. Stabilization of multi-input hybrid fractional-order systems with state delay. *ISA Transactions*, 50:21—27, 2011.

[92] Saeed Balochian and Ali Khaki Sedigh. Sufficient condition for stabilization of linear time invariant fractional order switched systems and variable structure control stabilizers. *ISA Transactions*, 51:65–73, 2012.

[93] B M Vinagre. *Modelado y control de sistemas dinámicos caracterizados por ecuaciones íntegro-diferenciales de orden fraccional.* PhD thesis, PhD thesis, Universidad Nacional de Educación a Distancia, Madrid, 2001.

[94] Antonio jose Calderon. *Control Fraccionario de Convertidores Electrónicos de Potencia Tipo Buck (in Spanish).* PhD thesis, University of Extremadura, Spain, 2003.

[95] C.A. Monje. *Design Methods of Fractional Order Controllers for Industrial Applications.* PhD thesis, University of Extremadura, Spain, 2006.

[96] A. Rodriguez. *Estimacion de Posicion y Control de Vehiculos Autonomos a Elevada Velocidad.* PhD thesis, University of Sevilla, 2007.

[97] Inés Tejado. *Some Contributions in Networked Control Systems Based on Fractional Calculus.* PhD thesis, University of Extremadura, Spain, 2011.

[98] Blas M. Vinagre, I. Podlubny, L. Dorcak, and V. Feliu. On fractional PID controllers: a frequency domain approach. In *Proceedings of the IFAC Workshop on Digital Control (PID'00)*, 2000.

[99] B. M. Vinagre, I. Petras, P. Merchan, and L. Dorcak. Two digital realization of fractional controllers: application to temperature control of solid. In *Proceedings of the European Control Conference*, 2001.

[100] YangQuan Chen, Kevin L Moore, Blas M Vinagre, and Igor Podlubny. Robust pid controller autotuning with a phase shaper. In *Proceedings of the First IFAC Workshop on Fractional Differentiation and its Applications (FDA04)*, 2004.

[101] C.A. Monje, B.M. Vinagre, Y.Q. Chen, and V. Feliu. On fractional PI^{λ} controllers: Some tuning rules for robustness to plant uncertainties. *Nonlinear Dynamics*, 38:369–381, 2004.

[102] C. A. Monje, B. M. Vinagre, Y. Q. Chen, V. Feliu, P. Lanusse, and J. Sabatier. Proposals for fractional $PI^{\lambda}d^{\mu}$ tuning. In *Proceedings of the 1st IFAC Symposium on Fractional Differentiation and its Applications (FDA'04)*, 2004.

[103] C.A. Monje, F. Ramos, B.M. Vinagre, and V. Feliu. Tip position control of a lightweight flexible manipulator using a fractional order controller. *IET Control Theory & Applications*, 1(5):1451–1460, 2007.

[104] B.M. Vinagre and V. Feliu. Optimal fractional controllers for rational order systems. A special case of the Wiener-Hopf spectral factorization method. *IEEE Transactions on Automatic Control*, AC-52(12):2385–2389, 2007.

[105] Blas M. Vinagre, C. A. Monje, A. J. Calderón, and J. I. Suárez. Fractional PID controllers for industry application. *Journal of Vibration and Control*, 13(9-10): 1419–1429, 2007.

[106] I. Tejado, B.M. Vinagre, and Y.Q. Chen. Fractional gain and order scheduling controller for networked control systems with variable delay. Application to a Smart Wheel. In *Proceedings of the 4th IFAC Workshop on Fractional Differentiation and Its Applications (FDA'10)*, 2010.

[107] S. Hassan HosseinNia and Blas M. Vinagre. Direct boolean integer and fractional order SMC of switching systems: Application to a DC-DC buck converter. In *Proceedings of the 4th IFAC Workshop on Fractional Differentiation and Its Applications (FDA'10)*, 2010.

[108] S. H. HosseinNia, D. Sierociuk, A. J. Calderon, and B. M. Vinagre. Augmented system approach for fractional order smc of a DC-DC Buck converter. In *Proceedings of the 4th IFAC Workshop on Fractional Differentiation and Its Applications*, 2010.

[109] SH Hosseinnia, R. Ghaderi, A. Ranjbar N, M. Mahmoudian, and S. Momani. Sliding mode synchronization of an uncertain fractional order chaotic system. *Computers & Mathematics with Applications*, 59(5):1637–1643, 2010.

[110] S.H. HosseinNia, I. Tejado, B.M. Vinagre, V. Milanés, and J. Villagrá. Low speed control of an autonomous vehicle using a hybrid fractional order controller. In *Proceedings of the 2nd international conference on control instrumentation and automation ICCIA*, 2011.

[111] I. Tejado, B.M. Vinagre, and Y.Q. Chen. Fractional gain scheduled controller for a networked Smart Wheel. Experimental results. In *Proceedings of the 18th IFAC World Congress*, pages 15043 –15048, 2011.

[112] I. Tejado, V. Milanés, J. Villagrá, J. Godoy, H. HosseinNia, and B. M. Vinagre. Low speed control of an autonomous vehicle by using a fractional pi controller. In *Proceedings of the 18th IFAC World congress*, 2011.

[113] S. Hassan HosseinNia, Inés Tejado, Blas M. Vinagre, Vicente Milanés, and Jorge Villagrá. Experimental application of hybrid fractional order adaptive cruise control at low speed. *Submitted to IET Control Theory and Applications*, -:–, 2012.

[114] S. Hassan HosseinNia, Inés Tejado, and Blas M. Vinagre. Stability of fractional order switching systems. In *Proceedings of the 5th Workshop on Fractional Differentiation and Its Applications (FDA'12)*, 2012.

[115] S. Hassan HosseinNia, Inés Tejado, and Blas M. Vinagre. Robust fractional order PI controller for switching systems. In *Proceedings of the 5th Workshop on Fractional Differentiation and Its Applications (FDA'12)*, 2012.

[116] Inés Tejado, Vicente Milanés, Jorge Villagrá, and Blas M. Vinagre. Fractional network-based control for vehicle speed adaptation via vehicle-to-infrastructure communications. *IEEE Transactions on Control Systems Technology*, (99): doi:10.1109/TCST.2012.2195494, 2012. doi: 10.1109/TCST.2012.2195494.

[117] S. Hassan HosseinNia, Inés Tejado, and Blas M. Vinagre. A method for the design of robust controllers ensuring the quadratic stability for switching systems. *Journal of Vibration and Control*, -:doi:10.1177/1077546312470480, 2013. doi: 10.1177/1077546312470480.

[118] I. Podlubny. *Fractional Differential Equations. An Introduction to Fractional Derivatives, Fractional Differential Equations, Some Methods of Their Solution and Some of Their Applications.* Academic Press, San Diego - New York - London, 1999.

[119] D. Sierociuk and B.M. Vinagre. Infinite horizon state-feedback lqr controller for fractional systems. In *Proceedings of the 49th IEEE Conference on Decision and Control (CDC)*, pages 6674–6679. IEEE, 2010.

[120] M. Shahiri, R. Ghaderi, A. Ranjbar N, SH Hosseinnia, and S. Momani. Chaotic fractional-order coullet system: Synchronization and control approach. *Communications in Nonlinear Science and Numerical Simulation*, 15(3):665–674, 2010.

[121] E. Naseri, A. Ranjbar, SH Hosseinnia, and S. Momani. Backstepping control of fractional-order chaotic systems. In *Proceedings of the 7th International Conference on Multibody Systems, Nonlinear Dynamics, and Control, San Diego, USA*, 2009.

[122] C. Tomlin. Hybrid systems: Modeling, analysis, and control. Course Lecture, Stanford University, 2004.

[123] L. Dorcak, V. Lesko, and I. Kostial. Identification of fractional-order dynamical systems. In *Proceedings of the ASRTP'96*, 1996.

[124] Z. Sun and S. S. Ge. *Switched Linear Systems: Control and Design*. Springer-Verlag, 2005.

[125] Jamal Daafouz, Pierre Riedinger, and Claude Iung. Stability analysis and control synthesis for switched systems: A switched Lyapunov function approach. *IEEE Transactions on Automatic Control*, 47(11):1883–1887, 2002.

[126] Jianjun Bai, Hongye Su, Jinfeng Gao, Tao Sun, and Zhengguang Wu. Modeling and stabilization of a wireless network control system with packet loss and time delay. *Journal of the Franklin Institute*, 349:2420–2430, 2012. ISSN 0016-0032.

[127] M.C.F. Donkers, W.P.M.H. Heemels, D. Bernardini, A. Bemporad, and V. Shneer. Stability analysis of stochastic networked control systems. *Automatica*, 48(5):917–925, 2012. ISSN 0005-1098.

[128] Magdi S. Mahmoud, Hazem N. Nounou, and Yuanqing Xia. Robust dissipative control for internet-based switching systems. *Journal of the Franklin Institute*, 347(1):154–172, 2010. ISSN 0016-0032.

[129] Fang Yang and Huajing Fang. Control structure design of networked control systems based on maximum allowable delay bounds. *Journal of the Franklin Institute*, 346(6):626–635, 2009. ISSN 0016-0032.

[130] M. Yu, L. Wang, T. Chu, and G. Xie. Stabilization of networked control systems with data packet dropout and network delays via switching system approach. In *43rd IEEE Conference on Decision and Control (CDC'04)*, 2004.

[131] A.Baos and A.Vidal. Design of reset control systems: The pi+ci compensator. *Journal of Dynamics Systems, Measurement and Control*, 134(5):051003–1–11, 2012.

[132] Blas M. Vinagre, Concha A. Monje, and Inés Tejado. Reset and fractional integrators in control applications. In *Proceedings of the International Carpathian Control Conference, Strbske Pleso (Slovak Republic)*, pages 754–757, 2007.

[133] P.M. Pardalos and J.B. Rosen. Constrained global optimization: Algorithms and applications. *Lecture Notes in Computer Science*, 268, 1987.

[134] S. Boyd, L. El Ghaoui, E. Feron, and V. Balakrishnan. *Linear Matrix Inequalities in System and Control Theory*. SIAM, 1994.

[135] R. N. Shorten and K.S. Narendra. Necessary and sufficient conditions for existence of a common lyapunov function for finite number of stable second order linear time invariant system. *International Journal of Adaptive Control and Signal Processing*, 16(10):709–728, 2002.

[136] M. Kunze and A. Karimi. Frequency-domain controller design for switched systems. *Preprint submitted to Automatica*, 2012.

[137] H. Hu, Y. Zheng, Y. Chait, and CV Hollot. On the zero-input stability of control systems with clegg integrators. In *Proceedings of the American Control Conference*, volume 1, pages 408–410. IEEE, 1997.

[138] O. Beker, CV Hollot, Q. Chen, and Y. Chait. Stability of a reset control system under constant inputs. In *Proceedings of the American Control Conference*, volume 5, pages 3044–3045. IEEE, 1999.

[139] Q. Chen. *Reset control systems: Stability, performance and application*. PhD thesis, University of Massachusetts Amherst, 2000.

[140] Y. Zheng, Y. Chait, CV Hollot, M. Steinbuch, and M. Norg. Experimental demonstration of reset control design. *Control Engineering Practice*, 8(2):113–120, 2000.

[141] Q. Chen, Y.S.S. Chait, and CV Hollot. Analysis of reset control systems consisting of a fore and second-order loop. *ASME Journal of Dynamic Systems, Measurements, and Control*, 123:279–283, 2001.

[142] A. Oustaloup. *La dérivation non entière: théorie, synthèse et applications*. Hermes, 1995.

[143] S. Manabe. The non-integer integral and its application to control systems. *Journal of Institute of Electrical Engineers of Japan*, 80(860):589–597, 1960.

[144] D. Valério and J. Sá da Costa. Fractional reset control. *Signal, Image and Video Processing*, pages 1–7, 2012.

[145] Y. Luo, Y. Q. Chen, Y. Pi, C. A. Monje, and B. M. Vinagre. Optimized fractional order conditional integrator. *Journal of Process Control*, 21(6):960–966, 2011.

[146] D. Sierociuk and B. M. Vinagre. State and output feedback fractional control by system augmentation. In *Proceedings of the 4th IFAC Workshop on Fractional Differentiation and Its Applications (FDA'10)*, 2010.

[147] Q. Chen, CV Hollot, and Y. Chait. Stability and asymptotic performance analysis of a class of reset control systems. In *Proceedings of the 39th IEEE Conference on Decision and Control*, volume 1, pages 251–256. IEEE, 2000.

[148] Jean-Jacques E Slotine, Weiping Li, et al. *Applied nonlinear control*, volume 199. Prentice-Hall Englewood Cliffs, NJ, 1991.

[149] P. Ioannou and G. Tao. Frequency domain conditions for strictly positive real functions. *IEEE Transactions on Automatic Control*, 32(1):53–54, 1987.

[150] National Center for Statistics and Analysis. Motor vehicle traffic crash fatality counts and estimates of people injured for 2005. Technical report, Department of Transportation, U.S., 2006.

[151] D. F. Llorca, V. Milanes, I. P. Alonso, M. Gavilan, I. G. Daza, J. Perez, and M. A. Sotelo. Autonomous pedestrian collision avoidance using a fuzzy steering controller. *IEEE Transactions on Intelligent Transportation Systems*, 12(2):390–401, 2011. doi: 10.1109/TITS.2010.2091272.

[152] M. Heddebaut, F. Elbahhar, C. Loyez, N. Obeid, N. Rolland, a. Rivenq, and J. Rouvaen. Millimeter-wave communicating-radars for enhanced vehicle-to-vehicle communications. *Transportation Research Part C: Emerging Technologies*, 18(3):440–456, June 2010.

[153] D. Lelono and F. Muldani. Prototype of automatic parking aid based on microcontroller at89s52. In *Proceedings of the International Instrumentation, Communications, Information Technology, and Biomedical Engineering (ICICI-BME) Conf*, pages 1–5, 2009. doi: 10.1109/ICICI-BME.2009.5417303.

[154] A. Shaout and M. Jarrah. Cruise control technology review. *Computers & Electrical Engineering*, 23(4):259–271, July 1997.

[155] G. Naus, J. Ploeg, M. Van de Molengraft, W. Heemels, and M. Steinbuch. Design and implementation of parameterized adaptive cruise control: An explicit model predictive control approach. *Control Engineering Practice*, 18(8):882–892, August 2010.

[156] Fanping Bu, Han-Shue Tan, and Jihua Huang. Design and field testing of a cooperative adaptive cruise control system. In *Proceedings of the American Control Conf. (ACC)*, pages 4616–4621, 2010.

[157] U. Holmberg and K. Sjöberg. A modular cacc system integration and design. *IEEE transactions on intelligent transportation systems (Print)*, 13(3): 1050–1061, 2012.

[158] R. Kianfar, B. Augusto, A. Ebadighajari, U. Hakeem, J. Nilsson, A. Raza, R.S. Tabar, N.V. Irukulapati, C. Englund, P. Falcone, S. Papanastasiou, L. Svensson, and H. Wymeersch. Design and experimental validation of a cooperative driving system in the grand cooperative driving challenge. *IEEE Transactions on Intelligent Transportation Systems*, 13(3):994–1007, 2012.

[159] V. Milanes, J. Villagra, J. Godoy, and C. Gonzalez. Comparing fuzzy and intelligent pi controllers in stop-and-go manoeuvres. *IEEE Transactions on Control Systems Technology*, 99:1–9, 2012. doi: 10.1109/TCST.2011.2135859.

[160] W.U.N. Fernando and S. Kumarawadu. Discrete-time neuroadaptive control using dynamic state feedback with application to vehicle motion control for intelligent vehicle highway systems. *Control Theory & Applications, IET*, 4(8): 1465–1477, August 2010.

[161] D. Valério and J. Sá da Costa. Introduction to single-input, single-output fractional control. *Control Theory & Applications, IET*, 5(8):1033–1057, May 2011.

[162] P. Li and J. Cao. Stabilisation and synchronisation of chaotic systems via hybrid control. *Control Theory & Applications, IET*, 1(3):795–801, May 2007.

[163] J. Lygeros, D.N. Godbole, and S. Sastry. Verified hybrid controllers for automated vehicles. *Automatic Control, IEEE Transactions on*, 43(4):522 –539, apr 1998. ISSN 0018-9286. doi: 10.1109/9.664155.

[164] T. Samad and G. Balas. *Software-Enabled Control:Information Technology for Dynamical Systems*, chapter A Maneuver-Based Hybrid Control Architecture for Autonomous Vehicle Motion Planning, pages 299–323. Wiley-IEEE Press, 2003.

[165] Emilio Frazzoli. *Robust Hybrid Control for Autonomous Vehicle Motion Planning*. PhD thesis, Massachusetts Institute of Technology, Cambridge, MA, 2001.

[166] C.W. Seibel, J.M. Farines, and J.E.R. Cury. *Hybrid Systems V*, volume 1567, chapter Towards using hybrid automata for the mission planning of unmanned aerial vehicles. Springer-Verlag, 1999.

[167] M. Mukai, T. Azuma, and M. Fujita. A collision avoidance control for multi-vehicle using pwa/mld hybrid system representation. In *Proceedings of the IEEE International Conference on Control Applications*, volume 2, pages 872–77, September 2004. doi: 10.1109/CCA.2004.1387478.

[168] A. Balluchi, P. Soueres, and A. Bicchi. Hybrid feedback control for path tracking with a bounded-curvature vehicle. In *Proceedings of the 4th International Workshop on Hybrid Systems: Computation and Control*, pages 133–146, Italy, 2001.

[169] João Pedro Hespanha. *Stabilization Through Hybrid Control*, volume Control Systems, Robotics, and Automation, chapter Stabilization Through Hybrid Control. Developed under the Auspices of the UNESCO, Eolss Publishers, Oxford, UK, 2004.

[170] J. Lygeros, C. Tomlin, and S. Sastry. Controllers for reachability specifications for hybrid systems. *Automatica*, 35:349–370, 1999.

[171] E. Onieva, V. Milanés, C. González, T. de Pedro, J. Pérez, and J. Alonso. Throttle and brake pedals automation for populated areas robotica. *Robotica*, 28: 509–516, 2010.

[172] V. Milanés, C. González, J. Naranjo, E. Onieva, and T. De Pedro. Electro-hydraulic braking system for autonomous vehicles. *International Journal of Automotive Technology*, 1(11):89–95, 2010.

[173] A. Kamga and A. Rachid. Speed, steering angle and path tracking controls for a tricycle robot. In *Proceedings of the IEEE International Symposium on Computer-Aided Control System Design*, pages 56–61, 1996.

[174] J. Villagrá, V. Milanés, J. Pérez, and T. de Pedro. Control basado en pid inteligentes: Aplicación al control de crucero de un vehículo a bajas velocidades. *Revista Iberoamericana de Automática e Informática Industrial*, 7(4):44–52, 2010.

[175] J. Zhou and H. Peng. Range policy of adaptive cruise control vehicles for improved flow stability and string stability. *IEEE Transaction on Intelligent Transportation System*, 6(2):229–237, 2005.

[176] Peter A Cook. Stable control of vehicle convoys for safety and comfort,. *IEEE Transactions on Automatic Control*, 52(3):526–531, 2007.

[177] R Alur, K-E Arzen, John Baillieul, TA Henzinger, Dimitrios Hristu-Varsakelis, and William S Levine. *Handbook of networked and embedded control systems*. Birkhäuser Boston, 2005.

[178] Jeff S Shamma and Michael Athans. Gain scheduling: Potential hazards and possible remedies. *Control Systems, IEEE*, 12(3):101–107, 1992.

[179] Feedback Instruments Ltd. *Analogue Servo. Fundamentals Trainer 33-001*. UK.

[180] National Instruments Corporation. *DAQ M Series. M Series User Manual*, 2008.

[181] E Onieva, V Milanés, C González, T De Pedro, J Pérez, and J Alonso. Throttle and brake pedals automation for populated areas. *Robotica*, 28(4):509, 2010.